SPARC, a matricellular protein that protects cancer from therapy

Thesis

Alessandra Santangelo

Cell and Molecular Biology Master's Degree

SPARC, a matricellular protein that protects cancer from therapy

A thesis submitted to the Open University of London

for the degree of Doctor in Philosophy

in Life and Biomolecular Sciences

Molecular Immunology Unit
Department of Experimental Oncology
Fondazione IRCCS Istituto Nazionale Tumori
Via Amadeo, 42 20133 Milan, Italy

January 2014

ACKNOLEDGMENTS

First of all, I would like to thank to Dr. Colombo who gave me the great opportunity of working in this interesting field of research and for spending 4 years in his outstanding laboratory.

I would like to express my sincere gratitude to Dr. Sabina Sangaletti for her training and her advices about experiments and thesis outlines, I enjoyed the time spent with her and our interpretation of experiment results and to her being part of new scientific ideas. My thanks goes to Dr. Tagliabue and her colleague Dr.Triulzi for have shared with me their results and their collaboration to the conclusive part of this thesis with data in Human breast patients. I express my gratitude to her for giving me the possibility for validation of my hypothesis in ECM3 breast tumors samples. Many other thanks go to to Dr. Tripodo for providing pathologist outlines about SN25ASP and N3DSPARC tumors EMT phenotype and Zometa effect on EMT.

I would like to thank Dr. Claudia Chiodoni for her collaboration to this work concerning the part of in vivo validation of the MDSC suppressive activity. I would like to thank Dr. Caterina Vitali for her suggestions about FACS analysis concerning MDSC characterization. I would like to thank Dr. Chronowska for her collaboration in the area of qPCR analysis performed to validate MDSC phenotype.

I would like to thank to Dr. Silvia Piconese for her great collaborative spirit that she never hesitated in sharing with me, for her special support during the first part of my PhD and our great friendship. I would to thank for their special technical support Mariella Parenza, Ivano Arioli, Barbara Cappetti, Paola Portararo, who guided me in setting up protocols and methods. Above all, I would like to thank the Scientific Directorate of the Institute which supported me in the final part of the thesis, with a particular gratitude to Dr. Daniela Majerna. Finally all the laboratory members and colleagues for making my time during the PhD delightful.

ABBREVIATIONS

(GMCSF) Granulocytes colony stimulating factor

(EMT) Epithelial to mesenchymal transition

(CCL5) Chemokine C-C motif ligand 5

(CCL2) Chemokine C-C motif ligand 2

(iNOS) Inducible nitric oxide synthase

(EMDR) Enviromental mediated drug resistance

(CSFE) 5,6-carboxy fluorescein diacetate succinimidyl ester

(Doxil) Doxorubicin Hcl Liposome Injection

(H&E) Haematoxylin and Eosin

(M1) Pro-inflammatory macrophages, M1 phenotype

(M2) Pro-tumor macrophages, M2 phenotype

(Mac 1) Macrophage antigen 1

(MDSCs) Myeloid-derived suppressor cells

(MCP-1) Monocyte chemotactic protein-1

(N1) Pro-inflammatory neutrophils, N1 phenotype

(N2) Pro-tumor neutrophils, N2 phenotype

(N-BPs) Nitrogen-containing bisphosphonates

(NF κ b) Nuclear factor- κ b

(TGF- β) Recombinant transforming growth factor-beta

(E-CAD) E-Cadherin

(N-Cadh) N-Cadherin

(ECM) extracellular matrix

(LOX) Lysil Oxydase

(SPARC) secreted protein acid and rich in cysteine

(LAIRs) leukocytes-associated Ig-like receptors

(AAMs) alternatively activated macrophages

(Treg) T regulatory cells

(M-CSF) macrophage colony-stimulating factor

(GITR) glucocorticoid-induced TNF receptor family-related gene

(nTreg) natural Treg (nTreg)

(iTreg) induced (or adaptive) Treg

(G-MDSC) granulocytic MDSCs

(M-MDSC) monocytic MDSCs

(BCL-XL) B-cell lymphoma XL

(CDK4) cyclin-dependent kinase 4

(PDGF) platelet-derived growth factor

(VEGF) vascular endothelial growth factor

(ATRA) all-trans retinoic acid

(MMP-9) matrix metalloproteinase-9

(PMNs) Polymorphonuclear lymphocytes

(GEP) Gene Expression Profile analysis

LIST OF TABLES

LIST OF FIGURES

ABSTRACT

The matricellular protein SPARC (secreted protein acidic and rich in cysteine) is a master regulator of tissue stroma; it is expressed during tissue remodeling and repair and its impaired regulation has a role in fibrotic responses, in determining the composition of the tumor-associated stroma and, less expected, in regulating the immune response. The complexity of studying SPARC in cancer stems from its concomitant or alternative expression in tumor and/or stroma cells depending on the tumor histotypes. Extracellular matrix (ECM) gene profile of human breast carcinomas correlates SPARC expression with prognosis and response to therapy. In particular, a subgroup of breast tumors can be identified based on ECM gene signature headed by SPARC that correlates with tumor grade, bad prognosis and poor response to therapy. Epithelial to mesenchymal transition (EMT) has been associated to drug resistance and SPARC has been implicated in EMT. Nevertheless the source of SPARC and its path toward EMT and the associated drug resistance have not been identified yet. I have used a well-defined model of transgenic mouse mammary carcinoma expressing the mutated rat oncogene c-erB2 (HER-2/neu), under the mouse mammary tumor virus promoter, backcrossed with *Sparc*$^{-/-}$ mice to establish mammary carcinoma cell lines devoid of SPARC expression, in which SPARC can be restored by retroviral gene transduction. With this isogenic cell lines I have been able to show that SPARC expression in tumor cells induces EMT only in vivo, indicating that EMT is a microenvironmental and not a cell autonomous process. Moreover, SPARC expressing tumors became resistant to treatment with Doxil (Doxil, a pegylated form of Doxorubicin). Investigating the environmental players responsible of EMT in SPARC transduced tumors, I found that myeloid cells and particularly the so called myeloid derived suppressor cells (MDSC) have a role in EMT and drug resistance depending on SPARC. SPARC does not change the number or ratio between the Ly6G^{high} and the Ly6G^{low} fractions of CD11b MDSC rather it determines the immunosuppressive phenotype of recruited myeloid cells. The data show that SPARC-forced expression increased the activation of pro-tumoral (CCL2, CCL5) and immunosuppressive (ArgI, NOS2, Cox-2) genes in monocyte-MDSC (the Ly6G^{low} fraction). Furthermore, the role of myeloid cells recruited in Doxil resistance and EMT has been proven adding bisphosphonate to Doxil during treatment. Bisphosphonates have been shown to inhibit induction and function of myeloid suppressor cells. Indeed, Bisphosphonates addition reverted EMT, the immunosuppressive phenotype of myeloid cells and rendered SPARC-producing tumors sensitive to Doxil administration.

1. GENERAL INTRODUCTION

1.1 The Tumor Microenvironment

1.1.1 The tumor stroma

For decades, pathologists have recognized that the stroma surrounding tumours is, in many cases altered with changes in cellular and ECM composition [1]. Over the years descriptive studies have verified that gene expression is altered in the carcinoma –associated stroma and suggested it would be reasonable to look at the role of the tumour stroma in tumorigenesis and to find out new possible targets for cancer therapy within the tumour microenvironment [2]. The basic concept of this cancer perspective is that carcinomas (and other tumours) do not exist in isolation but instead emerge and exhibit a range of behaviors regulated by host cells comprising the tumour stroma. During tumor progression and metastasis an active cross-talk occurs between tumor cells and their associated stroma, mainly mediated by cell-to-cell contact or paracrine cytokines and growth factors; signaling that is reminiscent of the communication between epithelial and mesenchymal cells during embryonic development. As a result of these interchanges, tumor stroma undergoes a number of morphological changes (desmoplasia) allowing tumor growth, invasion and metastasis. It is now widely accepted that tumor cells lacking the intrinsic ability to initiate angiogenesis, proliferate, resist apoptosis or invade and metastasize can acquire such properties via their interaction with the microenvironment. Stroma can also limit the influx of inflammatory cells, or the access of therapeutics to the tumor, alter drug metabolism and contribute to the development of drug resistance. Areas of tumor-host interaction are populated by different types of extracellular matrix (ECM) components and stroma cells all contributing to the final tumor outcome. Among the identified cells are fibroblasts, epithelial cells, adipocytes and vascular cells. The ECM is a network of

fibrous structural proteins, such as collagens and fibronectin, which are embedded in a viscoelastic gel of glycosaminoglycans, proteoglycans and glycoproteins. Fibrous proteins not only form the scaffold of the stroma and provide tensile strength, but also represent channels for communication and movement of cells and might exert a regulatory function on a variety of cells.

1.1.2 Matrix stiffness regulates tumor growth and progression

Although tightly controlled during embryonic development and organ homeostasis, ECM deposition is commonly deregulated and disorganized in diseases such as cancer. Abnormal ECM affects cancer progression by directly promoting cellular transformation and metastasis. An increase in collagen deposition or ECM stiffness, alone or in combination, up-regulates integrin signaling and can promote cell survival and proliferation [3, 4]. In mouse models Lenvental et al. demonstrated that an increase in collagen deposition or ECM stiffness resulting from overproduction of lysyl oxidase (LOX), an enzyme that cross-links collagen fibers and other ECM components, promotes focal adhesion assembly, ERK and PI3 kinase signaling and facilitates Neu-mediated oncogenic transformation [5]. In addition, mammary fad pad conditioned by fibroblasts constitutively expressing LOX promoted the transformation and invasion of pre-malignant mammary cell lines. The regulatory role of the ECM is not restricted solely to tumor cells, but also extends to immune cells. Inflammation, characterized by massive influx of immune cells, plays a causative role in cancer development. Although their initial function is supposed to suppress tumor growth, at later stages immune cells, including macrophages, are often altered and recruited by tumor cells to promote cancer. In this context, abnormal ECM might affect many aspects of immune cell behaviors, including infiltration, differentiation, and functional activation. For example, mice lacking the ECM glycoprotein SPARC (secreted protein

acidic and rich in cysteine) have an increased number of macrophages in tumors, suggesting that the ECM can influence the number of immune cells. One way the ECM affects the immune cells is by regulating cell proliferation. The ECM also regulates the activation of immune cells. For example, increased ECM stiffness can promote integrin-mediated adhesion complex assembly and activate T cells. Although collagen type I promotes infiltration of immune cells, it inhibits the ability of macrophages to kill cancer cells by blocking polarization and, thus, activation of macrophages. These findings highlight the complex ways in which ECM deregulation may affect behaviors of different groups of immune cells. The inhibitory effect of collagen I on immune cells is likely mediated by its binding with the leukocyte-associated Ig-like receptors (LAIRs), which are expressed at the surface of most immune cells. At present, it is not clear whether LAIRs and integrins cooperate; however, the activation of LAIRs is a plausible mechanism whereby high levels of tumor collagen can attenuate the otherwise tumor-suppressive function of immune cells.

1.1.3 The immune microenvironment of solid tumors.

In homeostatic tissue, resident immune cells serve as sentinels that safeguard tissue and organ integrity. Following acute damage (e.g., infiltration/infection by pathogens or physical trauma), one activity of resident leukocytes is to limit tissue damage while engaging tissue repair programs (e.g., activation of stromal fibroblasts and vasculature for matrix resynthesis and angiogenesis, respectively, and recruitment of leukocytes from peripheral blood to remove damaged cells and debris) and facilitate re-epithelialization, all without inducing autoimmunity. Following resolution of wound responses, tissue damage is (hopefully) minimal and homeostatic maintenance programs return such that organ physiology is unperturbed. In cancer, immune cells play dual roles with potential to either eliminate or promote malignancy. Premalignant

tissues contain proliferating cells harboring genomic damage (e.g., "initiated" cells) that typically activate critical proliferation/survival pathways. In these tissues, chronic engagement/activation of immune cells, stromal fibroblasts, and vascular and mesenchymal support cells together fosters survival of "initiated" cells, culminating in tissue expansion and development of premalignant lesions via a process reminiscent of typical "inflammatory-type" responses observed in tissues responding to acute damage/trauma [6]. When these chronic inflammatory-type events are sustained, neoplastic progression can ensue. Unresolved chronic immune responses thus resemble the resolution phase of wound healing, where the tumor microenvironment contains significant infiltrations of cells with immunosuppressive activity akin to a wound failing to heal [6]. Consistent with this, studies evaluating leukocyte complexity by flow cytometry in human (and murine) tumors have identified multiple immune cell types that variably contain immunosuppressive activity and, among them, three types of leukocytes in particular have emerged as playing significant roles in suppressing anti-tumor immune responses: macrophages, particularly alternatively activated macrophages (AAMs); regulatory T cells (Treg) and immature myeloid cells.

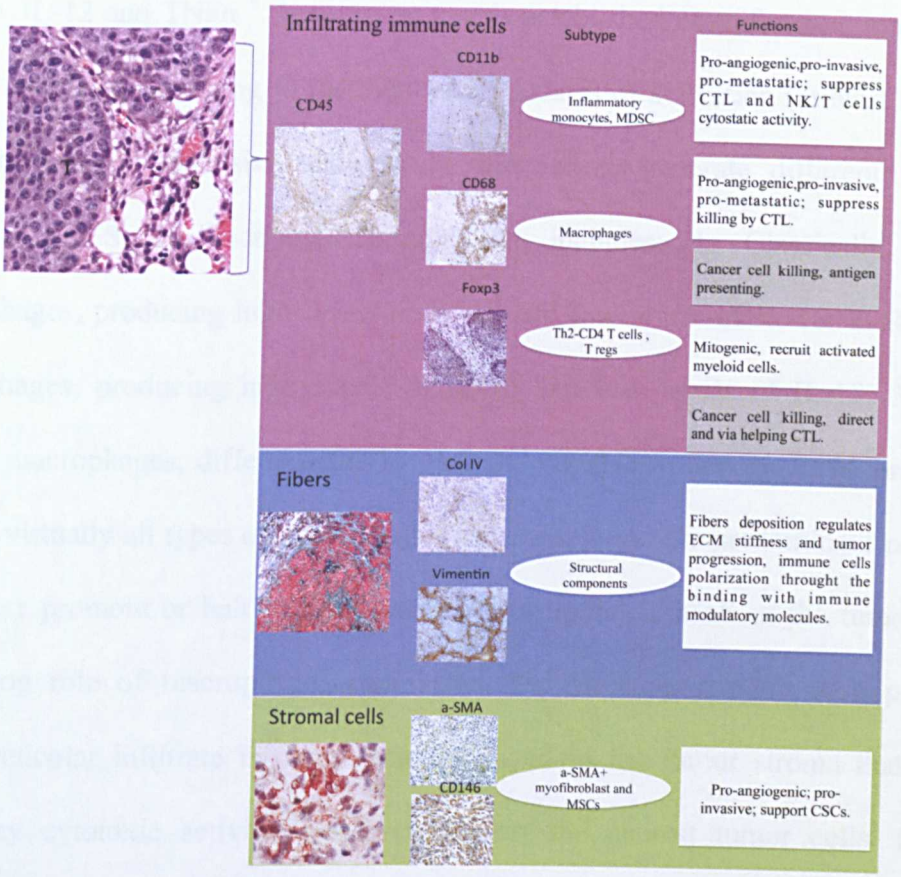

Fig.1.1.1 Schematic representation of the tumor stroma.

CD45 staining (violet box) on OCT tumor sections isolated from a transplantable model of breast tumor identified the immune components of tumor stroma in which different immune cells subtypes are recognized for antagonistic functions highlighted in gray; (blue box) structural components of tumor stroma, here IHC staining of Col IV and Vimentin of breast tumor sections; (green box) stromal cells like CAFs and MSC, herein stained with a-SMA and a-CD146 mAbs.

1.1.3.1 Tumor-associated macrophages

Derived from hematopoietic precursor cells, macrophages have advanced plasticity and key functions in both immune response and tissue homeostasis and integrity. Macrophage activities result from their state of activation as function of the predominant cytokine milieu characterizing the microenvironment in which they are recruited. A common simplification classifies macrophages as M1 or M2 when referring to classically activated or alternatively activated macrophages, respectively [7]. M1 macrophages are pro-inflammatory, producing high levels of IL-12, IFNγ and TNFα, whereas M2 macrophages are anti-inflammatory, producing high levels of IL-

10, low IL-12 and TNFα [8]. In addition to this established classification, macrophages can be classified according to the their various states of activation (at least three) that are not mutually exclusive and can be blended to generate different functional outcomes [9]. Such functional classification includes: 1. Classically activated macrophages, producing high levels of IL-12 and low levels of IL-10; 2. Regulatory macrophages, producing high levels of IL-10 and low levels of IL-12; 3. Wound healing macrophages, differentiated by IL4 and capable to deposit ECM proteins. In tumors, virtually all types of macrophages can coexist and the predominant population can either promote or halt tumor growth. The original hint about the tumor-growth supporting role of macrophages came from the early description of a prominent lymphoreticolar infiltrate in carcinomas localized in the tumor stroma that did not show any cytotoxic activity, not even against the nearest tumor cells. From an immunological point of view, these macrophages were called anergic. Nowadays, they are characterized as "homeostatic" macrophages that, recruited by the tumor, help to orchestrate the tumor microenvironment depositing ECM, releasing VEGF and MMPs and contributing to local immunosuppression. Large part of our knowledge on tumor-associated macrophages comes from studies in mice lacking macrophage- colony stimulating factor (M-CSF) or granulocyte macrophages-colony stimulating factor (GM-CSF). Colony-stimulating factors were first described for the ability to stimulate the formation of colonies from bone marrow (BM) precursors *in vitro*. The effects of M-CSF on macrophages and of GM-CSF on monocytes, granulocytes and dendritic cells (DCs) include: proliferation, survival, differentiation and functional activation[10]. Among CSFs, M-CSF is the most potent macrophage differentiation factor; M-CSF KO mice show general paucity of macrophages in various tissues that impacts on tissue homeostasis, for example impairing mammary gland development[11,12].

Homeostatic macrophages resemble M2-polarized macrophages. Accordingly, macrophages differentiated from BM in the presence of M-CSF release IL-10 and MCP-1 after LPS stimulation and show a more M2-polarized phenotype, whereas macrophages obtained in the presence of GM-CSF respond to LPS by releasing pro-inflammatory cytokines, thereby showing an M1-activation. Monocytes differentiate into macrophages under the influence of the cytokines present in the microenvironment while maintaining some plasticity. For example, it is possible to induce tumor regression re-directing their polarization from M2 to M1 by local delivery of TLR-9 ligand combined with a mAb to IL-10R [13] or by enriching, the tumor microenvironment with macrophages unable to activate NF-kB [14]. Contrary to the tumoral setting, liver injury and repair require two distinct subpopulation of macrophages one monocyte derived and the other derived from a nonhematogenous source, likely Kupffer cells [15]. Although the injury phase is characterized by high TNFα and little IL-10 and the recovery phase by little TNFα and IL-10, it is undetermined whether the functional distinction is related to the macrophage origin [16]. Thus, plasticity seems relevant at least in tumors. The potential plasticity of macrophages adapting their activity to the different phase of tumor development can be summarized as follow: 1. Initiate tumorigenesis by inducing inflammation and epithelial cell transformation (M1-macrophages). Inflammatory macrophages can also have a role in metastasis. 2. Sustain tumor growth and progression. Participate in TM architecture through production of ECM proteins and VEGFs (wound healing macrophages, M2-like macrophages not necessarily expressing predominantly IL-10 or IL-12). Contribute to an immunosuppressive environment by producing high level of IL-10 and low level of TNFα and IL-12 (M2-like, regulatory macrophages). 3. Halt TM growth or mediate tumor rejection if properly stimulated or redirected to undergo

classical activation. The most compelling data showing macrophage-assisted tumor growth and progression came from studies on VEGF and studies using M-CSF KO (*op/op* mice) that, in addition to general macrophages paucity, show defects in tissue development. VEGF is one of the most important factors involved in tumor angiogenesis and stroma reaction. Tumors have been defined as "wounds that never heal" because of their persistent VEGF production[17], but macrophages can produce this cytokine as well as respond to it [18]. In breast cancer, genetic depletion of macrophages in Polyoma Middle T oncoprotein (PyMT)-induced mammary tumors (PyMT plus op/op, double mutants) and the consequent absence of macrophages-produced VEGF delayed tumor progression because of reduced tumor angiogenesis, leukocyte infiltration and tumor-cell invasion. Such defects were caused by the absence of M-CSF, hence, of macrophages, and were reverted by the transgenic expression of VEGF-A directly into the tumors [19]. In the tumor microenvironment, M2-like macrophages are likely to sense the cytokines released in the tumor microenvironment such as IL-10 and can further polarize toward an M2 regulatory phenotype. In such phenotype, tumor-associated macrophages (TAMs) release high levels of IL-10 that contribute to the maintenance of the immunosuppressive phenotype of tumors. In this condition, TAMs are not able to present tumor-associated antigens (TAAs), which partly explains why immunotherapies with a single TAA or based on tumor cell transduction with a single cytokine capable of inducing macrophages recruitment failed or were restricted to particular conditions.

1.1.3.1.1 Macrophage role in tumor rejection

Macrophages plasticity opens up the interesting possibility of functionally reverting M2 macrophages fostering tumor growth into M1 macrophages that are capable of tumor rejection. Gene transduction of solid tumor cells with a gene encoding for a chemokine (CCL16) recruits new macrophages that exclusively display an M2 phenotype. The addition of a TLR-9 agonist (CpG) and inhibition of IL-10 (mAb to IL-10R) change the TAM phenotype to M1 and tumor debulking is quick (less than 24h) and massive, largely via a TNFα-dependent mechanism [13, 20]. Also, TAMs in the microenvironment of ovarian carcinoma can be redirected either by specifically blocking the NF-kB activity that, in this tumor type, contributes to the immunosuppressive phenotype of cancer, or by the use of Smac-mimetic compounds [14 21]. In tumor-bearing mice, the adoptive transfer of these re-directed macrophages impairs tumor growth and metastasis [14].

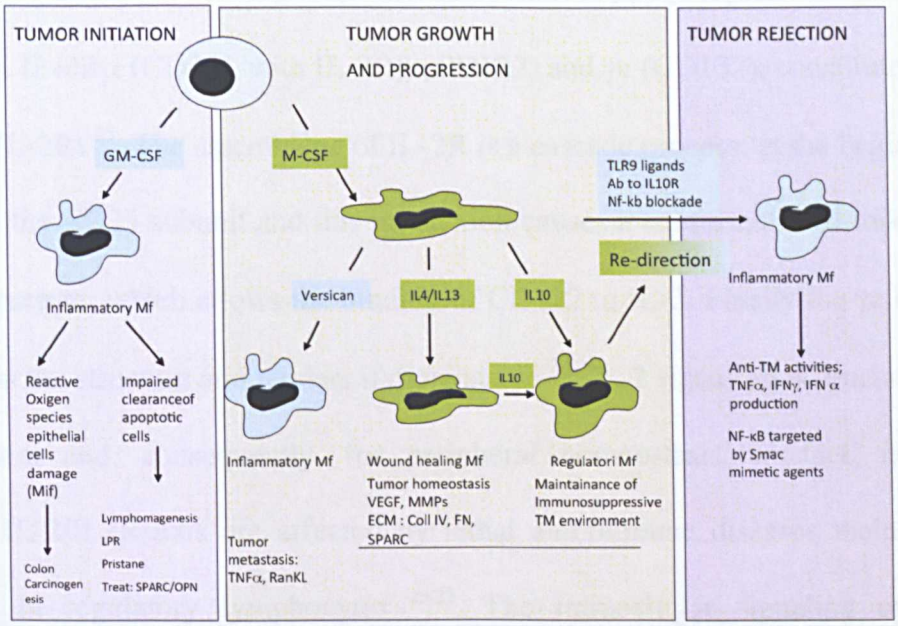

Fig.1.1.3.1 Plasticity of tumor-associated macrophages, from tumor initiation to tumor rejection.

M2-like Macrophages ROS activity are associated to cells damage in colon carcinogenesis; M2- alternative macrophages phenotype are challenging by IL4/IL13 and associated to wound healing. IL-10 is associated to tumor immunosuppressive M2 macrophages. The image was adapted from Sangaletti S. and MP Colombo AACR Educ. Book. 2008.

1.1.3.2 The biology of regulatory T cells

The first evidence about the existence of Treg was provided, at the beginning of 1970s, by Gershon and colleagues, who called them suppressive T cells [22,23]. Few years later, using mouse tumor models, it was also proven that these suppressive lymphocytes promote tumor growth [24]. Despite the immunological relevance of these studies, the field of Treg was abandoned for decades, up to 1995, when Sakaguchi and collaborators demonstrated that self-tolerance is regulated and maintained by suppressive T cells expressing the alpha-chain of interleukin 2 (IL-2) receptor (CD25). They showed that the inoculation of $CD4^{+}CD25^{-}$ non-suppressive lymphocytes in BALB/c nu/nu mice induces the development of autoimmune pathologies, and that the reconstitution of the suppressive $CD4^{+}CD25^{+}$ population prevents the development of those diseases. Since this discovery, numerous scientists focused their attention on this

particular T cell subset, investigating their roles in both physiological and pathological conditions. IL-2Rα (CD25), with IL-2Rβ (CD122) and γc (CD132), constitute the IL-2 receptor (IL-2R) [25]. The assemblage of IL-2R is a cascade process: at the beginning IL-2 binds to the CD25 subunit and this interaction causes a conformational modification in IL-2 structure, which allows the binding of CD122 to IL-2. Finally the γc subunit is included in the structure and renders it more stable [25]. IL-2 signaling is crucial for Treg development and, consequently, for peripheral homeostasis: in fact, mice with impaired IL-2/IL2R axis are affected by lethal autoimmune diseases mainly due to alteration in regulatory lymphocytes [25-27]. The intracellular signaling of IL-2 is primarily mediated by signal transducer and activator of transcription 5 (Stat5) [28]. It was also demonstrated that Treg cells constitutively express basal level of CD40L, so that, via CD40, DC (Dentritic Cells) is stimulated to produce an amount of IL-2 sufficient to ensure their survival. The relevance of CD40/CD40L axis in Treg cells biology was clearly observed in CD40 KO mice, in which Treg cells have lower proliferative and survival potential [29]. At the beginning of the 21st century, the discovery that the transcription factor forkhead box P3 (Foxp3), located on X chromosome, was mutated both in scurfy mice and in humans with immune dysregulation, polyendocrinopathy, enteropathy, and X-linked syndrome (IPEX) [30,31] led to the idea that this transcriptor factor could be involved in Treg development. In fact two years later Foxp3 was identified as the master regulator for Treg differentiation and functions [32]. It was demonstrated not only that in absence of Foxp3 the development of Treg is impaired, but also that the ectopic expression of Foxp3 in $CD4^+CD25^-$ naïve T cells endows them with suppressive functions [33,34]. Thanks to the generation of a knock-in Foxp3-GFP mice, in which the complete eGFP sequence was inserted in the first exon of the Foxp3 gene[35], it was possible to specifically identify

which cell subset expresses this transcription factor. It was found that Foxp3 is mainly expressed (>99,8%) by TCRβ$^+$ T cells, both in thymus and periphery, while macrophages, DC cells, NKT cells, NK cells, B lymphocytes and non hematopoietic cells are deficient in Foxp3 [35]. Foxp3 expression was confirmed in both CD25$^+$ and CD25$^-$CD4$^+$ T cells, whose suppressive ability was confirmed with different functional assays. In these studies, Foxp3 emerged as the most specific Treg marker, since CD25 and other surface molecules constitutively expressed by Treg cells, such as glucocorticoid-induced TNF receptor family-related gene (GITR), cytotoxic T lymphocytes-associated antigen 4 (CTLA-4) and OX40, are up-regulated also by activated Teff cells [35,36]. Treg cells were able to differentiate both in the thymus, from early common precursors, and in the periphery, from naïve CD4$^+$Foxp3$^-$ T cells in response to different immunosuppressive stimuli [37,38] the former are named natural Treg (nTreg), the latter induced (or adaptive) Treg (iTreg). In the thymus, Foxp3 expression is predominantly found at the stage of CD4$^+$ single positive (SP) cells, although a small percentage of cells expressing Foxp3 is found in the CD8$^+$ SP, CD4$^+$CD8$^+$ double positive (DP) and CD4$^-$CD8$^-$ double negative (DN) stages of thymic development[35]. Although the precise signals that guide nTreg differentiation, and consequently Foxp3 expression, are not yet well understood, the strong interaction between TCR and MHC/self-antigen presented by DC seems to have a crucial role in this process [38,39,32]. Also, IL-2 is a critical player in nTreg differentiation process [37]. It was demonstrated that mice with alteration in the IL-2/IL-2R pathway or in IL-2 signals transducers, like Stat5 and Jak3 [40], or treated with anti-IL-2 antibody [27] have fewer Treg cells, both in thymus and periphery, compared to wt mice. Furthermore, their Treg cells express Foxp3 at lower levels than wt Treg, resembling immature and non-suppressive regulatory T cells [41]. In 2008 Hsieh and Ferrar, in two distinct studies, using a two-step

model described nTreg development in the thymus as dependent on TCR and IL-2 signaling [42,43]. They proposed that nTreg precursors ($CD4^+CD25^{high}Foxp3^-TCR^+$), after receiving strong stimulation via TCR, further up-regulate CD25, thus becoming more sensitive and responsive to IL-2. This enhanced IL-2 responsiveness eventually promotes Foxp3 expression [42,43]. In addition to the stimuli provided by TCR and IL-2, other molecules were indicated as relevant in the nTreg differentiation process. Among these the costimulatory molecule CD28 [44] and the transcription factor NF-kB [45] were demonstrated to be necessary for nTreg differentiation. Unlikely nTreg, iTreg differentiate in periphery from naïve T cells in response to different stimuli. iTreg include different subsets of regulatory cells: Tr1, Th3 and Treg indistinguishable from nTreg [46]. When naïve T cells are in presence of high amount of IL-10 they acquire a suppressive phenotype and are defined Tr1 cells. These cells produce abundant IL-10, but do not secrete TGFβ. In contrast, Th3 cells are both induced by TGFβ and produce it themselves [47]. Both Tr1 and Th3 cells, even if endowed of suppressive functions, do not express Foxp3. Naïve lymphocytes can also differentiate in iTreg cells that are indistinguishable from nTregs when they are in the presence of TGFβ and receive insufficient antigen stimulation by immature/tolerogenic APC [46].

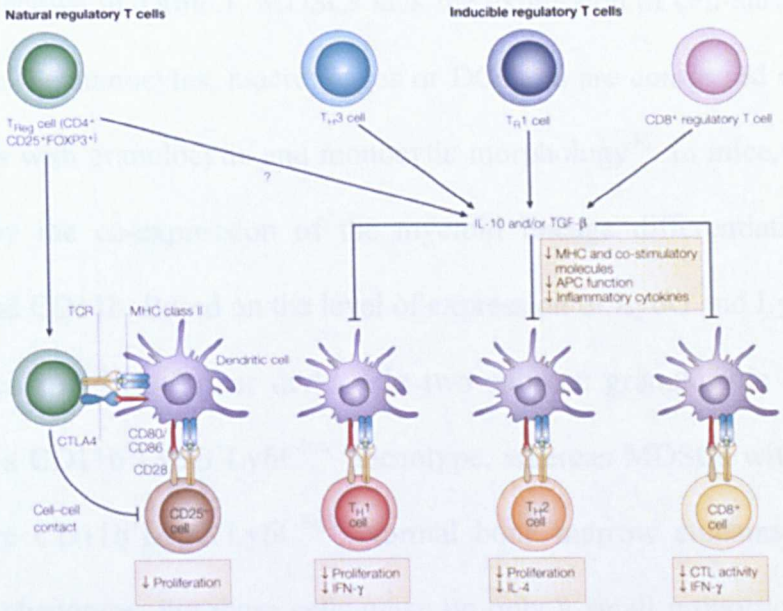

Fig.1.1.3.2 Representative scheme of Tregulatory cells subsets.
CD4+CD25+FOXP3+ (forkhead box P3) natural regulatory T cells (TReg cells) inhibit the proliferation of CD25- T cells. The mechanism of suppression seems to be multifactorial and includes cell–cell contact. CD4+CD25+ TReg cells express cytotoxic T-lymphocyte antigen 4 (CTLA4), which interacts with CD80 and/or CD86 on the surface of antigen-presenting cells (APCs) such as dendritic cells (DCs), and this interaction delivers a negative signal for T-cell activation. There is also some evidence that secreted or cell-surface transforming growth factor-B (TGF-B) or secreted interleukin-10 (IL-10) might have a role in suppression mediated by natural regulatory T cells. Image is adapted from Kingston H. G. Mills Nature Reviews Immunology 4, 841-855 (November 2004).

1.1.3.3 The biology of myeloid-derived suppressor cells

Myeloid-derived suppressor cells (MDSCs) are a heterogeneous population of cells that expands during cancer, inflammation and infection, and that has the ability to suppress T-cell responses. These cells constitute a unique component of the immune system that regulates immune responses in healthy individuals and in the context of various diseases. In addition to their suppressive effects on adaptive immune responses, MDSCs have also been reported to regulate innate immune responses by modulating the cytokine production of macrophages. Non-immunological functions of MDSCs have also been described, such as the promotion of tumor angiogenesis, tumor-cell invasion and metastasis. MDSCs are a heterogeneous population of activated immature myeloid cells that have been prevented from fully differentiating into mature cells. Schematic representation of different MDSCs population in distinct

tumor model is shown in **Table.1**. MDSCs lack the expression of cell-surface markers that are specific for monocytes, macrophages or DCs and are comprised of a mixture of myeloid cells with granulocytic and monocytic morphology[48]. In mice, MDSCs are characterized by the co-expression of the myeloid lineage differentiation antigens Ly6G, Ly6C and CD11b. Based on the level of expression of Ly6G and Ly6C antigens MDSCs in mice could be further divided in two subsets: granulocytic MDSCs (G-MDSCs) have a $CD11b^{+}Ly6G^{+}Ly6C^{low}$ phenotype, whereas MDSCs with monocytic morphology are $CD11b^{+}Ly6G^{-}Ly6C^{high}$. Normal bone marrow contains 20–30% of cells with this phenotype, but these cells make up only a small proportion (2–4%) of spleen cells and are absent from the lymph nodes in mice. In humans, MDSCs are most commonly defined as $CD14^{-}CD11b^{+}$ cells or, more narrowly, as cells that express the common myeloid marker CD33 but lack the expression of markers of mature myeloid and lymphoid cells and the MHC-class-II molecule HLA-DR. MDSCs have also been identified within a $CD15^{+}$ population in human peripheral blood. Different MDSC subsets are characterized on the basis of their immune phenotype (see **Table.2**). In healthy individuals, immature myeloid cells with the described phenotype comprise ~0.5% of peripheral blood mononuclear cells. MDSCs were first characterized in tumor-bearing mice and in patients with cancer. Inoculation of mice with transplantable tumor cells, or the spontaneous development of tumors in transgenic mice with tissue-restricted oncogene expression, results in a marked systemic expansion of these cells. In addition, up to a tenfold increase in MDSC numbers characterize the blood of patients with different types of cancer. In many mouse tumor models, as many as 20–40% of nucleated splenocytes are represented by MDSCs (in contrast with the 2-4% observed in tumor-free mice).

Tumor type	MDSC phenotype	References
Colon carcinoma (CT26, C26 cell lines); Melanoma (B16); fibrosarcoma (C3, 15-12 RM)	CD11b/Gr-1	Salvadori et al. 2000; Gabrilovich et al. 2001;Kusmartsev et al. 2000, 2005; Liu et al. 2003
Breast cancer (TS/A) and Lung cancer	CD11b/Gr-1/CD31	Young et al., 1996; Bronte et al. 1999; Bronte et al. 2000
Colon Carcinoma (C26-GM), Breast cancer (4T1), Sarcoma (MCA203)	CD11b/Gr-1/F4/80/ILRa	Gallina et al., 2006 ; Dolcetti et al., 2009
Timoma (EL-4), linfoma (EG7, BW-Sp3), Colon carcinoma (MCA26)	CD11b/Gr-1/F4/80/CD115^{int}	Kusmartsev et al., 2005; Movahedi et al., 2008; Huang et al., 2006
Ovarian cancer	CD11b/Gr-1/CD80	Yang et al., 2006
Transgenic mamary mouse model (BalbNeuT)	CD11b/Gr-1/CD31	Melani et al. 2003; Melani et al., 2007

Table.1 Immune phenotype of different MDSC recruited in transplantable or transgenic mouse tumor model.

Tissue	Cell population	Subpopulations	Phenotype
Mouse lymphoid organs	DCs	ND	CD11c$^+$F4/80$^-$GR1$^-$MHC-II$^+$
		Conventional DCs[a]	CD11c$^+$CD11b$^+$MHC-II$^+$CD205$^+$F4/80$^-$GR1$^-$CD115^{low}
		Plasmacytoid DCs	CD11c$^+$CD11b$^-$B220$^+$SIGLEC-H$^+$GR1$^+$F4/80$^-$
	Monocytes	ND	CD11b$^+$LY6C$^-$LY6G$^-$CD11c$^-$CD115$^+$
		Resident monocytes	CD11b$^+$LY6C^{low}LY6G$^-$CD115$^+$MHC-II$^-$F4/80^{hi}CD11c$^-$
		Inflammatory monocytes	CD11b$^+$LY6C^{hi}LY6G$^-$CD115$^+$MHC-II$^-$F4/80$^+$CD11c$^-$
	Macrophages	ND	F4/80$^+$CD11b$^+$GR1$^-$
		M1 macrophages	iNOS$^+$IL-12$^+$CD86$^+$MHC-II^{hi}
		M2 macrophages	CD206$^+$CD163$^+$CD36$^+$ARG1$^+$MHC-II^{low}IL-10$^+$IL-4Ra$^+$ FIZZ1$^+$YM1$^+$
	Granulocytes	Various	CD11b$^+$LY6G$^+$LY6C^{low}F4/80$^-$CD11c$^-$
Mouse tumours	MDSCs	ND	CD11b$^+$GR1$^+$CD11c$^-$F4/80$^{-/+}$CD124$^+$
		Polymorphonuclear MDSCs	CD11b$^+$GR1^{hi}LY6C^{low}LY6G$^+$CD49d$^-$
		Monocytic MDSCs	CD11b$^+$GR1^{int}LY6C^{hi}LY6G$^-$CD49d$^+$
Human blood	DCs[a]	ND	LIN$^-$HLA-DR$^+$BDCA1$^+$CD209$^-$
		Conventional DCs[a]	LIN$^-$CD11c$^+$CD11b$^+$CD33$^+$BDCA1$^+$BDCA3$^-$DC-SIGN$^+$
		Plasmacytoid DCs	LIN$^-$CD123$^+$BDCA2$^+$BDCA4$^+$
	Monocytes[a]	ND	CD14$^+$HLA-DR$^-$CD15$^-$
	Macrophages	ND	CD14$^+$CD68$^+$
		M1 macrophages	iNOS$^+$IL-12$^+$CD86$^+$HLA-DR$^+$
		M2 macrophages	CD206$^+$CD163$^+$CD36$^+$HLA-DR^{low}IL-10$^+$CD124$^+$
	Granulocytes[a]	ND	CD15$^+$CD14$^-$CD66b$^+$CD16$^+$
Human tumours	MDSCs[a]	ND	LIN$^-$CD11b$^+$HLA-DR$^-$CD33$^+$
		Polymorphonuclear MDSCs	In addition to the above MDSC phenotype, these cells express CD15 and/or CD66b
		Monocytic MDSCs	CD33$^+$CD14$^+$HLA-DR$^{low/-}$

ARG1, arginase 1; BDCA1, blood DC antigen 1 (also known as CD1c); BDCA2, blood DC antigen 2 (also known as CD303); BDCA3,

Table2. Phenotypic characterization used for isolated MDSC populations. Adapted from Gabrilovich DI, Review Immunology, 2012 Mar 22:12(4).

1.1.3.3.1 Soluble factors involved in MDSCs recruitment and function

Factors that induce MDSC expansion include cyclooxygenase-2 (COX2), prostaglandins, stem-cell factor (SCF), macrophage colony-stimulating factor (M-CSF), IL-6, granulocyte/macrophage colony-stimulating factor (GM-CSF) and vascular endothelial growth factor (VEGF) [49,50]. The signaling pathways in MDSCs that are triggered by the majority of these factors converge on Janus kinase (JAK) protein family members and downstream pathways that induce activation of transcription 3 (STAT3), which are signaling molecules involved in cell survival, proliferation, differentiation and apoptosis. STAT3 is arguably the main transcription factor that regulates the expansion of MDSCs. MDSCs from tumor-bearing mice have markedly increased levels of phosphorylated STAT3 compared with IMCs from naïve mice. Exposure of hematopoietic progenitor cells to tumor-cell-conditioned medium resulted in the activation of JAK2 and STAT3 and was associated with an expansion of MDSCs *in vitro*, whereas inhibition of STAT3 expression in hematopoietic progenitor cells abrogated the effect of tumor-derived factors on MDSC expansion. Ablation of STAT3 expression in conditional knockout mice or selective STAT3 inhibitors markedly reduced the expansion of MDSCs and increased T-cell responses in tumor-bearing mice. STAT3 activation is associated with increased survival and proliferation of myeloid progenitor cells, probably through upregulated expression of STAT3 target genes including B-cell lymphoma XL, (BCL-XL), cyclin D1, MYC and survivin. Accordingly, abnormal and persistent activation of STAT3 in myeloid progenitors has been shown to prevent their differentiation into mature myeloid cells and thereby promotes MDSC expansion. Recent findings suggest that STAT3 also regulates MDSC expansion by inducing the expression of S100A8 and S100A9 proteins. In addition, it has been shown that MDSCs also express receptors for these proteins on their cell

surface. S100A8 and S100A9 belong to the family of S100 calcium-binding proteins that have been reported to have an important role in inflammation. STAT3-dependent upregulation of S100A8 and S100A9 expression by myeloid progenitor cells prevented their differentiation and resulted in the expansion of MDSCs in the spleens of tumor-bearing and naïve S100A9-transgenic mice. By blocking the binding of S100A8 and S100A9 to their receptors on MDSCs *in vivo* with a carboxylated glycan-specific antibody reduced MDSC levels in the blood and secondary lymphoid organs of tumor-bearing mice. Although the mechanisms involved require further investigation, these studies suggest that S100A9 and/or S100A8 proteins have a crucial role in regulating MDSC expansion, and may provide a link between inflammation and immune suppression in cancer[48].

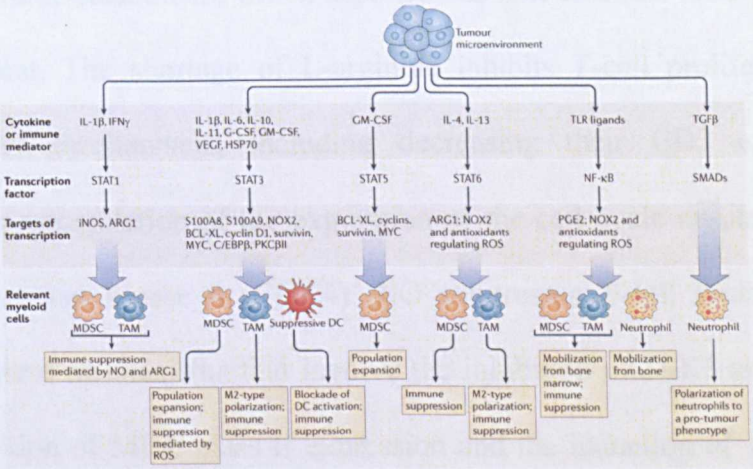

Fig. 1.1.3.3.1 Molecular mechanism affecting myeloid cells lineage proliferation and expansion.

Soluble factors, secreted by tumor microenvironment, affect myeloid cells progenitors as well as mature myeloid cells and regulate the activity of different transcriptional factors that in turn target the synthesis of different proteins. Adapted from Gabrilovich DI, Review Immunology, 2012 Mar 22:12(4).

1.1.3.3.2 Mechanisms of MDSC suppressive activity

A large number of studies have shown that the immunosuppressive functions of MDSCs require direct cell-to-cell contact, which suggests that they act either through cell-surface receptors and/or through the release of short-lived soluble mediators. Historically, the suppressive activity of MDSCs has been associated with the metabolism of L-arginine. L-arginine serves as a substrate for two enzymes: iNOS, which generates NO, and arginase, which converts L-arginine into urea and L-ornithine. MDSCs express high levels of both arginase and iNOS, and a direct role for both of these enzymes in the inhibition of T-cell functions is well established. Recent data suggest that there is a close correlation between the availability of arginine and the regulation of T-cell proliferation. The increased activity of arginase in MDSCs leads to enhanced L-arginine catabolism, which depletes this non-essential amino acid from the microenvironment. The shortage of L-arginine inhibits T-cell proliferation through several different mechanisms, including decreasing their CD3 expression and preventing their upregulation of the expression of the cell cycle regulators cyclin D3 and cyclin-dependent kinase 4 (CDK4). NO suppresses T-cell function through a variety of different mechanisms that involve the inhibition of JAK3 and STAT5 in T cells, the inhibition of MHC class II expression and the induction of T-cell apoptosis **(Fig.1.1.3.3.2)**.

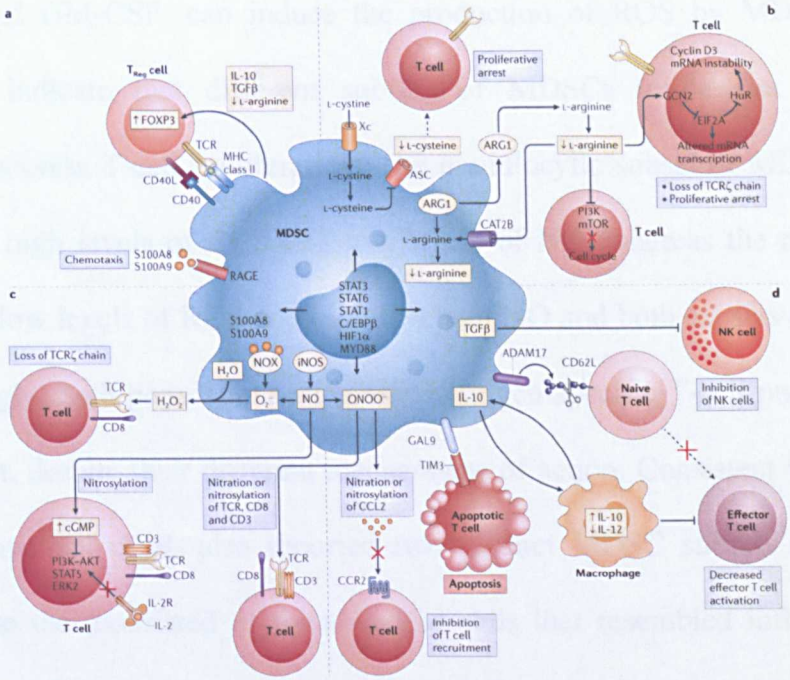

Fig. 1.1.3.3.2 Mechanisms of MDSC-dependent inhibition of T cells activity.

Myeloid-derived suppressor cells (MDSCs) inhibit efficient anti tumor T cell responses via different mechanisms. a) Tumor-associated MDSCs induce the development of regulatory T (Treg) cells or expand existing TReg cell populations trough the calcium-binding proteins S100A8 and S100A9 and S100A9. These effects are mediated in part through the activation of receptor for advanced glycation end-products (RAGE) and are responsible for the increased production of reactive oxygen species (ROS) by MDSCs. b) Tumor-associated myeloid cells deprive T cells of amino acids that are essential for their growth and differentiation. c) Tumor-associated myeloid cells release oxidizing molecules, such as hydrogen peroxide (H2O2) and peroxynitrite (ONOO–), that nitrosylate components of the T cell receptor (TCR) signaling complex. d) Tumor-associated myeloid cells can also interfere with T cell migration and viability. Adapted from Gabrilovich DI, Review Immunology, 2012 Mar 22:12(4).

1.1.3.3.3 Reactive oxygen species (ROS).

Another significant factor that contributes to the suppressive activity of MDSCs are ROS. Increased production of ROS has emerged as one of the main characteristics of MDSCs in both tumor-bearing mice and patients with cancer. Inhibition of ROS production by MDSCs isolated either from mice or patients with cancer completely abrogated the suppressive effect of these cells in vitro. Interestingly, ligation of integrins expressed on the surface of MDSCs was shown to contribute to increased ROS production following the interaction of MDSCs with T cells. In addition, several known tumor-derived factors, such as TGFβ, IL-10, IL-6, IL-3, platelet-derived growth

factor (PDGF) and GM-CSF, can induce the production of ROS by MDSCs[48, 51]. Recent findings indicate that different subsets of MDSCs might use different mechanisms to suppress T-cell proliferation. The granulocytic subset of MDSCs was found to express high levels of ROS and low levels of NO, whereas the monocytic subset expressed low levels of ROS and high levels of NO and both subsets expressed ARG1. Interestingly, both populations suppressed antigen-specific T-cell proliferation to an equal extent, despite their different mechanisms of action. Consistent with these observations, Movahedi et al. also reported two distinct MDSC subsets in tumor-bearing mice, one that consisted of mononuclear cells that resembled inflammatory monocytes and the other that consisted of polymorphonuclear cells that were similar to immature granulocytes[52]. Again, both populations were found to suppress antigen-specific T-cell responses, although by using distinct effector molecules and signaling pathways. The suppressive activity of the granulocytic subset was ARG1-dependent, in contrast to the STAT1- and iNOS-dependent mechanism of the monocyte fraction [53, 54].

1.1.3.4 Therapeutic targeting of MDSCs

1.1.3.4.1 Promotion of myeloid-cell differentiation

One of the most promising approaches to targeting MDSCs for therapy is to promote their differentiation into mature myeloid cells that do not have suppressive abilities. Vitamin A has been identified as a compound that can mediate this effect: vitamin A metabolites such as retinoic acid have been found to stimulate the differentiation of myeloid progenitors into DCs and macrophages. Mice that are deficient in vitamin A or that have been treated with a pan-retinoic-acid-receptor antagonist show an expansion of MDSCs in the bone marrow and spleen. Conversely, therapeutic concentrations of all-trans retinoic acid (ATRA) result in substantial

decrease in the presence of MDSCs in cancer patients and tumor-bearing mice [50, 55]. ATRA induced MDSCs to differentiate into DCs and macrophages *in vitro* and *in vivo*. It is probable that ATRA preferentially induces the differentiation of the monocytic subset of MDSCs, whereas it causes apoptosis of the granulocytic subset. [56].

1.1.3.4.2 Inhibition of MDSC expansion

MDSC expansion is regulated by tumor-derived factors. Different studies have focused on neutralizing the effects of these factors. SCF has been implicated in causing MDSC expansion and the inhibition of SCF-mediated signaling by blocking its interaction with its receptor, c-kit, decreased MDSC expansion and tumor angiogenesis. *Melani et* al showed that inhibition of matrix metalloproteinase 9 function in tumor-bearing mice decreased the number of MDSCs in the spleen and tumor tissues and resulted in a significant delay in the growth of spontaneous NeuT tumors in transgenic BALB/c mice. In this setting, the authors showed that both tumor and stromal cells express matrix metalloproteinase-9 (MMP-9), thereby increasing the levels of pro-MMP-9 in the sera of tumor-bearing mice. Treatment with amino-bisphosphonates (Zoledronic acid) impaired tumor growth, significantly decreased MMP-9 expression and the number of macrophages in tumor stroma, and reduced MDSC expansion both in bone marrow and peripheral blood by dropping serum pro-MMP-9 and VEGF [49]. The authors dissected the role of tumor-derived MMP-9 from that secreted by stromal leukocytes by transplanting bone marrow from MMP-9 knockout mice into BALB-neuT mice. Although bone marrow progenitor-derived MMP-9 had a major role in driving MDSC expansion, amino-bisphosphonate treatment of bone marrow chimeras further reduced both myelopoiesis and the supportive tumor stroma, thus enhancing tumor necrosis. Moreover, by reducing MDSC, amino-bisphosphonates overcame the tumor-induced immune suppression and

improved the generation and maintenance of antitumor immune response induced by immunization against the p185/HER-2. These data revealed that suppression of MMP-9 activity breaks the vicious circle linking tumor growth and myeloid cell expansion, and that amino-bisphosphonates trigger a specific MMP-9 inhibitory activity that may extend their application beyond their current usage. Very recently, it has been shown that amino-bisphosphonates could also inhibit MDSC activity by blocking the TGFβ axis that is crucial for their pro-tumoral function [57].

1.1.3.4.3 Inhibition of MDSC function

Another way to inhibit MDSCs is to block the signaling pathways that regulate MDSC production of suppressive factors. This might be achieved by targeting COX2. COX2 is required for the production of prostaglandin E2, which in 3LL tumor cells and mammary carcinoma has been shown to induce the upregulation of ARG1 expression by MDSCs, thereby inducing their suppressive function[58]. Accordingly, COX2 inhibitors were found to downregulate the expression of ARG1 by MDSCs, which improved antitumor T-cell responses and enhanced the therapeutic efficacy of immunotherapy [59]. Similarly, phosphodiesterase-5 inhibitors such as sildenafil are able to downregulate the expression of arginase and iNOS expression by MDSCs, thereby inhibiting their suppressive function in growing tumors[60]. This resulted in the induction of a measurable anti-tumour immune response and a marked delay of tumour progression in several mouse models. The main categories of targeting agents used to inhibit MDSC activity are listed in **Table.3**.

Therapeutic agents	Type of cancer tested	References
Therapeutic agents	Type of cancer tested	**Sinha P. Et al.** Prostaglandin E2 promotes tumor progression by inducing myeloid-derived suppressor cells. Cancer Res . 2007
Cyclooxygenase-2 inhibitors (SC58236)	Mammary carcinoma (mice)	**Melani C.et al.** Amino-biphosphonate-mediated MMP-9 inhibition breaks the tumor-bone marrow axis responsible for myeloid-derived suppressor cell expansion and macrophage infiltration in tumor stroma. Cancer Res 2007
Amino-biphosphonates	Mammary tumors (mice)	**Serafini P, et al.** Phosphodiesterase-5 inhibition augments endogenous antitumor immunity by reducing myeloid-derived suppressor cell function. J Exp Med 2006
Biphosphanate, sildenafil and tadalafil	Mammary carcinoma(mice) Colon Carcinoma (mice) Fibrosarcoma (mice)	**Pan PY, et al.** Reversion of immune tolerance in advanced malignancy: modulation of myeloid derived suppressor cell development by blockade of stem-cell factor function. Blood 2008
KIT-specific antibody	Colon Carcinoma (mice)	**De Santo C, et al.** Nitroaspirin corrects immune dysfunction in tumor-bearing hosts and promotes tumor eradication by cancer vaccination. Proc Natl Acad Sci U S A 2005
Nitroaspirin	Colon Carcinoma (mice)	**Kusmartsev S, et al.** All-trans-retinoic acid eliminates immature myeloid cells from tumor-bearing mice and improves the effect of vaccination. Cancer Res 2003; **Mirza N, et al.** All-trans-retinoic acid improves differentiation of myeloid cells and immune response in cancer patients. Cancer Res 2006
All-trans retinoic acid	Sarcoma, colon carcinioma (mice) Metastatic renal cell carcinoma(human)	**Lathers D. et al.** Phase IB study to improve immune responses in head and neck cancer patients using escalating doses of 25-hydroxyvitamin D3. Cancer Immunol Immunother 2004
Vitamin D3	Head and neck cancer (humans)	**Suzuki E. Et al.** Gemcitabine selectively eliminates splenicGr-1+/CD11b+ myeloid suppressor cells in tumor-bearing animals and enhances antitumor immune activity. Clin Cancer Res 2005
Gemcitabine	Lung cancer (mice)	**Fricke I, et al.** Vascular endothelial growth factor-trap overcomes defects in dendritic cell differentiation but does not improve antigen-specific immune responses. Clin Cancer Res; **Kusmartsev S, et al.**Oxidative stress regulatesexpression of VEGFR1 in myeloid cells: link to tumor-induced immunesuppression in renal cell carcinoma. J Immunol 2008
VEGF–trap* VEGF-specific antibody (avastin)	Solid tumors (humans) Metastatic renal cell cancer (humans)	**Diaz-Montero CM, et al.** Increased circulating myeloid-derived suppressor cells correlate with clinical cancer stage, metastatic tumor burden, and doxorubicin-cyclophosphamide chemotherapy. Cancer Immunol Immunother 2009;

Table 3. Pharmacological regulation of MDSC in cancer.

1.2 Cell intrinsic and environmental-mediated drug resistance.

Resistance to tumor therapy can be subdivided into two broad categories: intrinsic (or *de novo*) and acquired resistance. Acquired resistance develops over time as a result of sequential genetic changes that ultimately culminate in complex therapy-resistant phenotypes. One form of *de novo* drug resistance is the environment-mediated drug resistance (EMDR), in which tumor cells are transiently protected from apoptosis induced by either chemotherapy, radiotherapy or receptor-mediated cell death.

1.2.1 Enviromental-mediated drug resistance (EMDR)

This form of drug resistance arises from an adaptive reciprocal cross-talk between tumor cells and the surrounding stroma [61]. EMDR is rapidly induced by signaling events that are initiated by factors present in the tumor microenvironment and can be subdivided into two categories: soluble factor-mediated drug resistance (SFM-DR), which is induced by cytokines, chemokines and growth factors secreted by fibroblast-like tumor stroma; and cell adhesion-mediated drug resistance (CAM-DR), which is mediated by the adhesion of tumor cell integrins to stromal fibroblasts or to components of the extracellular matrix (ECM), such as fibronectin, laminin and collagen as shown in **Table.4**. Notably, EMDR is transient and appearing only when tumor cells are in contact with the microenvironment, and reverts rapidly when tumor cells are removed from the microenvironment.

Tumor	Matrix	Cytotoxic	Mechanism	Reference
SFM-DR				
MM U266		Fas ligation	IL-6 via Bcl-XL up-regulation	Catlett-Falcone et al. (22)
MM cell clones from patient specimens		Dexamethasone	IL-6	Frassanito et al. (24)
MM 8226, H-929, ANBL-6, MM1.S, KAS-6/1		Bortezomib	IL-6 via STAT1 and STAT3	Voorhees et al. (25)
Ovarian cell lines	BMS	Paclitaxel	IL-6 via STAT3	Duan et al. (32)
Prostate cancer, PC-3		Etoposide, cis-platinum	gp130	Borsellino et al. (73)
CAM-DR (epithelial)				
SCLC NCI-H82	FN, collagen, BMS	Etoposide	SDF-1 up-regulated VLA-4	Hartmann et al. (18)
Murine primary endothelial tumors	FN, collagen, laminin	Etoposide	α5, β3, β1	Hoyt et al. (50)
SCLC H345	FN, laminin	Etoposide, radiation	β1	Hodkinson et al. (51)
Breast MDA-MB-231, 435	FN, collagen	Paclitaxel, vincristine	β1, Akt	Aoudjit et al. (52)
SCLC H69, H345, H510	FN	Etoposide, cis-platinum, cyclophosphamide	β1	Sethi et al. (60)
Normal epithelial		Fas ligation	c-FLIP up-regulation	Aoudjit et al. (66)
CAM-DR (hematopoietic)				
AML, CML, and CLL cell lines, and primary CLL	BMS	Cytarabine	CXCR4	Zeng et al. (16)
MM 8226	FN	Doxorubicin, melphalan	VLA-4, VLA-5 (α5β1)	Damiano et al. (53)
CML K562	FN	AG957, STI-571, radiation	VLA-5 (α5β1)	Damiano et al. (54)
CML K562	FN	Imatinib, mitoxantrone	β1, Bim down-regulation	Hazlehurst et al. (64)
MM 8226	FN	Etoposide	β1, p27 up-regulation	Hazlehurst et al. (56)
Histiocytic lymphoma U937	FN	Mitoxantrone, doxorubicin, etoposide	β1	Hazlehurst et al. (57)
MM 8226	FN	Melphalan	Bim down-regulation	Hazlehurst et al. (59)
MM U266	BMS	Melphalan, mitoxantrone	p21 up-regulation	Nefadova et al. (61)
MM 8226, histiocytic lymphoma U937	FN	Fas ligation	c-FLIP redistribution	Shain et al. (65)

Abbreviations: SFM-DR, soluble factor–mediated drug resistance; CML, chronic myelogenous leukemia; CLL, chronic lymphocytic leukemia; SCLC, small cell lung cancer; MM, multiple myeloma; FN, fibronectin.

Table.4 Schematic representation of EMDR mechanisms exerted by different tumors Meads MA, Clin Cancer Res 14; 2519 (May, 2008).

1.2.2 CAM-DR (Cell-adhesion mediated drug resistance)

CAM-DR is particularly involved in conferring drug resistance in hematologic tumors in response to various chemotherapeutic agents [62]. CAM-DR mostly depends on the engagement of integrin receptors as the adhesion mediated by these receptors has been shown to influence cell survival and prevent programmed cell death. An example of the role of CAM-DR in drug resistance comes from multiple myeloma. This disease is mostly incurable mainly because of CAM-DR. In this context, Damiano et al have shown that human myeloma cells after doxorubicin or melphalan treatment increase the expression of VLA-4 (alpha4beta1) and VLA-5 (alpha5beta1) integrin that are fibronectin (FN) receptors, thus increasing cell adhesion and conferring drug resistance. The induction of VLA-4 and VLA-5 was reversible and reduced by drug removal from the culture medium. In another study performed on multiple myeloma, Noborio-Hatano K et al (oncogene 2009) performed a functional screening by using short hairpin RNA (shRNA) to define the molecule(s) responsible for CAM-DR of multiple myeloma [63]. Using four myeloma cell lines (KHM-1B, KMS12-BM, RPMI8226 and U266) and primary myeloma cells, they identified CD29 (beta1-

integrin), CD44, CD49d (alpha4-integrin, a subunit of VLA-4), CD54 (intercellular adhesion molecule-1 (ICAM-1)), CD138 (syndecan-1) and CD184 (CXC chemokine receptor-4 (CXCR4)) as major adhesion molecules expressed in multiple myeloma. shRNA-mediated knockdown of CD49d but not CD44, CD54, CD138 and CD184 significantly reversed CAM-DR of myeloma cells to vincristine, doxorubicin and dexamethasone. Interestingly, it was also showed that bortezomib was relatively resistant to CAM-DR because of its ability to specifically downregulate CD49d expression. This property was unique to bortezomib and was not observed in other anti-myeloma drugs. Pretreatment with bortezomib was able to ameliorate CAM-DR of myeloma cells to vincristine and dexamethasone, a finding suggesting that a combination of bortezomib and conventional anti-myeloma drugs might be useful in overcoming CAM-DR of MM. EMDR also plays an important role in determining the extent of tumor response to therapies in solid tumors. In small cell lung cancer (SCLC), β1-mediated adhesion of tumor cells to ECM protects tumor cells from chemotherapy-induced apoptosis by activating a tyrosine kinase pathway [64]. Similarly to SCLC also breast carcinoma [65] chemoresistance involves integrin activation. In humans, β1 integrin expression is also a prognostic factor for metastatic melanoma[66].

1.2.3 SFM-DR (Soluble factor mediated drug resistance)

SFM-DR depends on soluble factors released in the tumor microenvironment. Interestingly, a dynamic interaction between tumor cells and their stroma is required to produce the soluble factors that mediate drug resistance as Nefedova et al [55] reported that conditioned medium from stromal cells provided protection only if it was collected from cells grown in co-culture with myeloma cells. Consistent with this observation, IL-6 and stromal cell-derived factor 1 (SDF-1), the most widely studied mediators of SFM-DR, are known to mediate resistance to various chemotoxic compounds in *in*

vitro EMDR models of hematological and epithelial cancer [67, 68, 69, 70, 71] and are produced at higher levels in tumor-associated stroma than in normal bone marrow stroma. Recently, Perez et al. extended these findings by using immortalized stromal fibroblasts and conditioned medium from patient bone marrow stroma to show that paracrine interaction between myeloma cells and stroma is also required to prevent myeloma cell lines from binding to death receptor for TNF-related apoptosis-inducing ligand. IL-6 was found to contribute to this effect by increasing the expression of the anti-apoptotic protein FLIP. An earlier work by Catlett-Falcone et al. demonstrated that IL-6-induced signal transducer and activator of STAT-3 protects myeloma cells from FAS-mediated apoptosis by upregulating transcription of the anti-apoptotic molecule BCL-X_L. [68].

1.2.4 EMDR targeting as a potential way to overcome drug resistance.

Cancer cells and their associated stroma coexist in an evolving ECM and soluble factor milieu that is molded by their interaction. Reciprocal integrin- and soluble factor-mediated signaling interactions between these two groups of cells induce a transient EMDR phenotype in tumor cells, protecting them from therapy until more complex acquired drug resistance phenotypes can develop. Therefore, stroma-induced signaling pathways associated with the tumor microenvironment are increasingly being targeted by therapeutic approaches intent on combating environment-mediated drug resistance. In this context, Moshaver et al. [72] demonstrated that chemotherapy decreased the ability of BM stromal cells to protect primary acute AML cells from chemotherapy. Using stromal fibroblasts that were pretreated with chemotoxics, they showed that treatment of stroma reduced the ability of primary AML and AML cell lines to proliferate and survive subsequent exposure to chemotherapy, suggesting that these cells must also need to develop resistance to therapy to ensure tumor survival. An

earlier study by Spiotto et al. suggested that targeting tumor stroma with immunotherapy in vivo could be an effective strategy by showing that bystander elimination of subpopulations of antigen loss variant tumor cells by cytotoxic T cells was possible only when parental tumor cells expressed sufficient amounts of antigen to be cross-presented by tumor stroma cells, allowing stromal cells themselves to be targeted for killing by T cells [73]. Later work by Zhang et al. from the same group showed that irradiation or chemotherapy could also increase cytotoxic T cell killing of established tumors by causing enough antigen to be released from tumor cells to target antigen-presenting stroma for destruction. They later verified the important role of stroma in this effect by showing that cytotoxic T cell killing of only major histocompatibility complex (MHC)-restricted tumor stroma causes long-term inhibition of tumor growth. [74]. Collectively, these data illustrate the important role of stroma in tumor survival and resistance to therapy and suggest that directly targeting stroma and stroma-mediated pathways might be an effective means of tumor therapy.

1.2.5 Epithelial to mesenchymal transition and drug resistance

Increasing evidence suggest that epithelial to mesenchymal transition (EMT) is associated with increased drug resistance. The EMT is a highly coordinated process and a multistep event during which epithelial cells lose epithelial characteristics and assume properties that are typical of mesenchymal cells. Cells that have undergone EMT can migrate out of their epithelial layers to distant points and either remain mesenchymal or redifferentiate into epithelial cells by a process known as mesenchymal-epithelial transition (MET). This process also been involved in decreasing the tumor grade. In human breast cancer, Triulzi et al. have identified a subgroup of breast tumors up-regulating EMT genes in both neoplastic and adjacent stromal cells, and showing increased tumor grade [75] and drug resistance. EMT is best

characterized for its role in embryonic development; induction of EMT is necessary for formation of the mesoderm and endoderm during gastrulation and for delamination of the neural crest. Following EMT, disseminated mesenchymal cells act as progenitors for many different tissue types. A number of distinct molecular processes, intrinsic to the tumor cell, are engaged in order to initiate an EMT and enable it to reach completion, including activation of transcription factors, expression of specific cell-surface proteins, reorganization and expression of cytoskeletal proteins, production of ECM-degrading enzymes, and changes in the expression of specific microRNAs. A new concept is that besides the cell-intrinsic molecular events leading to EMT, also the immune cells present in the tumor microenvironment might promote EMT. In this context, recent findings have revealed that activated CD8 T cells can stimulate mammary epithelial tumor cells to undergo epithelial-mesenchymal transition (EMT) and to become breast cancer stem cells (BCSC) acquiring greatly increased tumorigenic capability and chemotherapeutic resistance [76]. Different myeloid cells have been also involved in EMT: in colon cancer models, BM-derived CD11b+Jag2+ cells have been shown to promote EMT through a Notch dependent pathway which can be blocked either with neutralizing antibodies, or by decreasing the tumor-infiltrating CD11b+Jag2+ cells [77] **(Fig.1.2.5)**. Using a spontaneous murine model of melanoma, it has also been showed that MDSC infiltrates the primary tumor and actively promotes cancer cell dissemination by inducing epithelial-mesenchymal transition (EMT). CXCL5 was found to be the main chemokine attracting MDSC to the primary tumor, whereas TGF-β, EGF, and HGF were the signaling pathways involved in this process[78].

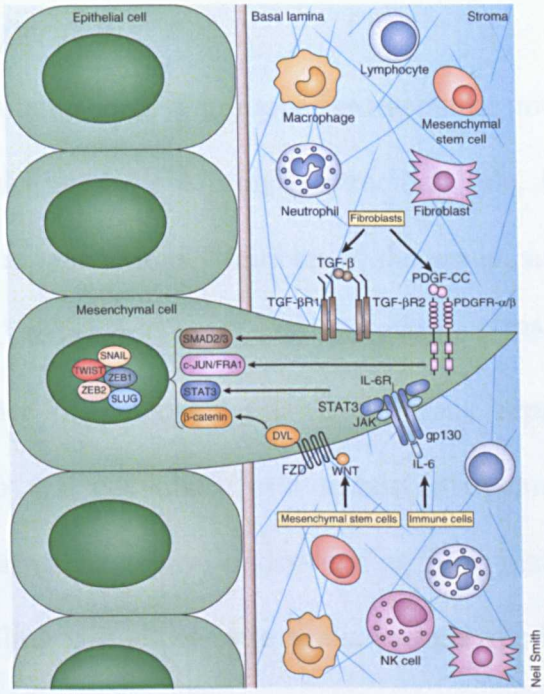

Fig 1.2.5 Tumor plasticity is regulated by a connection between extracellular signal and EMT transcription factors.

TGF-β, WNT proteins, platelet-derived growth factors (PDGFs) and interleukin-6 (IL-6), HGF, EGF arising from autocrine or paracrine signaling networks can activate intracellular signaling factors that influence the activation of transcriptional factors involving in EMT program from Wai Leong Tam and Robert A. Weinberg, Nature Medicine (November 2013).

1.3.Matricellular proteins

Matricellular proteins form a group of extracellular matrix (ECM) proteins, unlike collagens, that do not have a primary structural role, but rather function as modulators of cell-matrix interactions. Members of the group, such as thrombospondin (TSP)-1,TSP-2, SPARC, tenascin (TN)-C, and osteopontin (OPN), have been shown to participate in a number of processes related to tissue repair [79]. Tumor stroma continuously adapts to and coevolves with tumor enlargement through processes mimicking wound healing. Certainly, understanding how matricellular proteins are involved in wound healing will allow us to evaluate their role in cancer and probably to investigate the link of inflammation and cancer. SPARC (Secreted Protein Acidic and Rich in Cysteine, also known as osteonectin or BM-40) is a 32-kDa multifunctional glycoprotein that belongs to the matricellular group of proteins. It modulates cellular interaction with the extracellular matrix (ECM) by its binding to structural matrix proteins, such as collagen and vitronectin, and to surface receptors and growth factors. Its expression is spatially and temporally confined during embryogenesis, tissue remodeling, repair and tumorigenesis. SPARC functions to regulate cell–matrix interactions and thereby influences many important physiological and pathological processes. [80]

1.3.1 Structure and properties of SPARC

SPARC is a 32 kD protein, but the secreted form migrates at 43 kD on SDS-PAGE, in part due to the addition of carbohydrate [81]. The vertebrate SPARC gene encodes proteins of 298–304 amino acids (aa), including three distinct modules, as shown in Fig 1.3.1 Module I (aa 3–51), previously termed domain I [82], is encoded by exons 3 and 4, is highly acidic, and binds 5–8 Ca2+ ions with a Kd of 10-3–10-5 M. The structure of this module has not yet been solved. This NH2-terminal domain contains immunodominant epitope(s) and binds to hydroxyapatite. It is the major immunological epitope of SPARC and also the region that is the most distinct from the other members of the SPARC gene family. Therefore, antibodies against SPARC have not been found to cross-react with, or recognize, the SPARC-like protein [83]. Module II (aa 52–132) is encoded by exons 5 and 6 and contains 10 Cys and an N-linked complex carbohydrate. The sequence encodes a structure that is homologous to a repeated domain in follistatin, a protein that binds to activin and inhibin, members of the TGF- superfamily, and agrin, which induces aggregation of nicotinic acetylcholine receptors. Module II also contains bioactive peptides that have different effects on endothelial cells. Peptide 2.1 (aa 55–74), part of the EGF-like hairpin, inhibits the proliferation of endothelial cells and peptide 2.3 (aa 113–130), containing the Cu2+ binding sequence GHK and part of the Kazal protease inhibitor-like region, stimulates endothelial cell proliferation and angiogenesis [84]. Module III (aa 133–285, exons 7–9), formerly designated as the EC module, like Module II contains a sequence designated peptide 4.2 (aa 254–273), which has been shown to bind to endothelial cells and to inhibit their proliferation [85, 86]. The fibril-forming collagen types I, III, and V and the basement membrane collagen type IV bind to the EC module of SPARC in a Ca2+-dependent fashion.

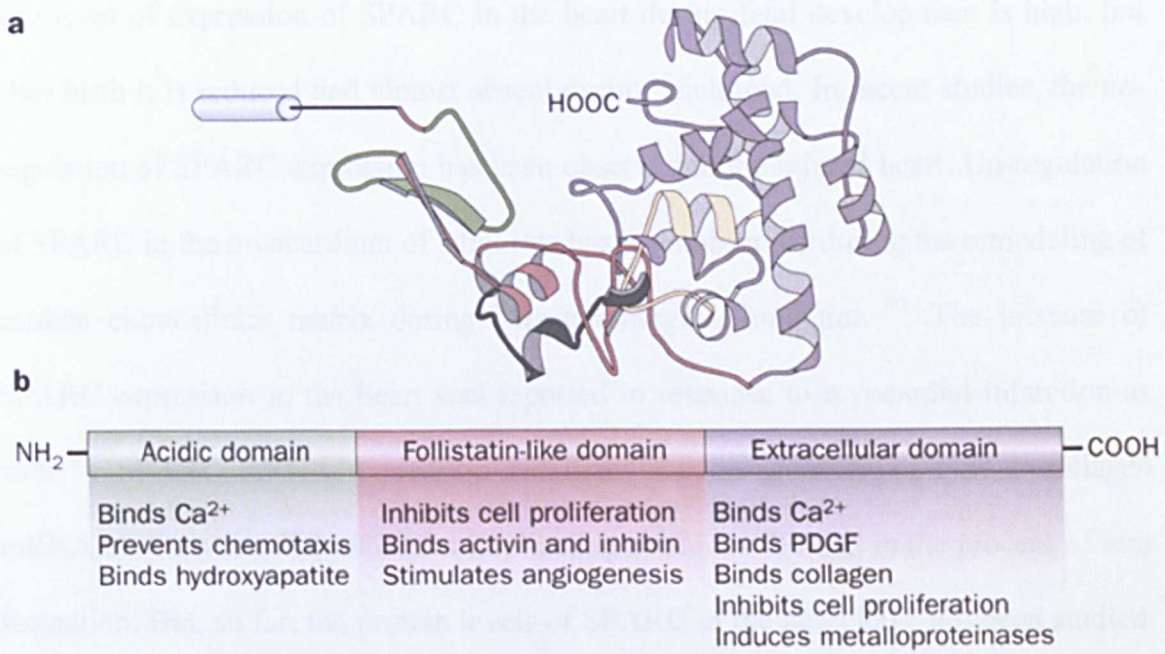

Fig.1.3.1 Crystallographic structure of human SPARC.

a. *The acidic domain is shown in green, the follistatin-like domain in red and the extracellular domain in purple.* ***b.*** *Functional properties of the three protein domains. Abbreviation: SPARC, secreted protein acidic and rich in cysteine (also known as osteonectin or BM-40). From Bradshaw, A. D. & Sage, E. H. J. Clin. Invest. 107, 1049–1054 (2001).*

1.3.2 Expression of SPARC

SPARC is expressed at high levels in breast tissue, is distributed widely in many other tissues and cell types, and is associated generally with remodeling tissues, e.g., tissues undergoing morphogenesis, mineralization, angiogenesis, and pathological responses to injury and tumor genesis. [87]. Although SPARC KO mice are born without obvious abnormalities, targeted disruption of the SPARC locus in mice has shown that SPARC is important for lens transparency, as SPARC-null mice develop cataracts shortly after birth. An impaired wound healing in mice deficient in SPARC has been reported [88]. Additionally, over expression of SPARC in nematodes also resulted in developmental abnormalities including an uncoordinated (Unc) phenotype in the F1 generation. Furthermore, worms overexpressing SPARC did not produce any viable offspring [89]. These results along with the data from SPARC-null mice, indicate that the

appropriate and regulated expression of SPARC is necessary for normal development. The level of expression of SPARC in the heart during fetal development is high, but after birth it is reduced and almost absent during adulthood. In recent studies, the up-regulation of SPARC expression has been observed in the injured heart. Up-regulation of SPARC in the myocardium of adult rats has been observed during the remodeling of cardiac extracellular matrix during beta adrenergic stimulation [90]. The increase of SPARC expression in the heart was reported in response to myocardial infarction as well [91]. SPARC mRNA expression paralleled the upregulation of type 1 collagen mRNA after myocardial infarction implicating a role for SPARC in the process of scar formation. But, so far, the protein levels of SPARC in the heart have not been studied. Interestingly, cardiac myocytes plated on fibronectin (FN) showed elevated expression of SPARC *in vitro*. Whether the absence of SPARC may lead to an altered formation of collagen in the normal heart is yet unknown.

1.3.3 Interaction of SPARC with ECM proteins

Vitronectin. SPARC binds preferentially to the multimeric form of vitronectin (mVN) rather than to the circulating plasma form, a fact indicates that these interactions are preferentially taking place within the ECM environment rather than in the soluble phase. Interestingly, active PAI-1 is able to induce directly the conformational transition from plasma to multimeric vitronectin. Moreover, contact with the vitronectin binding site of PAI-1 is required because the monoclonal antibody 2C8 prevented ECM protective activity of PAI-1. Finally, SPARC was demonstrated to induce PAI-1 production in some cells [92]. Vitronectin/PAI-1 complexes are linked to SPARC collagen type I-rich sites and additional observations also indicate that PAI-1 itself might have a major impact on the motility of cells. Competition studies with basic vitronectin-derived peptides, heparin and heparan sulphate, also demonstrated

that the heparin-binding site of multimeric vitronectin is an essential region for the interaction with SPARC. In contrast, plasma vitronectin, in which this region is cryptic, displayed virtually no binding to SPARC. This result indicates that the conformational transition of plasma vitronectin to the multimeric form is required for binding with SPARC. The fact that interactions with vitronectin can be inhibited by salt concentrations greater than 0.2 M and by Ca2+ ions (0.5±1 mM) indicates the involvement of Ca2+ binding acidic domain(s) of SPARC. These results agreed with observation that the complete or partial removal of domains III and IV (EC module), or a synthetic EF-hand, decreased the binding of SPARC to vitronectin. On the other hand, the partial deletion of domain I enhanced binding, probably because conformational changes in SPARC due to the internal binding of domain I to the C-terminal portion are able to affect its interaction with vitronectin.

Collagens. The binding of SPARC to collagen depends on SPARC N-glycosylation at Asn 99, a specific and highly conserved site [93 94 95]. Interestingly, BM-40 from bone and platelets migrates differently in sodium dodecyl sulphate-polyacrylamide gel electrophoresis (SDS-PAGE), and enzymatic digestion with N-glycosidase F and endoglycosidase H showed that the difference is due to variable N-glycosylation with the bone-derived protein carrying predominantly high-mannose oligosaccharides, whereas those on platelet BM-40 are mainly of the complex type[96]. The differences in the type of N-glycans have functional consequences, as the bone form of the protein binds to collagen I, III, and V, whereas the platelet form does not. The removal of N-linked oligosaccharides by N-glycosidase F treatment increases the affinity of BM-40 from both bone and platelets to collagen V to reach equal levels of affinity. Site-directed mutagenesis shows that only the glycosylation of Asn99 affects collagen binding [97]. The collagen affinity of BM-40 is of great functional importance.

The collagen affinity of BM-40 is of great functional importance. In fact, the collagen I-deficient Mov-13 mouse line does not retain SPARC in the extracellular matrix [98] and dermal collagen fibrils in SPARC-null mice have a decreased diameter and a reduced tensile strength [99]. Not only glycosylation but other forms of post-translational modification of SPARC modulate the collagen affinity. Limited proteolytic cleavage of SPARC occurs in tissues, and treatment with matrix metalloproteinases increases its affinity for collagens 7–20-fold due to a cleavage in helix {alpha}C[100] in the extracellular calcium-binding [101]. Indeed, deletion of helix {alpha}C in recombinant SPARC gives a similar increase in binding affinity, and X-ray crystallography shows that this is due to the removal of a steric constraint on the binding site, which was mapped to a loop between the two EF-hands in the extracellular calcium-binding domain [102]. One important aspect is that a different type of N-glycosylation can occur in SPARC, and it has been demonstrated that different types of N-glycosylation can affect in a different manner various cell behaviors. In experimental tumor models the most common aberrant N-glycosylations are an increase in terminal sialylation and a shift to more highly branched N-linked oligosaccharides; it has been shown that the metastatic potential of tumor cells correlates with these changes [103,104,105]. Glycosylation also has been implicated in the regulation of CD44-mediated cell binding of hyaluronan. Interestingly, N-linked oligosaccharides can both enhance and reduce the CD44 affinity for hyaluronan depending on the specific structure of the glycan [106]. Regarding SPARC certain work performed by Kaufmann and colleagues in 2001 demonstrated a highly variable N-glycosylation of SPARC derived from different sources [107]. The authors speculated that the type of glycosylation is dependent on the glycosyl transferase repertoire of the producing cell type, rather than being directed by the acceptor protein. It is known that SPARC binds to collagen, but the functional

significance of the interaction of SPARC with collagen in tissues is not clear. Collagen may serve as a storage site for SPARC in the ECM or may directly modulate the activity of SPARC, e.g. its counteradhesive or anti-proliferative functions. The fact that proteolytic cleavage of SPARC results in a higher affinity for collagen indicates that collagen is a potentially important ECM ligand for SPARC [108]. Interestingly, SPARC has been shown to increase the production and activity of MMPs [109,110]. These results suggest that SPARC might participate in an autocrine or paracrine positive feedback loop. For example, SPARC stimulates the expression and activity of MMP-2 and in turn, MMP-2 proteolytically cleaves SPARC, which increases the affinity of SPARC for collagen and presumably its localization to the basement membrane, an efficacious site for an anti-proliferative and counteradhesive protein.

1.3.4 Interaction of SPARC with growth factors and cytokines

Binding to cytokines is one of the major characteristics of SPARC. SPARC regulates the activity of at least three growth factors that are important for vascular homeostasis. SPARC was shown to bind the PDGF (platelet derived growth factor) dimers AB and BB, but not AA. PDGFs are a family of growth regulatory molecules capable of inducing directed cell migration, proliferation and altered cellular metabolism. The specific interaction of SPARC with the B-chain prevent binding of PDGF to its receptors on smooth muscle cells. The affinity of SPARC for this important growth factor could regulate the availability of PDGF dimers and thus affect the biological response to PDGF and may consequently control proliferative repair processes. (Raines, Lane et al. 1992) SPARC interaction with PDGF and its ability to inhibit cell proliferation induced by PDGF indicate the importance of SPARC in angiogenesis [111]. Because both SPARC and PDGF are found in platelet granules, and expression of both proteins is elevated in atherosclerotic plaque and in models of

kidney disease, it has been proposed that SPARC might regulate the activity or distribution of PDGF *in vivo* [112]. In addition to PDGF, VEGF, and bFGF, SPARC can also modulate the activity of TGF-β. TGF-β is an important and widely-distributed growth factor, which is associated with the rapid remodeling of connective tissues and has been shown to regulate the expression of extracellular matrix proteins [113] SPARC can upregulates TGF-ß1 expression (mRNA and protein) in cultured mouse mesangial cells [114] SPARC-null mesangial cells also showed significantly decreased synthesis of TGF-ß1 mRNA, and addition of SPARC to SPARC KO cells in culture restored the expression of TGF- ß to levels typical of WT cells [114]. Given the coincidence of TGF-ß and SPARC in embryonic development and wound healing [115] the modulation of SPARC by TGF-ß and that of TGF-ß by SPARC are likely to be significant. By contrast, TGF-ß had been shown to regulate the expression of SPARC in fibroblasts [116]. Whether TGF-ß and SPARC interact directly or not is unknown, but it is clear that both factors participate in a feedback loop that influences their production. There is considerable circumstantial evidence to indicate that SPARC interacts with TGF-ß and/or affects proteins of the TGF-ß signaling pathway.

1.3.5 SPARC as master stroma regulator

Because of its ability to promote collagen assembly and deposition, SPARC is now considered a key stroma regulator in both tumors and fibrotic diseases. By using a bone-marrow transplantation (BMT) strategy, Sangaletti et al [117], have demonstrated that SPARC helps organize the basement membrane structure that is required for tumor progression. Mammary carcinoma cells that express high levels of SPARC grow into solid tumors in WT mice. These tumors have a well-structured stroma that comprises collagen type IV. In *Sparc*-null mice, however, the same tumors grew much more slowly. Tumors were smaller and less vascularized, contained necrotic areas and were

devoid of collagen type IV-positive structures such as basement membranes of tumor lobules and blood vessels. So, SPARC production by the tumor environment, rather than the cancer cells themselves, is required for tumor progression. In this paper Sangaletti et al. also showed that when SPARC-expressing bone-marrow cells were transplanted into null mice, tumors grew at the same rate as those in WT mice. The transplanted bone-marrow-derived leukocytes localized to the tumors, where they expressed SPARC, allowing the tumor to develop a well-organized stromal compartment. Finally, the different immune cell infiltration characterizing tumor from wt or *Sparc*-null mice have also suggested that the lack of SPARC production in the tumor environment beside preventing proper basement-membrane assembly might also protect the tumor from immune-cell infiltration. This finding together with the increased contact-hypersensitivity response in *Sparc*-null mice [118] characterized by thin collagen in the dermis, prompted the hypothesis that a different ECM composition might induce a different immune response. The immune modulatory role of the ECM and of SPARC was also investigated in melanoma. By injecting human melanoma cell lines in nude mice in which SPARC expression was knocked down using an antisense RNA or shRNA led to tumor was rejected through a mechanism PMN dependent [119]. Loss of SPARC expression in melanoma cancer cell lines induced PMN recruitment and tumor rejection through a mechanism that involved the release of chemotactic factors like IL-8 and leukotrienes [120]. In the context of pulmonary fibrosis, Sangaletti et al. demonstrated that SPARC distinctly regulates inflammation and collagen deposition depending on its cellular origin. Reciprocal *Sparc*-null and WT bone marrow chimeras revealed that SPARC expression in host fibroblasts is required and sufficient to induce collagen fibrosis in a proper inflammatory environment. Accordingly, *Sparc*-null >WT chimeras showed exacerbated inflammation and fibrosis due to the inability of *Sparc*-

null macrophages to downregulate tumor necrosis factor production because of impaired responses to tumor growth factor-β. The use of bone marrow cells expressing a dominant-negative form of tumor growth factor-β receptor type II under the monocyte-specific CD68 promoter as a decoy, phenocopied Sparc-null donor chimeras pointing to a dual role of SPARC in oppositely influencing the outcome of fibrosis [121]. Such a dual role of SPARC has been observed in bone-marrow fibrosis [122]. In this setting, Tripodo et al. have demonstrated that SPARC contributes to the development of significant bone marrow fibrosis in a model of thrombopoietin-induced myelofibrosis. They found that SPARC deficiency in the radioresistant BM stroma compartment impairs myelofibrosis but, at the same time, associates with an enhanced reactive myeloproliferative response to thrombopoietin. In agreement with these with this pre-clinical data in humans, SPARC has been implicated in the pathogenesis of several fibrotic disorders, such as adipose tissue fibrosis, hepatic fibrosis [123], lung fibrosis, [124], scleroderma or myelofibrosis where the degree of SPARC expression in BM stromal elements, including $CD146^{+}$ mesenchymal stromal cells, correlates with the degree of stromal changes, and the severity of BM failure [122]. **Fig.1.3.5** summarizes the involvement of SPARC in stroma regulation.

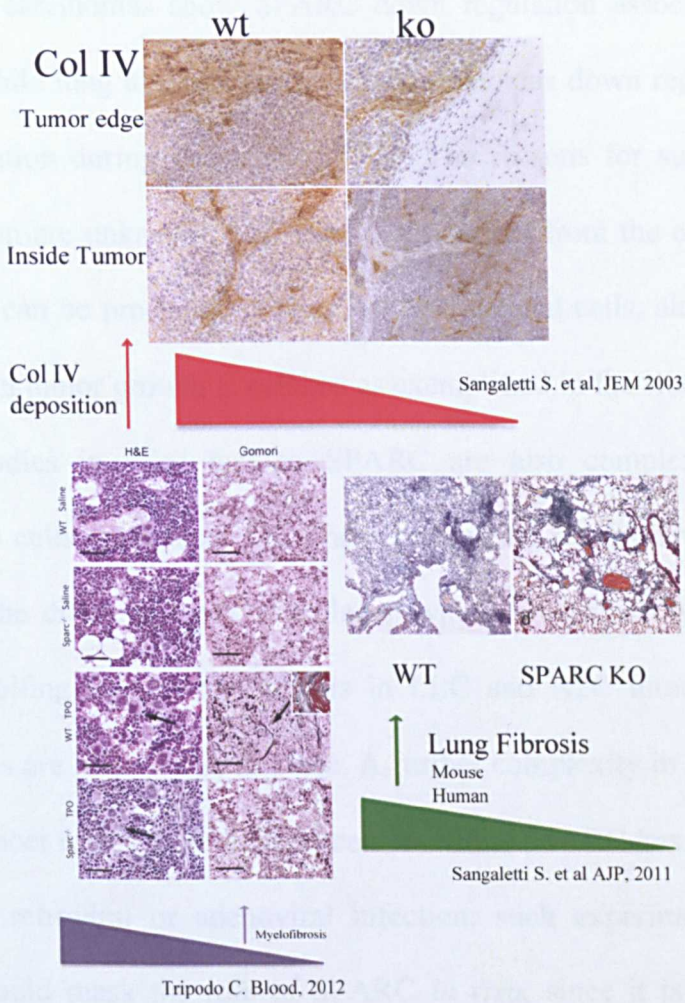

Fig.1.3.5 SPARC acts as a master stroma regulator.

SPARC stromal deficiency is responsible to increase BM-fibrosis in a experimental setting of myelofibrosis TPO-induced; on the contrary the absence of SPARC in stromal cells protect mice from Bleomycin-induced fibrosis; N2C mammary cells tumor composition injected respectively in wt and SPARC KO mice, SPARC KO mice present a defective Collagen IV deposition in tumor stroma.

1.3.6 Role of SPARC in tumor progression

Most of the well-known biological properties of SPARC come from *in vitro* studies but the implication of such observations *in vivo* and, in particular, the in vivo role of SPARC are not completely understood and frequently studies on SPARC and cancer, both in murine models and in humans, show contradictory results. In general, SPARC has been associated with advanced cancer of breast, head and neck, stomach, prostate and cancer esophagus as well as melanoma and glioma [125,126, 127, 119, 120]. By

contrast, ovarian carcinomas show SPARC down regulation associated with tumor progression [128] while lung and pancreatic adenocarcinomas down regulate SPARC by promoter methylation during progression [129,130]. The reasons for such differences in SPARC expression are unknown. This complexity arises from the cell-origin and the fact that SPARC can be produced by tumor and/or stromal cells, although the role of stromal-SPARC in tumor growth is debated as exemplified in the studies on melanoma cells. Tumor studies in mice lacking SPARC are also complex as Lewis lung carcinoma (LLC) cells grow faster [131]. These contrasting results have been explained on the basis of the different types of collagen whose proteolysis generate fragments favoring or inhibiting tumor angiogenesis in LLC and N2C tumours, respectively, other mechanisms are likely to be in place. A further complexity in dissecting the role of SPARC in cancer arisen from experiments in which SPARC has been "artificially" up-regulated by retroviral or adenoviral infection: such experimental conditions a condition that could mask the role of SPARC *in vivo*, since it is known that some functions of SPARC (e.g. the counter-adhesive one) depend on the amount of SPARC that is available. Accordingly, in glioma as the ability of SPARC to suppress proliferation is regulated to a greater degree by the level of SPARC and this suppressive effect is not influenced by the presence of any of the ECMs. The oncosuppressor activities of SPARC on ovarian cancer cells are multifaceted and are attributable to four different SPARC-mediated-effects: 1) SPARC induces apoptosis of ovarian cancer cells was demonstrated *in vitro* different ovarian cancer cell lines; 2) SPARC inhibits integrin-mediated adhesion and growth factor-dependent survival signaling in ovarian cancer 3) SPARC inhibits mesothelial-ovarian cancer cells cross-talk; 4) SPARC dampens inflammation in the ovarian cancer microenvironment. By contrast, SPARC in gliomas and more generally in tumors of the cerebellar system, is

up-regulated during progression. In such tumors SPARC mediates cellular survival of gliomas through AKT activation, accordingly the targeting of SPARC expression decreases glioma cell survival and invasion that is associated with reduced activities of FAK and ILK kinase. This aspect has been related to the capability of SPARC to promote integrin clusters on the cell surface and to stimulate signaling. Such an effect is in contradictory with SPARC effect on ovarian cells. It would be interest to understand the reasons why these opposing effects occur.

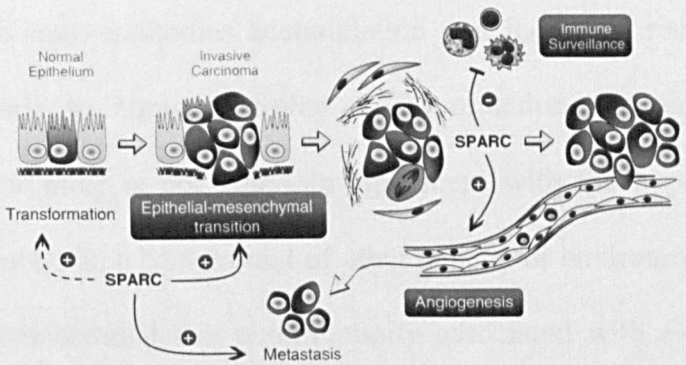

Fig.1.3.6 SPARC throughout tumor progression.

SPARC affects tumor progression at different levels; in malignant transformation during the early development stage; later on, SPARC is expressed both by tumor cells and stromal cells skips tumor immunity and regulates tumor escape

1.3.7 Role of SPARC in autoimmunity and associated transformation

Numerous studies have linked so far several different autoimmune disorders, or chronic inflammatory conditions, with benign lymphoproliferation or malign lymphoproliferation. The disregulation of immune cells that occurs in these conditions depends on not only defects that are intrinsic to the immune cells (like germline or somatic mutations) but also on defective signals coming from stromal cells in the tumor miroenviroment. In addiction to prosurvival factors for resting B and T cells (i.e. Baff, April) stromal cells of secondary lymphoid organs also produce insoluble factors like ECM molecules and SPARC. The finding that ECM molecules like collagens and

fibronectin are regulatory ligand for immune cells, including B cells, prompted the idea that the ECM and ECM-regulatory proteins might play a role in the maintenance of SLO homeostasis and its defective remodeling also in secondary lymphoid organs (SLO), for example related to the absence of SPARC, associated to autoimmunity and lymphomagenesis. To test this hypothesis Sangaletti et al [21] in our laboratory established an ad hoc murine model by crossing autoimmunity-prone *Fas* mutant (*lpr-lpr*) mice to *Sparc-null* mice. *Fas* mutant mice, similar to the human counterpart, develop an autoimmune lymphoproliferative disease characterized by lymph node and spleen enlargement, auto-antibodies accumulation and increased risk of developing lymphomas. Similarly to human carrying a *Fas* mutation the penetrance of this phenotype in *lpr-lpr* mice is not 100% in agreement with the hypothesis that *Fas* mutation might operates in a background of other genetic or environmental influences. Sangaletti et al. demonstrated that autoimmunity associated with *Fas* mutation was exacerbated toward lymphomagenesis due to SPARC lack. The absence of SPARC resulted in defective collagen assembly, with uncompartmentalization of lymphoid and myeloid populations within secondary lymphoid organs (SLO), and decreased inhibitory signals from the ECM. These conditions promoted unforeseen interactions between neutrophil extracellular traps (NET) and CD5+ B cells that underwent malignant transformation due to defective apoptosis under the pressure of neutrophil-derived trophic factors and NF-kB activation. Interestingly, this model of defective stromal remodeling during lymphomagenesis correlates with human lymphomas in a SPARC-defective environment, which is prototypical of CD5+ B cell chronic lymphocytic leukemia (CLL).

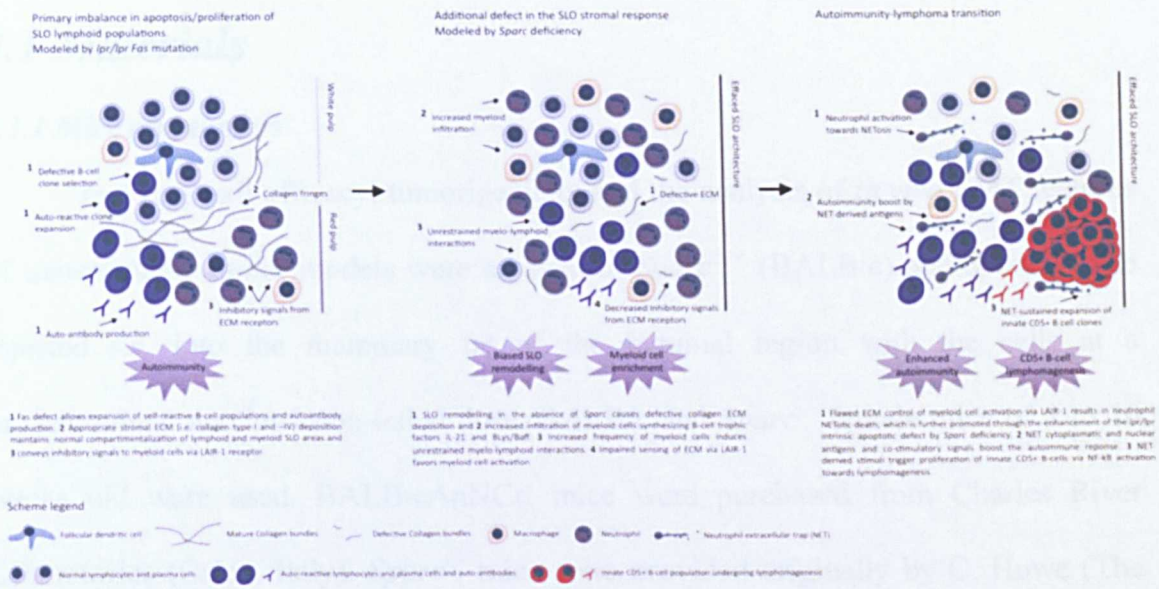

Fig 1.3.7 Schematic model of SPARC regulation of autoimmunity to lymphoma transition.

SPARC deficiency in a model of based Fas-mutated gene causes defective collagen deposition with an increased infiltration of myeloid cells. These conditions promoted unintended interactions between myeloid cells and the lymphoid clone and decrease the inhibitory signals mediated by LAIR-1 on MDSC activation. This condition regulated by SPARC is associated to an increased NETosis induced in PMN that lost their antiapoptotic signals impaired tolerance and enhance autoimmunity responses. In this condition CD5+ B cells proliferation is determined which underwent malignant transformation due to defective apoptosis under the pressure of neutrophil-derived trophic factors and NF-kB activation. Furthermore, this model of defective stromal remodeling during lymphomagenesis correlates with human lymphomas arising in a SPARC-defective environment, which is prototypical of CD5+ B cell chronic lymphocytic leukemia (CLL) in periphery and a SLE-like condition in dLNs. Picture is adapted from Sangaletti et al. Cancer Discov. 2014 Jan;4(1):110-29.

2. MATERIALS AND METHODS

2.1 Materials

2.1.1 Mice and tumors

In vivo Doxil efficacy, tumorigenicity and the analysis of *in vivo* EMT features of transpantable tumor models were assayed in *Sparc*$^{+/+}$ (BALB/c) and *Sparc*$^{-/-}$ mice injected s.c. into the mammary fat of the inguinal region with the cells at a predetermined maximal non-lethal dose. BALB/c and *Sparc*$^{-/-}$ female mice of 8 to 10 weeks old were used. BALB/cAnNCrl mice were purchased from Charles River Laboratories (Calco, Italy). *Sparc*$^{-/-}$ mice were provided originally by C. Howe (The Wistar Institute, Philadelphia, PA) on a mixed 129SV/ C57BL/6 background and were backcrossed afterwards for 12 generations with BALB/cAnNCrl (Charles River Laboratories) in order to obtain congenic *Sparc*$^{-/-}$ mice. *Sparc*$^{-/-}$ mice used in this study are maintained on a BALB/c background. Tumor take and volume were monitored twice per week. Tumors were measured with calipers in the two perpendicular diameters, and tumor volume (mm^3) was calculated as longest diameter × (shortest diameter)^2. To derive primary mammary carcinoma cell lines, spontaneous mouse model of mammary carcinomas BALB-neuT mice and SPARC-neuT were used. BALB-neuT mice are transgenic for the activated form of the rat c-erB2 oncogene and develop mammary tumors involving all mammary glands [132]. SPARC-neuT mice were derived from BALB-neuT mice that were back-crossed with *Sparc*$^{-/-}$ mice.

Mice were bred and maintained at the Istituto Nazionale Tumori under standard conditions according to institutional guidelines.

2.1.2 Cell lines

Primary mammary carcinoma cell lines (SN25A, SN25D, SN25E) were derived from female SPARC-neuT mice. N3D (inguinal) primary mammary carcinoma cell lines were derived from female BALB-neuT mice. Tumors were removed and, in a sterile environment, cleaned of fat, large vessels, and necrotic areas, minced with scissors, and placed in warm trypsin (37 C for 30 min). After washing with DMEM (GIBCO) and the addition of 10% heat-inactivated FCS (Bio Whittaker), tissue was passed through strainers and washed again. Cells were counted and seeded in 6-well plates at 0.4 10^6 cells/ml in DMEM plus 20% FCS. Mammary carcinoma cell lines that were unable to produce SPARC (SN25A, SN25E, SN25D) were infected with the retroviral vector LXSPARCSH and forced to express SPARC expression. SPARC expression has been analyzed by Western blotting using a specific rat a-mouse SPARC mAb as described in the *Section 2.2.8.* The most stable clone SN25A and its co-isogenic transduced counterpart (SN25ASP) were selected and were used for the majority of the experiments herein presented. Key experiments were confirmed using N3D and N3DSPARC pair obtained through infection with the same LXSPARCSH retroviral vector as the N3D w-t counterpart. Parental cell lines were maintained in monolayer cultures in Dulbecco's modified Eagle's medium (DMEM) (GIBCO) supplemented with 10% fetal bovine serum (FBS). Cells were maintained at 37°C humidified atmosphere with 5% CO2. Transduced stable clones were maintained in DMEM plus 10% FBS added 600 ug/ml Hygromicin dissolved in PBS 1% provided by (Santa Cruz). To establish the effects of tumor-derived SPARC, the above cell lines were compared with their wildtype counterparts. A possible experimental bias could be caused by SPARC anti-proliferative effect [133], therefore, transduced cell lines

selected for intermediate expression (similar to that of spontaneous tumors) were used for the injection into a *Sparc*$^{+/+}$ and *Sparc*$^{-/-}$ mice.

2.1.3 Antibodies used

Specificity-Antibody	Clone-brand	Diluition	Incubation
Byotinalated Ly6G and Ly-6C	**BD, Ebioscence** The monoclonal antibody RB6-8C5 reacts strongly with neutrophil-specific Ly6G Ag, but it has also been described to cross-react with the Ly6C Ag.	1:50	1h RT
Polyclonal iNOS antibody	**Cayman Chemical** Purified enzyme from mouse macrophages (RAW264.7) cells	1:1000	1 h RT
Polyclonal Cox-2 (Cyclo-oxygenase-2 antibody)	**ACRIS antibdodies** **Purified Rabbit Ig anti Ms and Hu**	1.50	1 h RT
Purified Mouse anti-IL-10	**BD, Pharmingen** The purified JES5-2A5 antibody (Cat. No. 551215) is useful as a capture antibody for a sandwich ELISA for measuring mouse IL-10 protein levels.	1:100	1 h RT
iNOS Polyclonal Antibody	**Cayman Chemical** Purified enzyme from mouse macrophages (RAW 264.7) cells.	1.1000	1 h RT

Table.5 Antibodies used for IHC analysis

2.2 Methods

2.2.1 Doxil treatment

To assess chemotherapy sensitivity *in vivo*, and to avoid cardiotoxicity and improve transcytosis, "Doxil" (Doxil, a Pegylated form of Doxorubicin) Caelyx 2mg/ml (Sterling A) was used[134,135]. $1*10^6$ SN25A and SN25ASP tumor cells were injected in the mammary fad pad of 8 old-week (*Sparc*$^{+/+}$) BALB/c mice (Charles River Laboratories, Wilmington, MA) (n=20) and *Sparc*$^{-/-}$ BALB/c mice (n=20), generated as described in *Section 2.1.1*, and when tumors reached a volume of approximately 20 mm^3 (day 15), animals were randomized into treatment groups. Mice were then either given 10 mg/kg of Caelyx twice, i.v., on day 15 and 30, or left

untreated as control. Tumor sizes were measured by a caliper 2 days per week and recorded as tumor volume calculated as longest diameter × (shortest diameter)^2. Growth was monitored for 40 days from tumor injection. Mice were sacrificed when tumors in control mice reached a volume of 1 cm3. At day 40, Doxil efficacy, estimated as % of tumor volume was calculated by the formula (Mean tumor volume (MTV) untreated-MTV treated/MTV Untreated*100).

2.2.2 Doxil plus Zometa treatment

BALB/c female were subcutaneously injected with $1*10^6$ of SN25ASP tumor cells. When tumors reached 20mm^3 size, mice were randomized into different groups. Beginning on day 15 after tumor cell injection, mice were treated with Doxil (10 mg/kg body weight via i.v. as described above in *Section 2.2.1*, Zometa (100 μg/kg body weight s.c.), Doxil plus Zometa, Doxil followed 30 min later by Zometa [136] (n = 20 mice per group).

2.2.3 Zometa treatment

Zoledronate (Zometa; Novartis Europharm, Ltd.) at a dose of 0.1 mg/kg was diluted in saline and administered daily s.c. 5 days a week. Mice were weighed weekly, drug concentration was adjusted to their actual weight. Mice were monitored for tumor growth, EMT and the expansion of MDSC in the peripheral blood was also evaluated. EMT features were evaluated after treatment, when tumors reached a volume of 600 mm^3.

2.2.4 Celebrex treatment

Anti-Cox-2 inhibitor, used for *in vivo* study, was provided by Novartis as 200 mg capsules (Celebrex). The content of each capsule was dissolved in DMSO to a final concentration of 25 mM. To test the role of COX-2 *in vivo*, BALB/c mice were injected with SN25ASP tumor cells. Starting on day 15 after tumor injection, animals were treated with COX-2 inhibitor (5 mg/kg) or vehicle control (DMSO) every other day in the contralateral side of the tumor. Mice were monitored for tumor growth twice a week. EMT and MDSC expansion in the peripheral blood were also evaluated. To establish the efficacy of the Doxil plus Celebrex combined treatment, drugs were administrated simultaneously, each according to its schedule.

2.2.5 Histopathology and IHC

Tumors were harvested for morphologic analysis and embedded in paraffin. Sections of 3 to 4 μm thick were cut from paraffin blocks and stained with H&E (SIGMA-Aldrich) for the evaluation of *in vivo* EMT features; Masson's trichrome (SIGMA-Aldrich) for Collagen distribution quantification; Gomori Trichrome for detection of interstitial fibers. Analysis included 15 cases per condition. For the evaluation of lung metastasis, lungs were removed from mice after sacrifice and were fixed *in situ* by intratracheal injection of 10% neutral buffered formalin. The trachea was canulated and the lungs fixed *in situ* with 10% formalin at a constant rate. The optimal instilled volume for mouse lungs was 0.3 mL for 20 g of weight. Lungs were removed, maintained 24 hours in formalin, and then embedded in paraffin. Sections of 3 to 4 μm thick were cut from paraffin blocks and stained with H&E. To characterize infiltrating immune cells, IHC analysis was performed on OCT sections. For immunohistochemestry, 5-μ m cryostat sections were fixed in acetone and incubated for 1 h with the reported Abs. After antibodies incubation, sections were washed and

overlaid with biotynilated goat anti-rabbit IgG for 30 min and with avidin-peroxidase complex for 30 min. A list of antibodies used is showed in *Section 2.1.3*. Avidin-peroxidase complex was used as secondary antibody to detect sections incubated with biotinylated primary antibody. Cox-2 immunostaing reactivity was revealed with alkaline phosphatase (LSAB+ kit AP, Dako Denmark) method. Sections were counterstained with Mayer's hematoxylin, dehydrated in graded alcohol (70%, 95%, and 100% ethanol), and mounted in BDH mounting medium (Merck Eurolabs). The immunostaining of IL-10 in SN25A and SN25ASP tumors was performed by intracellular staining of cytokines. Tumors, embedded in OCT compound were fixed with 2% of paraform-aldehyde for 20 min and then washed. Sections were incubated sequentially with a blocking and a permeabilization buffer both made in PBS (1% bovine serum albumin; 0.1% saponin/1% FCS, respectively). Subsequently, sections were incubated with avidin-biotin blocking solution (Vectashield) for 15 min and finally they were incubated overnight with a rat anti –IL-10, (see *Section 2.1.3* for datasheet informations). The following day, sections were washed with PBS 1%v/v and incubated with secondary antibodies provided by DAKO and revealed as previously described. Immunostained sections were evaluated under a NIKON E1000 invert epifluorescence miscroscope optical microscope using 20× (numeric aperture 0.4) and 40× (numeric aperture 0.65) objective lenses.

2.2.6 Immunofluorescence and laser confocal microscopy

Immunofluorescence analysis of EpCAM and ß-catenin expression was performed on SN25A and SN25ASP mammary tumor cell lines. Cells were seeded at approximately $2*10^5$ cells/35 mm poly-d-lysine coated glasses. Cells were fixed with 4% PFA, subsequently permeabilized with Triton-X-100 (0.1%) and incubated in blocking buffer (10% v/v FBS in PBS). Cells were re-hydrated in PBS and incubated

for 1 h with a primary antibody. Cells were then washed in PBS and incubated for 30 min with the appropriate goat Alexa Fluor 488/546 antibody (1:500; Invitrogen, Probes, eugene, Oregon). Primary antibodies used were rabbit anti-mouse CD326 (EpCAM) antibody purified G.8.8 (1:100; BD eBiosciences); rabbit anti-mouse ß-Catenin mAb (1:100; Sigma–Aldrich, St. Louis). Nuclei were stained with 4′,6-diamidino-2-phenylindole. Slides were mounted with Prolong anti-fade reagent (Life Technologies, Monza, Italy) and examined under a RADiance-2000 (Bio-Rad, Milan, Italy) Nikon-TE300 laser scanning confocal microscope (Nikon Instruments S.p.A, Florence, Italy). Images in .tif format were analysed with ImageJ as single chanel and then merged with Photoshop CS4 EXTENDED version 10.0.

2.2.7 Flow cytometry analysis

FACS analysis were performed on PBMCs (Peripheral blood mononuclear cells), BM (bone marrow) and SPL (spleen) in order to assess the frequency of circulating $Ly6G^{high}Ly6C^{low}$ $CD11b^{+}$ myeloid cells subsets. The frequency and distribution of myeloid progenitors (Lin-$cKit^{+}$; LK), including common myeloid progenitors (CMP), granulocyte-macrophage progenitor (GMP), and megakaryocytic/erythroid progenitor (MEP) was also evaluated. Analysis of circulating MDSC was performed collecting blood samples from retroorbital sinus and mixed with equal volume of 5 mmol/L EDTA, erythrocytes were lysed by hypotonic shock in NH4Cl lysis buffer. After that, cell suspension was centrifuged at 300 g for 5 min and washed twice with PBS containing 2% fetal bovine serum (FACS buffer). Finally, cells were blocked with 10 μ g/mL of rat anti-mouse CD16/CD32 Ab (clone 2.4G2; BD PharMingen) before staining with the combination of antibodies: Rat anti-mouse PerCP-CY5.5-Conjugated CD11b (M1-70), Anti-Mouse Ly-6G (Gr-1) FITC (RB6-8C5) and APC-conjugated rat anti-mouse Ly6C in FACS buffer. SPL and BM

samples were cut in small pieces and processed with a 0.5 ml syringe in sterile conditions. Suspensions were filtered by a cell strainer (BD, Franklin Lakes, NJ). After that, cells were washed, re-suspended in 1× PBS, and stained with the indicated monoclonal antibodies. To prevent nonspecific binding, Fc Blocker (anti-mouse CD16/32, BioLegend) was added to single cell suspensions for 5 min on ice and then stained with a pool of antibodies for lineage (Lin)-positive markers, including CD3, CD11b, CD45R, Ly6G, CD4, CD8, Ter-119 (all PE-conjugated) and stem cell and progenitor cell markers, including CD117 (FITC-conjugated), CD34. (APC-conjugated), all purchased from eBioscience. *In vitro* evaluation of EMT features was performed by FACS analysis. 6 well cultured SN25A, SN25ASP, N3D and N3SPARC, N2C cell lines (used as positive control) were gently detached and single stained for 60 min at room temperature with primary antibodies. To dectect N-CAM and integrin B1, polyclonal rabbit antibody specific for anti-mouse N-CAM (AbCAM), rat antibody for integrin B1 (CD29) (clone HMB1-1; Biolegend), anti mouse APC-conjugated EpCAM (CD326) (clone G8.8; eBioscience) were used. Primary antibodies were delivered with the following antibodies: a anti-Rbt FITC conjugated and anti-Rat antibody PE conjugated used 1:200. All the primary antibodies were diluted in PBS for cell surface staining or in saponin buffer 0.2% saponin and 0.5% bovine serum albumin (Sigma-Aldrich) for intracellular staining. Isotype-matched IgGs were used as controls. All samples were purchased by FORTESSA (Becton Dickinson) and data were subsequently analyzed using Flowjo 9.4.10.

2.2.8 Western blot analysis

Cells were collected in the eppendorf or falcon, centrifuged at 335 g for 15 min at RT. Cells were lysed in a RIPA buffer containing 50 mM Tris, PH 7.4, 1% NP-40, 150 mM NaCl, 1 mM EDTA, 1 mM Na3VO4 and protease inhibitor cocktail (Roche). Proteins were separated by SDS-PAGE and subjected to immunoblotting. Cell lysates were microcentrifuged at 14,000 × g for 20 minutes at 4°C and supernatants collected and stored at −80°C. Protein concentration in each sample was determined by the BCATM Protein Assay kit (Thermo Fisher Scientific, Waltham, MA). Cell lysates containing equal amounts of protein (25 μ g) were analyzed by SDS-PAGE on precast minigels (Invitrogen, Carlsbad, CA) and proteins were transferred to a nitrocellulose membrane (GE Healthcare, Waukesha, WI). Nonspecific binding sites were blocked in 5% non-fat dry milk in Tris-buffered saline–Tween (100 mmol/L Tris, 0.9% NaCl, pH 7.5, 0.1% Tween 20) solution. For the detection of SPARC expression in tumor cells, membrane was incubated overnight at 4°C with a polyclonal antibody to SPARC (R&D), washed three times each for 5 minutes with Tris-buffered saline containing 0.1% Tween 20, and then incubated with horseradish peroxidase–conjugated antibody (1:2500; Zymed, San Francisco, CA) for 1 hour at room temperature. For western blot analysis of TNF-α and TGF-ß expression in macrophages culture, $1*10^6$ differentiated *Sparc*$^{+/+}$ and *Sparc*$^{-/-}$ macrophages were cultured in a 6 well. Equal amounts of total protein (25 µg) were loaded in each lane. Blots were blocked and incubated overnight at 4°C with a monoclonal rat anti-mouse TNF-α antibody (Becton Dickinson) and with an anti-TGF-ß Functional Grade Purified (clone 1D11.16.8). After washing, blots were developed with an enhanced chemiluminescence system (ECL-plus; GE Healthcare).

2.2.9 MMT proliferation assay

To test proliferation of tumor cell lines *in vitro* proliferation, cells were plated into 96-well U-bottom microplates (Nunc, Denmark) at a density of $1^* 10^6$ cells/ well in 200 ul of DMEM medium supplemented with 10% FBS and cultured for 1, 3, 7 days selected as the experimental time point (t=s). Tumor cells viability was assessed by incubating tumor cells with MTT solution (5 mg/mL Thiazolyl blue Tetrazolium Bromide) for 4h at 37° C (Sigma). After incubation, crystalized MMT solution was dissolved in 100 of dimethyl sulfoxide (DMSO), and measured at 590 nm using an ELISA reader. The ratio of cell proliferation was calculated as (OD mean t=0/OD mean t=s).

2.2.10 Cytotoxicity assay

In vitro the efficacy of Doxil was tested for SN25A and SN25ASP cell lines using the previously described colorimetric MMT assay. Cells suspensions were dispensed into different 96 U-bottom well (as described in *Section 2.2.9)* one for each evaluated time point, and incubated for 24 h at 37 °C in a fully humidified atmosphere of 5% CO2. Then Doxil to final concentration of 5 μ M) was added in a volume of 200 μ l. Tumor cells inhibition mediated by Doxil was evaluated 6, 12, 24, 48 h after treatment. Results were measured using an ELISA plate reader as previously described (*Section 2.2.9*). The cytotoxic/cytostatic effect of doxorubicin was calculated as % of tumor cells Doxil inhibition was calculated by the formula (experimental absorbance-background absorbance)/ (absorbance of untreated controls-background absorbance) × 100.

2.2.11 Enzyme-Linked Immunosorbent Assay (ELISA).

To quantify the amount of GMCSF and GCSF, cells were seeded at a ratio of 1:1 (10^6 cell/10 ml) in a 96 well-plate and cultured. The supernatants were collected after 48 h. Quantification of mouse GMCSF levels was performed using a BD OptEIA™ kit (Cat#555167) specific for mouse GMCSF. For the quantification of GCSF levels, a RayBiotech (Cat#: ELM-GCSF-001) G-CSF ELISA Kit specific for G-CSF was used. To quantify serum levels of MMP-9 and VEGF in tumor- bearing mice recipients of the adoptive transfer, a specific ELISA Kit that detects total levels of MMP9 was purchased from R&D (Cat#Kit- MMPT90) while for VEGF (isoforms A-B) a specific kit was purchased from Peprotech (Cat# 0608099) was used. Results are reported as mean of OD values ±SEM.

2.2.12 Isolation and functional characterization of splenic and tumor-derived MDSCs

2.2.12.1 Isolation of splenic MDSCs for RNA preparation

G-MDSC (CD11b+Ly6G^{high}Ly6C^{low}) and M-MDSC (CD11b+Ly6G^{low}Ly6C^{high}) were isolated from the spleen of tumor-bearing mice through immunomagnetic separation using a specific kit obtained from Miltenyi (Myeloid derived Suppressor Isolation kit; MACS ®). The purity of G-MDSC and M-MDSC populations were checked by FACS analysis by using a mixture of the following antibodies: PerCP-CY5.5-Conjugated anti-mouse CD11b (M1-70); FITC-conjugated anti-Mouse Ly-6G (Gr-1) (RB6-8C5); APC- conjugated Ly6C anti- mouse (clone HK1.4).

2.2.12.2 Cell sorting of tumor-derived MDSC

MDSC and their subsets were isolated from tumors of tumor-bearing or control mice using cell sorting on FACSAria cell sorter (BD Biosciences). The purity of cell populations was >99%. For isolation, tumor tissues were cut into small pieces and treated with collagenase (type IV, 1 mg/ml, Sigma-Aldrich) and Elastase (6U/ml, Sigma-Aldrich) for 45 minutes at 37°C, and dead cells were removed by centrifugation over a Ficoll-Hypaque gradient (Atlanta Biotechnology). Cell suspensions were stained with the following mixture of antibodies: PerCP-CY5.5-Conjugated Rat anti-mouse CD11b (M1-70); Anti-Mouse Ly-6G (Gr-1) FITC (RB6-8C5) and APC-conjugated rat anti-mouse Ly6C (clone HK1.4).

2.2.12.3 RT-PCR for TaqMan probes based Real Time PCR (qPCR)

For quantitative RT-PCR, myeloid cells were lysated with Trizol (Invitrogen Life Technologies) and RNA was extracted by using RNeasy Kit (Qiagen, Valencia, CA). Traces of DNA were removed by treatment with DNase I. The cDNA was synthesized from 1 μg total RNA according to the manufacture protocol of Kit Applied Biosystems. RNA was retrotranscribed with a kit provided by Invitrogen (18021-071).

2.2.12.4 Quantitative real-time PCR

PCR was performed using Taqman Universal PCR master mix (Applied Biosystems, Foster City, CA, USA) and target gene assay mix containing sequence-specific primers for *ARG-I, CCL2, CCL5, COX-2, NOS-2* genes. Gene-specific primers (all 5'–3' direction) were purchased from Applied Biosystems (**Ccl2**, Ref. Seq. NM_011333.3; **Ccl5** Ref Seq.NM_013653.3; **Stat3** NM_0114886.4; **ARG1** NM_000036.2; **Nos-2-iNOS** NM_010927.3; **PTGS2** (COX-2) NM_0111983). The reaction was set according to the standard TaqMan qPCR conditions reported in the Applied Biosytem protocol, and was performed in duplicates for each samples. The

qPCR reactions were run using ABI PRISM ® 7900 Fast Real Time PCR system and ABI PRISM 7900 HT Sequence Detection System (Applied Biosystems) and analyzed with SDS Software 2.3 (Applied Biosystems). The target gene mRNA was quantified by measuring CT to determine the relative expression. Results have been reported using the fold change in the target gene expression of the target genes relative to the internal control gene (GAPDH).

The mean fold change in target gene expression was calculated as $2^{-\Delta\Delta CT}$ where $\Delta\Delta CT=((CT,\text{Target} - CT,\text{GAPDH})\text{sample}-(CT,\text{Target} - CT,\text{GAPDH})\text{internal control})$[137].

2.2.13 In vitro functional characterization of MDSC phenotype

2.2.13.1 In vitro *suppression assay.*

In vitro suppression assay was performed by using total CD11b+Ly6G+Ly6C+ myeloid cells without separating them in the two subsets (G- and M-MDSC). Myeloid derived suppressor cells were purified using CD11b-conjugated microbeads and Myeloid-Derived Suppressor Cell Isolation Kit (both from Miltenyi Biotec) following the manufacturer's instructions. In *vitro* T cell suppressive activity was measured, labeling 4 x 10^5 naïve BALB/c splenocytes with CFSE (Carboxyfluorescein Succinimidyl ester; SIGMA Aldrich) and co-culturing them with the MDSCs. Different concentrations of MDSCs ($1x10^4$ to 5×10^4) were cocultured with a fixed concentration (1×10^4) of activated splenocytes for 72 h in complete medium containing RPMI 1640 (Sigma-Aldrich) supplemented with 5% FCS, 2 mM L-glutamine, 200 U penicillin, and 200 mg/ml streptomycin (Sigma-Aldrich). Each sample was seeded in triplicate. Total splenocytes were stimulated with 2 mg/ml of soluble anti-CD3 and 1 mg/ml of anti-CD28 added to medium or left unstimulated as negative control. Proliferation of CD4 and CD8 T cells has been assessed 2 and 3 days later, by and

evaluating CFSE dilution in the CD4+ and CD8+ gated populations. Results are shown as percentage of proliferated cells (mean±SEM).

2.2.13.2 Cytostatic assay to test antitumor activity of PMNs

To test antitumor activity of PMNs (Polymorphonuclear leukocytes) in tumor cells, conditioned PMNs were isolated using agar plugs method. Blocks of 2% agarose and 0.2% gelatin in saline (agar plugs) were implanted in *Sparc*$^{+/+}$ and *Sparc*$^{-/-}$ mice and after 5 days, agar plugs were removed and PMNs were collected by washing 3 times agar blocks with IMDM supplemented with 10% of FCS (GIBCO, Life Technologies). 70%-75% of these cells are PMNs that are enriched up to the 95% after 30 minutes of adherence on plastics. In some cases, naive PMNs were obtained through immunomagnetic cell separation from spleen using a specific kit (anti-Ly6G MicroBead Kit, Miltenyi). Cytostatic activity of PMN was evaluated in a spectrophotometric assay. Briefly, tumor cells (SN25A and SN25ASP cell lines) (10^4) were incubated with PMNs in a float-bottom coated 96-well (Costar, Cambridge) using 12:1 to 100:1 ratios of attached cells (PMNs) to target cells (tumor cells). 72 h after incubation, culture wells were fixed with 5% formalin and stained with 1% methylene blue in 0.01 M borate buffer, pH 8.5. After eluting the dye from cells with 0.1 N HCl, absorbance was read at 620 nm. The percentage of growth inhibition was calculated as [1 -(A-B-C)/(D-C)], where A= absorbance in cultures of tumor cells and PMNs; B=PMNs alone; C=10^4 tumor cells after 2h adhesion; D= dye alone. Results are presented as mean of OD values (±SD) of six replicates.

2.2.13.3 Coculture experiments

Lineage negative cells were obtained from BM through negative selection by using a specific kit, Lineage Cell Depletion Kit (MACS, Order No. 130-090-858). Lineage negative cells (10^5 cells) were seeded directly onto a monolayer of tumor cells (SN25A and SN25ASP cell lines) or in the presence of a Transwell (0.4 μ m pore size from Corning LifeSciences) to ensure Lin- cells feeling of tumor-derived cytokines and avoid cell-to-cell contact. Control Lin- cells were cultured in the presence of the following cytokines: rGM-CSF (10 ng/ml), rGSCF (5 ng/ml), rTGF-β 1 (10 ng/mL) (all cytokines/chemokines were provided by R&D). Six days later, cells were harvested and Lin-cells differentiation towards the different subsets of myeloid cells was checked by FACS analysis using the following Abs: PerCP-CY5.5-Conjugated Rat anti-mouse CD11b (M1-70); Anti-Mouse Ly-6G (Gr-1) FITC (RB6-8C5) and APC-Conjugated Rat anti-mouse Ly6C. Results were reported as mean percentage of $Ly6G^{hi}Ly6C+$ and $Ly6G^{low}$ Ly6C+subsets gated on CD11b+ cells.

2.2.14 Adoptive transfer of MDSC in tumor-bearing mice

To directly test *in vivo* the capability of MDSC to promote EMT and tumor growth, also according to their *Sparc* genotype, tumor bearing *Sparc*$^{-/-}$ mice (SN25ASP) were i.v. injected with 10^6 myeloid cells isolated from the spleen of donors mice. As donors, we used *Sparc*$^{+/+}$ and *Sparc*$^{-/-}$ mice, previously injected with SN25ASP tumor cells (40 days before, a condition that ensured the presence of tumors and subsequent MDSCs expansion). The adoptive transfer was performed once a week for 4 consecutive weeks using a tumor size of 8 mm3 in recipient mice as a starting point. Mice adoptively transferred with MDSCs were checked for tumor growth, VEGF and MMP9 serum levels. At endpoint, tumors were harvested and histologically analyzed for aggressiveness and EMT.

2.2.15. In vitro macrophage preparation

Sparc$^{+/+}$ and *Sparc*$^{-/-}$ macrophages were obtained from bone marrow precursors by plating them in the presence of 10 ng/mL of granulocyte-macrophage colony-stimulating factor (GM-CSF) and 10 ng/mL of IL-4. On days 2, 4, and 6, floating cells mainly consisting of dendritic cells were eliminated and supplemented medium was replaced. On day 7, up to 90% of the adherent population consisted of macrophages as determined by flow cytometry analysis using the F4/80-specific monoclonal antibody (Caltag-Medsystems, Buckingham, UK).

2.2.16 Detection of intracellular cytokines in activated macrophages

Sparc$^{+/+}$ and *Sparc*$^{-/-}$ macrophages were seeded at $2*10^5$ cells/well on 96 well and cultured for 24 h. To detect intracellular cytokines production, macrophages were stimulated with 50 ng/ml PMA, 500 ng/ml Ionomycin (SIGMA-Aldrich) and Monensin (eBioscience) for 4 h at 37°C, fixed in Fix/Perm buffer (eBioscience) and stained for a mAb TNF-a APC conjugated antibody and FITC conjugated mAb F4/80 (Ebioscience).

2.2.17 Statistical analysis

Statistical analysis of single treatments (Celebrex or Zometa) was performed using the Mann-Whitney test. Significance of different combined treatments was assessed with one-way Anova with Dunn's Multiple Comparison Test. For other analyses related to MDSC frequency or ELISA data, differences between groups were tested for significance using a two-tailed unpaired t-test. Values were considered statistically significant at $p < 0.05$. All the analyses were performed using Prism software Version 5.0d (GraphPad).

3. AIMS OF THE THESIS

Communication between cancer cells and leukocytes occurs through a complex network of pro-inflammatory mediators in which the NF-kB pathway is predominant. Among the ECM proteins induced by remodeling and inflammation, SPARC (Secreted Protein Acidic and Rich in Cysteine) has been indicated as marker of poor prognosis and poor response to therapy in independent series of mammary carcinomas analyzed using expression array technology. Using carcinoma cells from MMTV-HER-2/neu transgenic mice, we have shown that host-derived rather than tumor-derived SPARC determines collagen density and leukocyte infiltration of the stroma, thus defining the lobular structure of mammary carcinoma. This finding, together with the above mentioned gene array results, prompts the hypothesis that tumor-derived SPARC and infiltrating inflammatory cells are a major obstacle to chemotherapy and/or biological therapy. In order to validate this hypothesis, I studied the effect of tumor-derived and stroma-derived SPARC on the outcome of chemotherapy in transplantable tumor model of mammary carcinomas.

4. RESULTS

4.1 SPARC PROMOTES IMMUNE-MEDIATED EMT

4.1.1 Replacing SPARC expression in primary spontaneous mammary carcinoma cell lines from transgenic MMTV-Her2 mice (BALBNeuT) also SPARC knock-out.

To establish primary mammary tumor cell lines defective for SPARC expression, MMTV-Her2 Neu (BALBNeuT) [132] were crossed with SPARC-KO mice to obtain the double mutant (SPARC-NeuT). Inguinal and thoracic tumors were removed from SPARC-NeuT mice and, in a sterile environment, cleaned of fat, large vessels, and necrotic areas, minced with scissors, and placed in warm trypsin (37°C for 30 min). After washing with DMEM and the addition of 10% heat-inactivated FCS, tissue was passed through strainers and washed again. Cells were counted and seeded in 6-well plates at 0.4×10^6 cells/ml in DMEM plus 20% FCS. Three of these *Sparc*-deficient mammary carcinoma cell lines, namely SN25A, SN25D and SN25E and the BALB-NeuT-derived N3D line, characterized for low SPARC expression [138], have been transduced with the retroviral vector LSPARCSH to replace or over-express SPARC, respectively. SPARC expression was then evaluated by Western Blot as shown in **Fig 1-A**. The most stable SN25A cell line and its co-isogenic SN25ASP counterpart were selected and key experiments were confirmed with the N3D and N3D/SPARC pair. SPARC overexpression did not change cell proliferation *in vitro* of both SN25SP and N3D/SPARC cell lines compared with their wt counterpart (**Fig. 1B-C**).

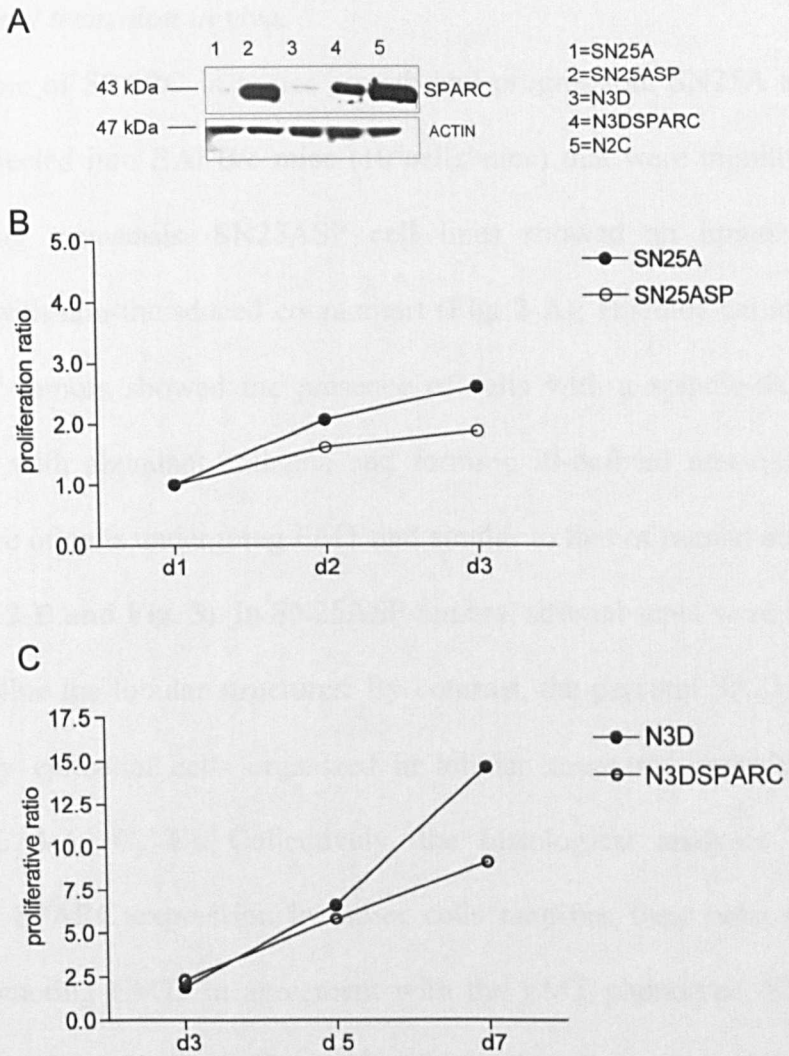

Fig.1 SPARC-induction has no effect on tumor cell proliferation in vitro.

(A) Western Blot analysis for SPARC expression in SN25A, SN25ASP, N3D, N3DSPARC cells lines. The N2C murine mammary cell line, previously characterized for high SPARC expression, was used as positive control (**B**) Proliferation of SN25A or SN25ASP cells was measured in vitro through an MTT assay The ratio of cell proliferation for each time point was calculated as (OD mean t=0/OD mean t=s); (**C**) the same analysis was performed for N3D, N3DSPARC cell lines at the indicated time points

4.1.2 SPARC-overexpressing cells, but not the parental cell lines, undergo epithelial-to-mesenchymal transition in vivo.

To test the role of SPARC in tumor growth and progression, SN25A and SNA25SP cells were injected into BALB/c mice (10^6cells/mice) that were monitored for tumor take and lung metastasis. SN25ASP cell lines showed an impaired growth in comparison with non-transduced counterpart (**Fig. 2-A**); Histological analysis (H&E) of SN25ASP tumors showed the presence of cells with a spindle-like morphology intermingled with abundant collagen and forming ill-defined nest-like structures, a typical feature of cells undergoing EMT and similar to that of human ductal mammary tumors **(Fig. 2-B and Fig. 3)**. In SN25ASP tumors, stromal septa were interrupted and unable to define the lobular structures. By contrast, the parental SN25A tumors were composed by epithelial cells organized in lobular structures embedded in a dense stroma (**Fig. 3-A, C, E**). Collectively, the histological analyses suggested that replenishing SPARC expression in tumor cells modifies their behavior *in vivo*, for instance promoting EMT. In agreement with the EMT phenotype, SN25ASP tumor cells were more aggressive and capable of invading the surrounding tissue margins **(Fig. 3-B, D, F)** despite the reduction of their mitotic index. The difference between SN25ASP and SN25A in terms of *in vitro* proliferation and *in vivo* tumor outgrowth was confirmed in the N3D and N3DSPARC mammary cell lines pair. Over-expression of SPARC in the N3D cell line did not affect their *in vivo* growth (**Fig.4-A**) but, as in the SN25ASP cell line, SPARC promoted a change in tumor grade and acquisition of spindle-shape morphology of the tumor cells, less-defined lobular structures and invasion of surrounding tissue margins **(Fig. 4-B)**. Interestingly, N3DSPARC tumors showed increased collagen content consistent with their mesenchymal phenotype **(Fig. 4-D).** To confirm that SN25ASP and N3DSPARC, but not the parental counterparts, underwent EMT, IHC analysis was performed for E-cadherin and N-cadherin

according to their epithelial and mesenchymal marking, respectively. Parental cell lines SN25A expressed E-cadherin but not N-cadherin on the cell surface, whereas their SPARC-transduced counterparts showed the reverse behavior: down-regulation and cytoplasmic or nuclear re-localization of E-cadherin and up-regulation of N-cadherin. Collectively, these data demonstrate that SPARC-overexpression in tumor cells promotes EMT (**Fig.5**). Finally, according to the increased tumor grade, lung metastases were only found in BALB/c mice injected with SN25ASP or N3DSPARC cells, but not with the wt counterpart. SPARC transduction into SN25A mammary cells endowed them with the ability to metastasize to lung tissues. Indeed, the quantification of digital images performed on multiple lung sections indicated that SN25ASP tumor-bearing mice present a statistically significant increase in the frequency of lung metastasis compared with SN25A tumor-bearing mice, (85% vs 15%, p-0.095) (**Fig.6-A**) as well as in the number of lung metastasis lesions (9.5 vs 0.2, p-0.001) as shown in **Fig. 6-B**. Accordingly, the increased number of metastatic areas/lung observed for SN25ASP tumor-bearing mice was associated to increased metastatic tumor burden (8500 μm^2 vs 200 μm^2, p-0.0081), here presented as mean values (±SD) of disseminated tumor cells areas measured by ImageJ software and expressed as pixel/um^2 units (**Fig. 6-C**). Collectively these data indicate that only upon SPARC-transduction we can observe an overall massive substitution of lung tissues with tumor cells. Interestingly, the injection of SN25ASP cells into the mammary fat pad of syngeneic BALB/c mice, as showed in the representative section, resulted in the formation of nested tumor cells that, disseminated in lung parenchyma, destroy the lung typical structure, and are often associated with bone marrow-derived cells with different myeloid morphology (**Fig. 6-D**).

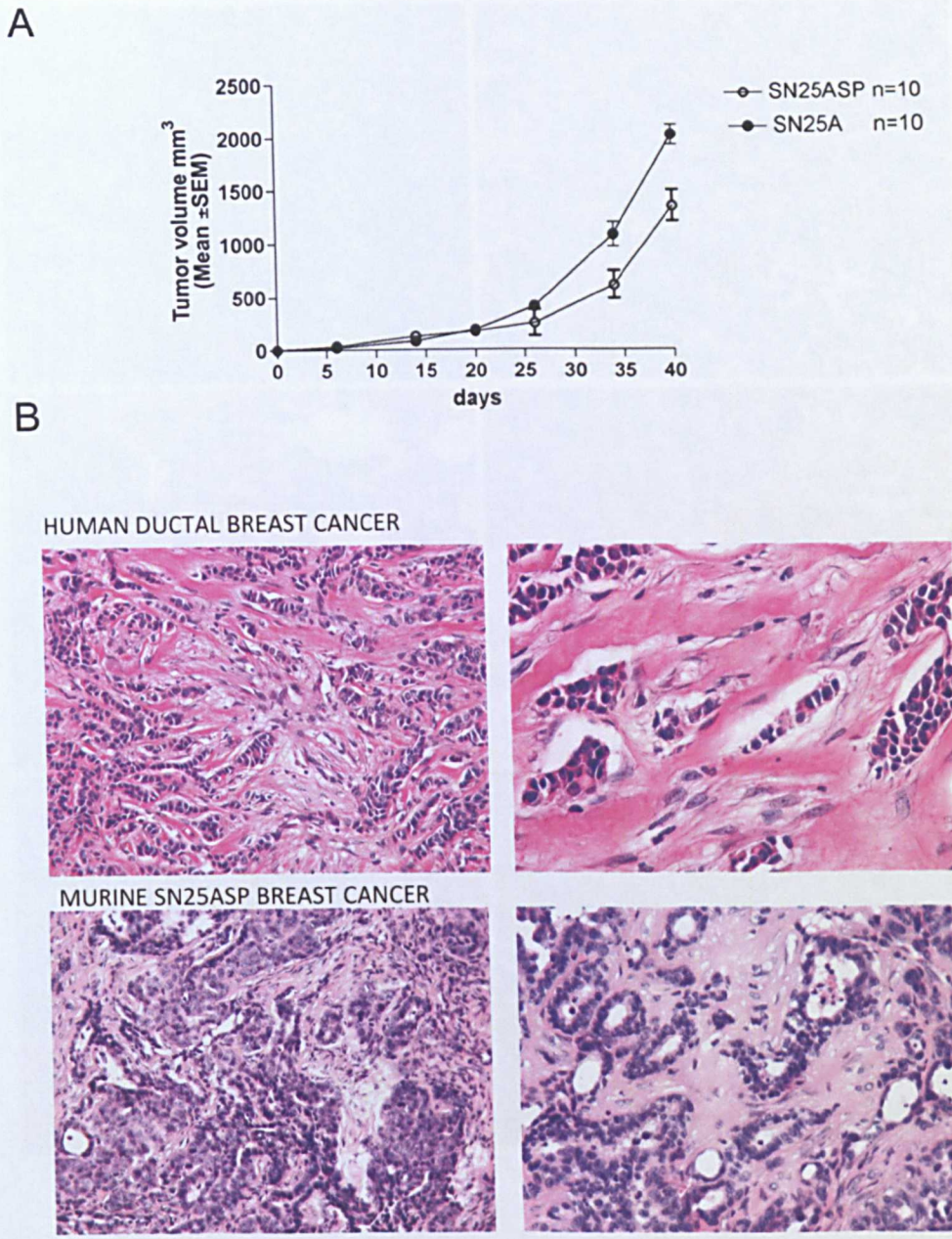

Fig.2 SPARC-transduction in SN25A cells promotes breast cancer aggressiveness.

(A) Tumorigenicity of SN25A and SN25ASP cell lines subcutaneously injected in BALB/c mice. Results show the mean of tumor volumes ±SEM. One representative experiment out of 4 performed is shown. (**B**) SN25ASP murine breast tumor has features of human invasive ductal carcinoma. Invasive human ductal breast cancer (upper panels) is characterized by tumor cells infiltrating the dense stroma. Similarly murine SN25ASP tumors show cords of tumor cells intermingled with the abundant stroma (lower panels).

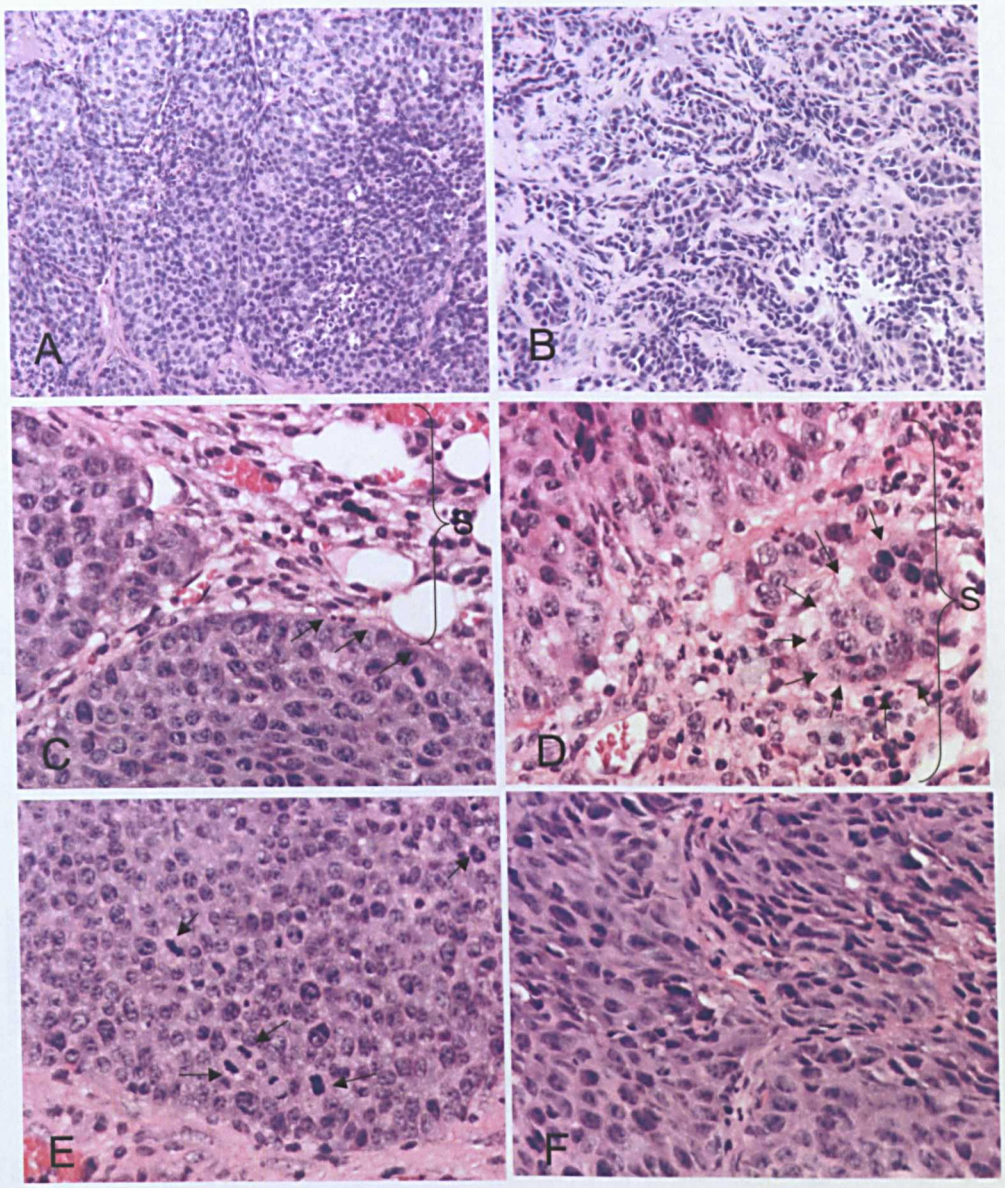

Fig.3 SN25ASP but not SN25A tumors have "mesenchymal" features in vivo.

H&E shows that SN25A tumors are well-differentiated adenocarcinomas with a lobular structure in which nest of tumor cells are surrounded by a stromal septa **(A)** on the contrary SN25ASP tumors are characterized by the absence of a lobular structure, in these tumors lobular septa are interrupted and interposed with spindle-like shape tumor cells (**B**). In SN25ASP **(D)** but not SN25A tumor **(C)** tumor cells (arrows) invade the surrounding stromal margins (**S**, graph parenthesis). Mitosis are evident in SN25A **(E)** but not SN25ASP tumors **(F)** that have a reduced proliferative capacity in vivo, according to the "mesenchymal" phenotype.

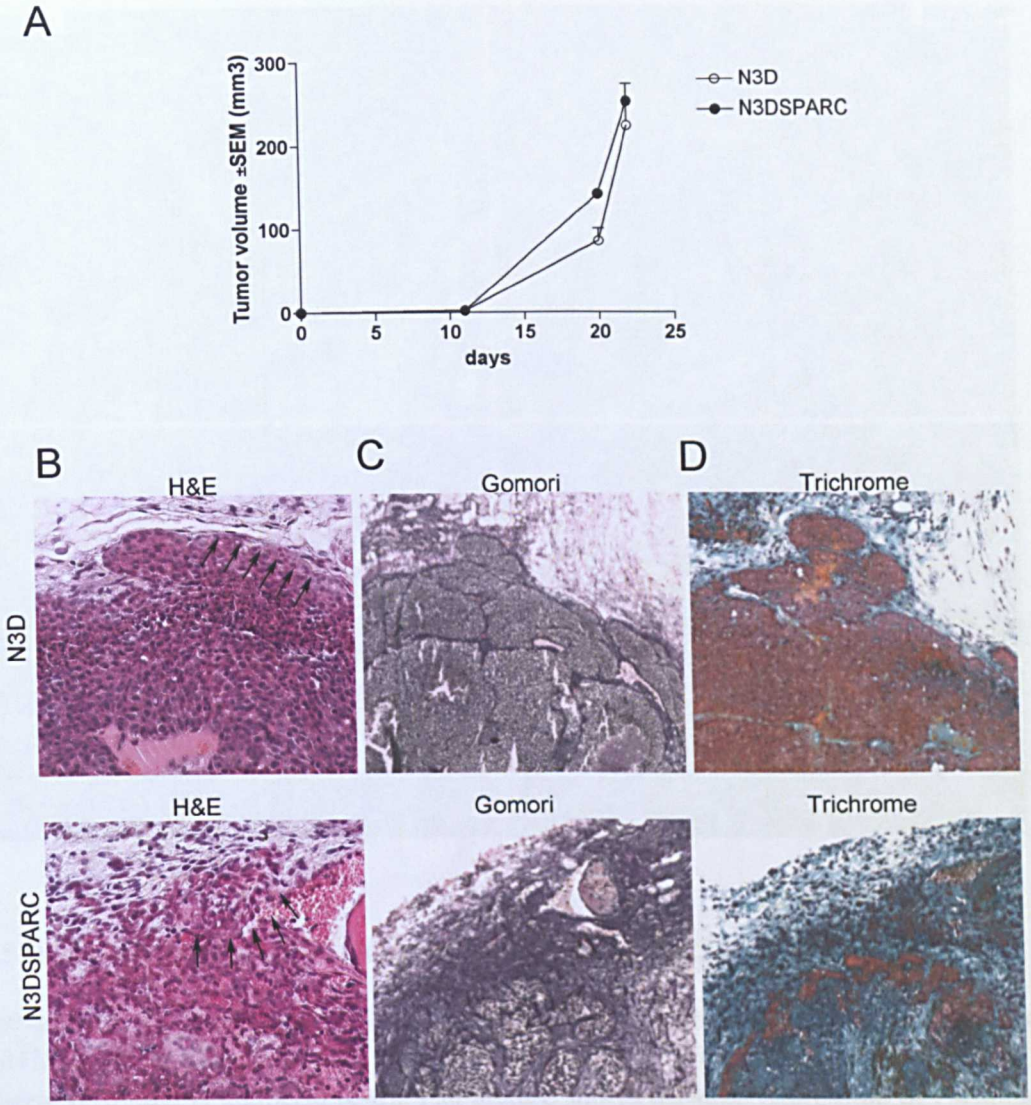

Fig.4 SPARC overexpression in N3D tumors does not affect tumor growth but promotes EMT and collagen deposition.

(A) BALB/c female mice were subcutaneously injected with N3D or N3DSPARC cells. Results are shown as mean of tumor growth ±SD. *P<0.05. (n=10) **(B)** Histological (H&E) analysis shows the presence of spindle-shape tumor cells invading the surrounding stroma in N3DSPARC tumors but not in N3D parental counterpart (arrows). **(C)** As in the SN25SP tumors, also in N3DSPARC model we found cords of tumor cells intermingled with the abundant stroma fibers (Gomori staining) In parental N3D tumors, the stroma was less abundant and defining the lobular architecture. (**D**) The mesenchymal phenotype of N3DSPARC tumor cells is confirmed, the high collagen production not restricted to the stromal cells, as in the parental N3D tumors, but extending to the tumor cells (Masson's trichrome staining).

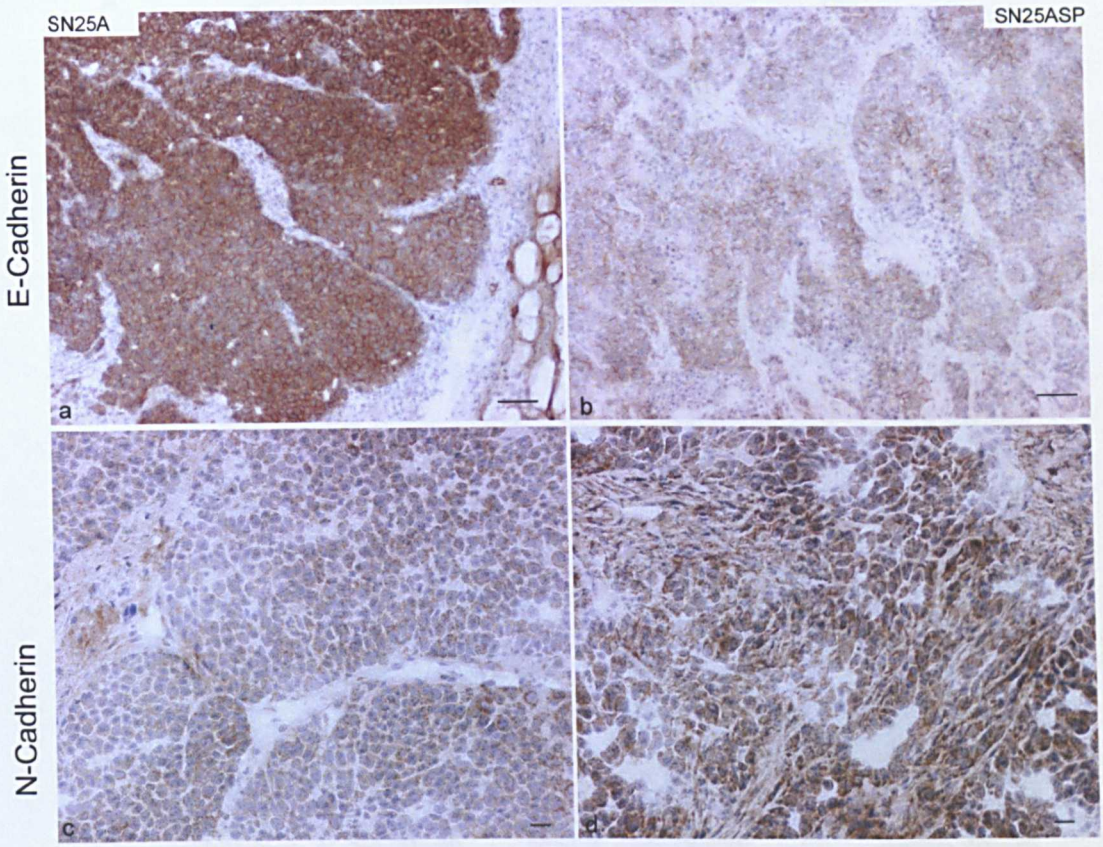

Fig.5 In vivo analysis of EMT markers in SN25A and SN25ASP tumors.

Expression of E-Cadherin and N-Cadherin in SN25A and SN25ASP tumors. Frozen sections of SN25A and SN25ASP tumors obtained from BALB/c mice were stained with Abs to E-cadherin **(a-b)** and N-cadherin **(c-d).** The picture shows the high expression of E-cadherin in SN25A tumor but not in the SN25ASP counterpart in which tumor cells gain the expression of N-cadherin. In SN25A tumors E-cadherin shows a cell membrane localization that is functional for the epithelial phenotype. On the contrary in SN25ASP tumor were E-cadherin is almost lost, N-cadherin shows a nuclear pattern, that is functional for EMT (original magnification x100) (**a-b**); (original magnificationx200) (**c-d**).

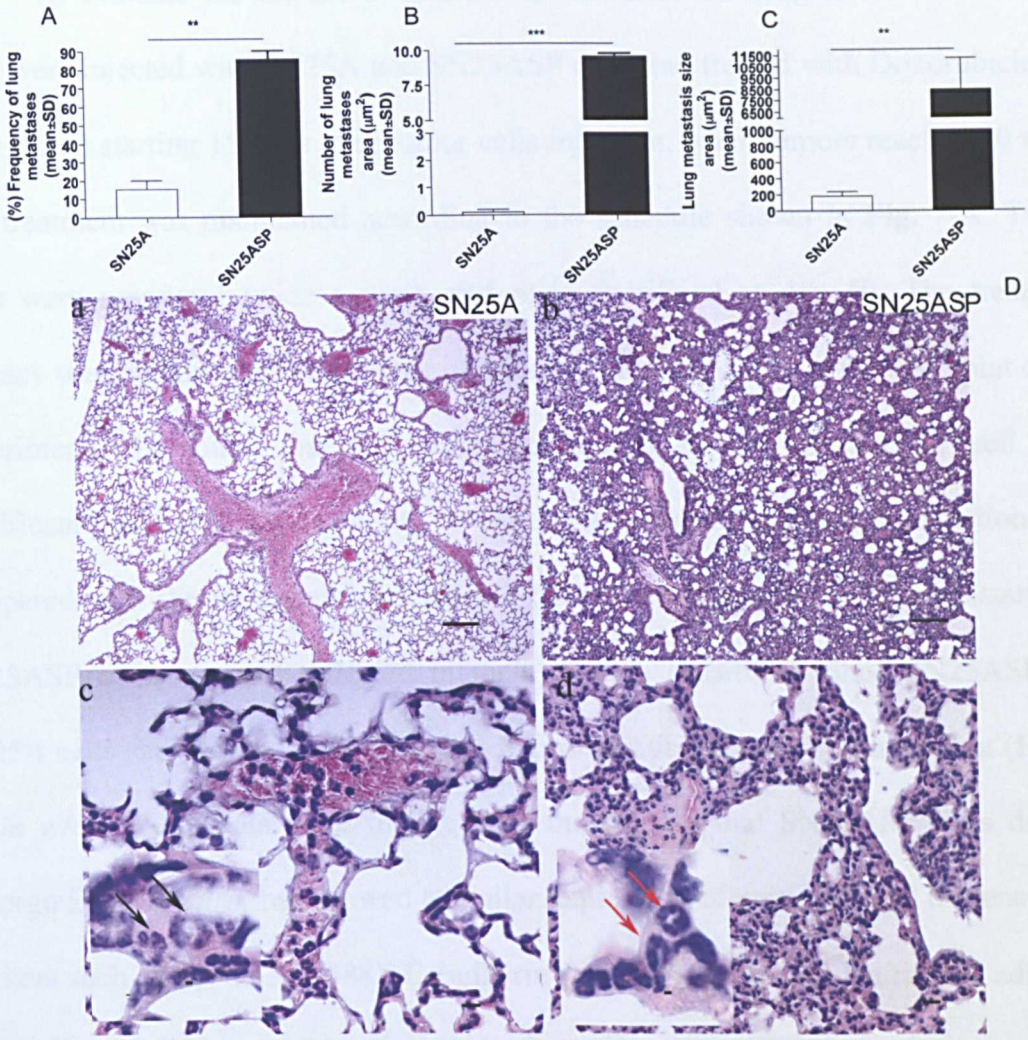

Fig. 6 Tumor-derived SPARC promotes tumor aggressiveness and lung metastasis.

SN25A and SN25ASP cell lines were injected in BALB/c mice s.c. and metastases were checked 40 days after tumor injection (**A**) Quantification of lung metastasis frequency (mice with lung metastases per total mice %) after SN25A and SN25ASP cell lines injection in BALB/c mice. Results are reported as mean values (±SD) expressed as percentage n=10 (Student's t-test p=0.095) (**B**) Metastatic lesions for lung surface were counted in the group described in (**A**). The graph shows the average number of metastases (±SD) in each group. The number of metastatic lesions was counted considering a total number of 10 areas for lung (Student's t-test p=0.001). (**C**) Digital quantification of lung metastasis burden obtained by objective morphometric analysis using ImageJ. The values reported in the graph represent the mean area occupied by tumor indicated as μm^2. The analysis included a group of n=10 mice; error bars indicated SD (Student's t-test p=0.0081). (**D**) Representative image of lungs tissues isolated from SN25A and SN25ASP tumor bearing mice. Lungs from SN25ASP but not SN25A tumors show an overall increased cellularity depending from the presence of tumor cells invading the normal parenchyma structure **(a-b).** Notably the presence of lung metastases in SN25ASP tumor-bearing mice correlated with the enrichment in pro-tumoral (circular nuclei, black arrows) myeloid cells infiltration (original magnification x200). By contrast, lungs from SN25A tumor-bearing mice showed the presence of anti-tumor (hypersegmented nuclei, red arrows) myeloid cells (**a-c**). This data represents the first observation of SPARC-expression in tumor cells skewing the myeloid cells phenotype.

4.1.3 EMT determines Doxil (Pegylated Doxorubicin) resistance

To evaluate the impact of SPARC-driven EMT on drug resistance, BALB/c mice were injected with SN25A and SN25ASP cells and treated with Doxorubicin (10 mg/kg, i.v.) starting 15 days after tumor cells injection, when tumors reached 10 mm^3. The treatment was maintained according to the schedule shown in **Fig. 7-A**. Tumor sizes were measured twice a week and mice sacrificed at day 40. The treatment efficacy was calculated as percentage of tumor volume reduction at the end point of the experiment. We found that the overexpression of SPARC in SN25A cell lines significantly reduced the sensitivity to Doxil (60% vs 90% of tumor reduction rate) compared with the wt counterpart (**Fig. 7-B**). Interestingly, the *in vivo* resistance of SN25ASP cells was not reflected in their *in vitro* sensitivity since SN25ASP and SN25A cells showed the same reduction in proliferation upon Doxil treatment (**Fig. 7-C**) *in vitro*. These data were in line with the finding that SN25ASP cells did not undergo EMT *in vitro,* but showed a similar expression of epithelial and mesenchymal markers such as Ep-CAM (G88), E-cadherin (E-CAD), ß-catenin, neural cell adhesion molecule (N-CAM), Vimentin and integrin ß1 (CD29) as assessed by immunefluorescence (**Fig.8-A**) or flow cytometry (**Fig.8-B**). The only significant difference was related to the increased expression of CD29 in SN25ASP compared to SN25A in agreement with published data showing SPARC directly associated with CD29 [139, 140](**Fig. 8-B**). Collectively, these data suggest that the EMT-driven by SPARC is not cell-intrinsic, occurs *in vivo* and not *in vitro*, and is therefore likely to need the support of host cells either from the immune system or the mesenchymal reservoire.

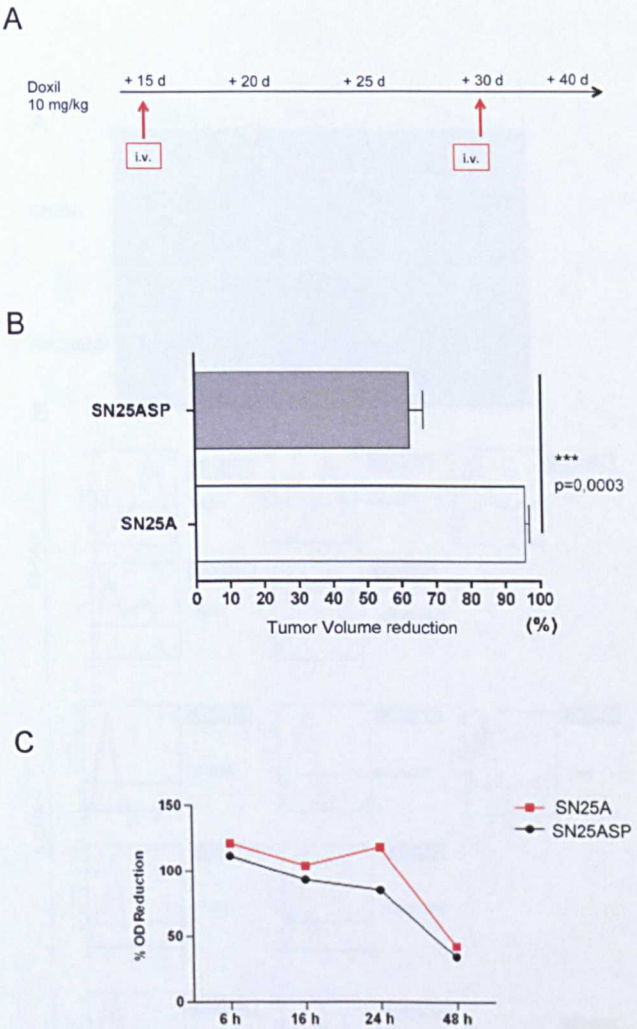

Fig. 7 SPARC overexpression increases in vivo Doxil resistance.

(A) SN25A and SN25ASP cell lines were injected in BALB/c and tumors were treated twice, on days 15 and 30, with 10 mg/kg of Doxil according to the schedule reported. **(B)** The efficacy of Doxorubicin treatment on SN25A and SN25ASP tumors was calculated at day 40 and showed as % of tumor volume reduction (Mean tumor volume (MTV) untreated-MTV treated/MTV Untreated*100) ***$p<0.001$ n=20. Data represent a pull of 4 independent experiments each one of n=5 /group. (**C**) In vitro Doxil cytostatic effect. Cells were treated with Doxil for 24 h, 48 h, and 72 h. Proliferation was evaluated with MMT assay as ratio of OD values referred to untreated cells.

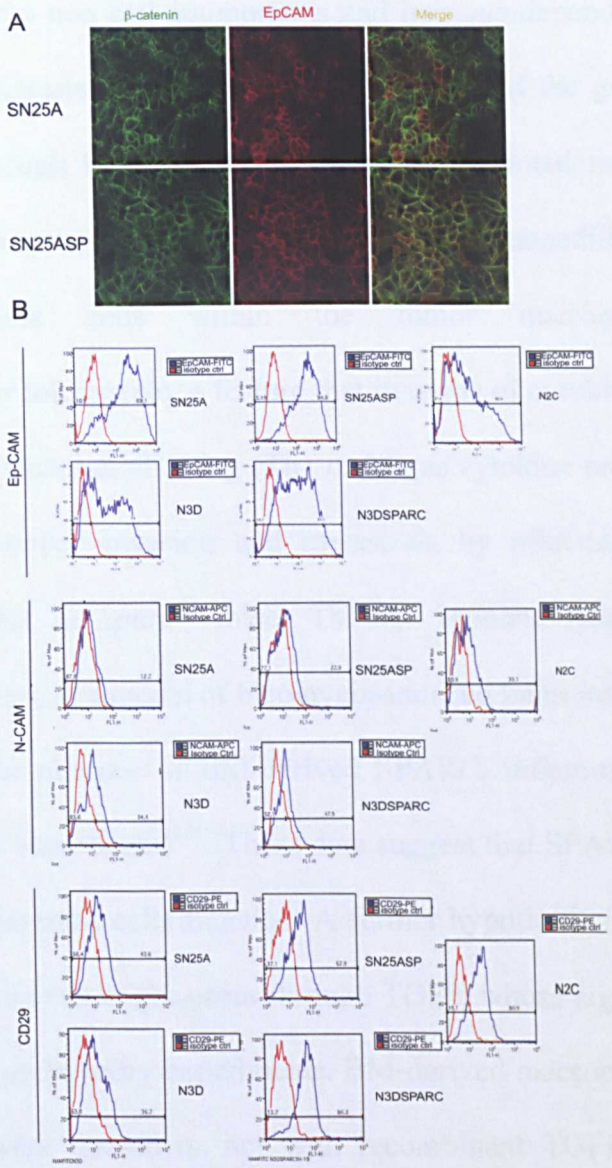

Fig. 8 Tumor-derived SPARC is not sufficient to induce EMT in vitro.

(A) Immunofluorescence analysis of B-catenin and Ep-CAM expression by SN25A and SN25ASP cells. SN25A and SN25ASP cells were seeded onto poly-lysine coated glasses for 24h at 70% of confluence, fixed and stained with mAb to b-catenin and Ep-CAM. Both cell lines express both markers on the cell membrane as typical for epithelial cells. (**B**) Expression of Ep-CAM, N-CAM and CD29 by SN25A and SN25ASP, N3D, N3DSPARC, N2C cells in vitro. FACS analysis shows tumor-derived SPARC do not influences Ep-CAM and N-CAM regulation in SPARCNeuT derived mammary cell lines The only difference observed is the increased CD29 expression by the SN25ASP in comparison to SN25A.

4.1.4 SN25ASP tumors do not undergo EMT in vivo if injected into Sparc$^{-/-}$ mice.

The concept of a non cell-autonomous and immune-dependent EMT is recent and relatively new. Santisteban and colleagues[141] described the generation of breast cancer stem cells through EMT as dependent on a functional immune system and suggested that EMT may be a potential mechanism of immunoediting. In this line, the skewing of immune cells within the tumor microenvironment from immunosuppressive or tolerogenic, a feature that in terms of cytokines was reported as Th2 or M2, to tumor tumor-eradicating (Th1 or M1 as cytokine profile) may have the potential to reduce tumor invasion and metastasis by affecting EMT. We have previously shown that in *Sparc*$^{-/-}$ mice, Th1/M1 immune responses[118] are more pronounced. In addition, in a model of bleomycin-induced pulmonary fibrosis, we have also found that in the absence of BM-derived SPARC, inflammation increases and pulmonary fibrosis is exacerbated[121]. These data suggest that SPARC may be involved in the regulation of immune cells function. A further hypothesis is that such SPARC-regulation on immune cells might occur through TGFß, whose signaling pathway may lead to EMT. In our preliminary experiments, BM-derived macrophages from *Sparc*$^{+/+}$ and *Sparc*$^{-/-}$ mice were treated or not with recombinant TGFß to test the down-modulation of TNF-α expression, a mechanism that is implicated in the resolution of inflammation. We found that *Sparc*$^{+/+}$ but not *Sparc*$^{-/-}$ were able to down-modulate TNF-α after TGF-ß stimuli (**Fig.9-A**). Interestingly, *Sparc*$^{-/-}$ macrophages were not affected for TGF-ß production (**Fig. 9-B**) that was even greater than in *Sparc*$^{+/+}$ macrophages. This feature is shared by other cell types, i.e. fibroblasts and MSC, in which SPARC affects TGF-ß signaling, but not its production [114]. The tight link between SPARC and the immune system suggests its possible involvement in immune-driven EMT *in vivo*. In other words, if our EMT phenotype was immune-mediated, the

injection of SN25ASP tumor cells in *Sparc*$^{-/-}$ mice whose immune system is per se skewed towards a Th1M1 phenotype could prove our hypothesis. Thus SN25A and SN25ASP cell lines have been injected in *Sparc*$^{-/-}$ mice. H&E staining of those tumors showed that SN25ASP tumors no longer displayed EMT features and did not invade the surrounding tissues compared with as they did in *Sparc*$^{+/+}$ mice (**Fig. 10A-D**). IHC analysis also showed that in SN25ASP tumors from *Sparc*$^{-/-}$ mice, E-cadherin was mainly expressed in the cell membrane, while it was preferentially expressed in the cytoplasm in tumors from *Sparc*$^{+/+}$ mice. In agreement with the retention of an epithelial phenotype, the SN25ASP tumors injected into *Sparc*$^{-/-}$ mice were more sensitive to Doxil growth-inhibition compared with the SN25ASP injected into *Sparc*$^{+/+}$ mice (**Fig. 11**). By contrast, parental SN25A was equally sensitive to Doxil treatment in both strains. These data suggest that EMT *in vivo* in SN25ASP tumors is likely to be promoted by an immunosuppressive (Th2/M2) phenotype molded by pro-tumor myeloid cells.

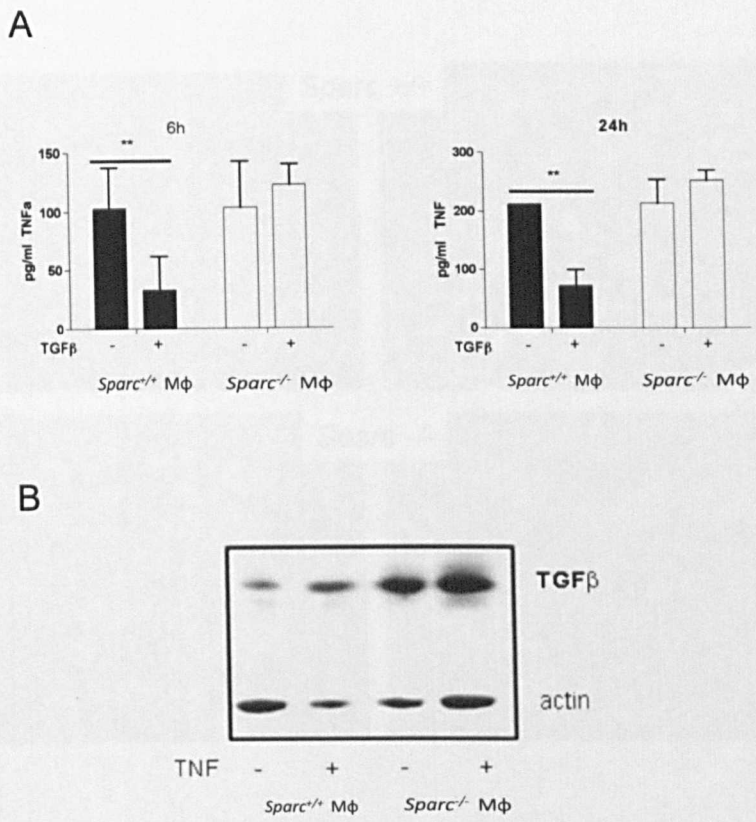

Fig. 9 TNF and TGFß1 are reciprocally regulated in macrophages.

(**A**) TGF-ß inhibition of TNF- production by BM-derived macrophages. BM-macrophages were seeded into a 96-well plate and treated with TGF-ß-1 (10 ng/ml) for 6 and 24h and evaluated for TNF production by ELISA: TGF-ß1 inhibited TNF production by *Sparc*$^{+/+}$ but not *Sparc*$^{-/-}$ macrophages. (**B**) TGF-ß1 production is not defective in *Sparc*$^{-/-}$ macrophages. WB analysis of TGFb1 production by *Sparc*$^{+/+}$ and *Sparc-/-* shows that *Sparc*$^{-/-}$ macrophages are competent for synthesizing TGF-ß-1 basally and upon TNF stimulation. BM-derived macrophages from *Sparc*$^{+/+}$ and *Sparc*$^{-/-}$ mice were seeded into 6-well culture plate in IMDM 2% FCS in the presence of recombinant murine TNF (10 ng/ml) for 16h. Cells were then harvested and analysed for TGF-ß production by Western Blot by using a specific purified rat anti-mouse TGF-ß.

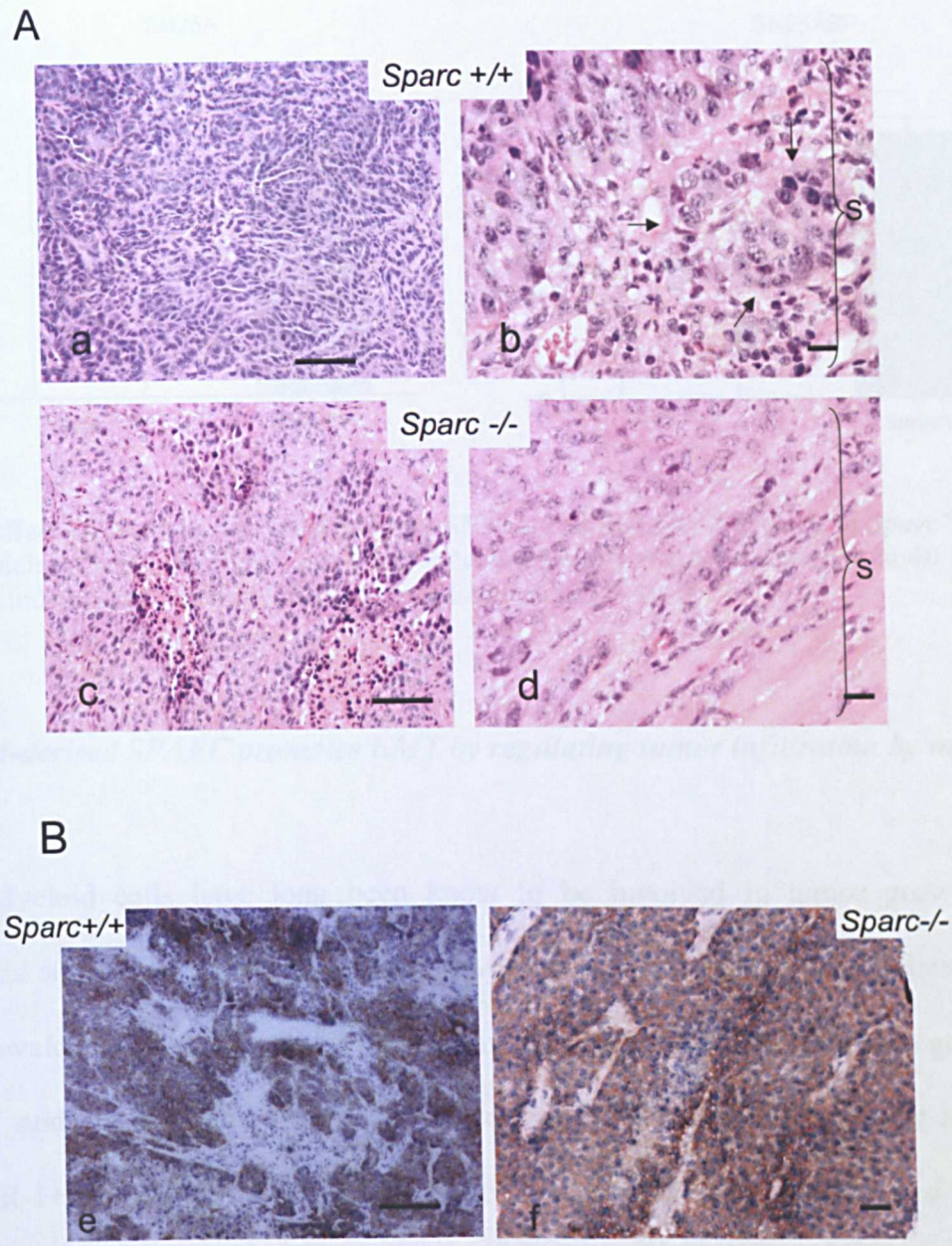

Fig. 10 Histological analysis of SN25ASP tumors from *Sparc*$^{+/+}$ and *Sparc*$^{-/-}$ mice.

(A) H&E shows that SN25ASP tumors from *Sparc*$^{-/-}$ contrary to that from *Sparc* $^{+/+}$ mice (**a-b**), lost any EMT feature with tumor cells rounded (**c**) and not invading (arrows) the surrounding stromal (**d**) margins (**S**, graph parenthesis); **(B)** E-cadherin expression in SN25ASP tumors from *Sparc*$^{-/-}$ mice is mostly on the cell membrane, while cytoplasmic in tumors from *Sparc*$^{+/+}$ mice.

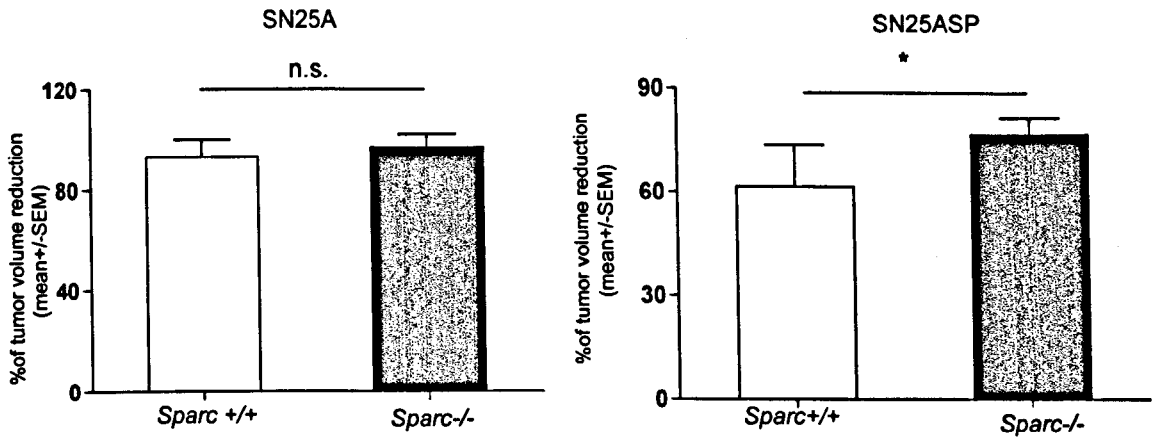

Fig.11 Effect of Doxorubicin treatment on SN25A and SN25ASP growth in *Sparc*$^{-/-}$ mice. Doxorubicin efficacy in *Sparc*$^{-/-}$ mice was calculated as % of tumor reduction at 40 day. A pull of 4 independent experiments (n=5, each experiment) is shown.

4.1.5 TM-derived SPARC promotes EMT by regulating tumor infiltration by myeloid cells

Myeloid cells have long been know to be involved in tumor growth and metastasis and recently their possible involvement in EMT was also hypothesised [78, 142]. We evaluated myeloid cells recruitment in SN25A and SN25ASP tumors grown in *Sparc*$^{+/+}$ and *Sparc*$^{-/-}$ mice. In *Sparc*$^{+/+}$ mice, we found a higher number of myeloid cells (GR-1+) infiltrating SN25ASP tumors compared with the non transduced SN25A tumors. **(Fig. 12 A-B)** When both cell lines were injected in *Sparc*$^{-/-}$ mice, we found no difference in the number of infiltrating myeloid cells in the tumors, in agreement with the hypothesis that the absence of host-derived SPARC activates the immune system **(Fig.12 C-D)** also by promoting myeloid cells recruitment [138]. Thus, if the hypothesis of the immune-mediated EMT is true, myeloid cells recruited in *Sparc*$^{+/+}$ mice by SN25ASP tumors should be functionally different from those recruited in the total absence of SPARC. In fact, an interesting corroborating evidence emerged from the analysis of tumors from *Sparc*$^{-/-}$ mice: in these tumors the distribution of Gr-1 cell

seemed to attack tumors creating area of necrosis and vascular lacunae (**Fig. 12-E**). We have previously demonstrated that GR-1+ neutrophils isolated from agar plugs injected into the dorsal skin of mice[143] are able to inhibits tumor cells proliferation. Thus, we performed an *in vitro* proliferation assay in which SN25A and SN25ASP cells were co-cultured for 24h with different doses of PMN from *Sparc*$^{+/+}$ and *Sparc*$^{-/-}$ mice. We found that SN25A was more sensitive to the citostatic effect of *Sparc*$^{+/+}$ PMN as, even at the lower PMN-tumor cells ratio, the inhibition of tumor proliferation was nearly 70% in SN25A while it was 10-20% in SN25ASP, indicating that, as for our hypothesis, this cell line is capable to re-direct PMN to a more tumor supportive phenotype (**Fig. 13-A**). Interestingly, this effect was partially inhibited in the presence of *Sparc*$^{-/-}$ PMN (30-50% growth inhibition) suggesting that in absence of SPARC, PMNs increase their capability to kill tumor cells (**Fig. 13-B**). In the *Sparc*$^{-/-}$ host, the reduced ECM deposition favors myeloid cells infiltration, as we have previously demonstrated. However, in the *Sparc*$^{-/-}$ host, myeloid cells are more activated and capable of attacking tumor cells, explaining why in both SN25A and SN25ASP tumors, we have areas of necrosis related to PMN recruitment. Moreover, in tumor from *Sparc*$^{-/-}$ mice, IL10 is reduced and a less suppressive environment is expected. Another way to test whether *Sparc*$^{-/-}$ GR-1 cells are more prone to becoming effector rather then protumoral cells, was to isolate notably immunosuppressive myeloid cells (MDSCs) from tumor bearing SPARC-NeuT and BALB-NeuT mice[49], to inject them into SN25ASP bearing mice and evaluate the effect on tumor growth (**Fig. 14**). We found that MDSCs from *Sparc*$^{+/+}$ tumor-bearing mice significantly increased the growth of SN25ASP tumors compared with mice that did not receive MDSCs i.v. By contrast, MDSCs from *Sparc*$^{-/-}$ tumor-bearing mice, despite their increased production of VEGF, a factor that was involved in their tumor-promoting activity, were less

efficient in sustaining tumor growth. Finally to demonstrate that defective-myeloid cells in *Sparc*$^{-/-}$ mice are responsible for the reversion of the EMT phenotype we performed an experiment in which tumor-bearing *Sparc*$^{-/-}$ mice were adoptively transferred with myeloid cells from wt mice and tumors evaluated for EMT features. In detail *Sparc*$^{-/-}$ mice were injected with SN25ASP cells and transferred with $1*10^6$ myeloid cells once a week considering a size of 8 mm^2 the starting point for myeloid cell transfer. We found that myeloid cells from wt, but not from *Sparc*$^{-/-}$ mice were able to promote EMT in SN25ASP tumors injected into *Sparc*$^{-/-}$ mice **(Fig.15)**. Taken together, these data suggest that chemotherapy resistance may be related to the acquisition of an EMT phenotype and that the interaction with the immune system is very relevant to the acquisition of such phenotype. Within these cross-communications, SPARC might be relevant in two ways:

1. SPARC produced by tumor cells is required for EMT. In line with this, SPARC-negative tumor cells do not undergo EMT *in vivo* in *Sparc*$^{+/+}$ mice;

2. SPARC produced by host cells sustains EMT *in vivo*, by affecting myeloid cells functionality.

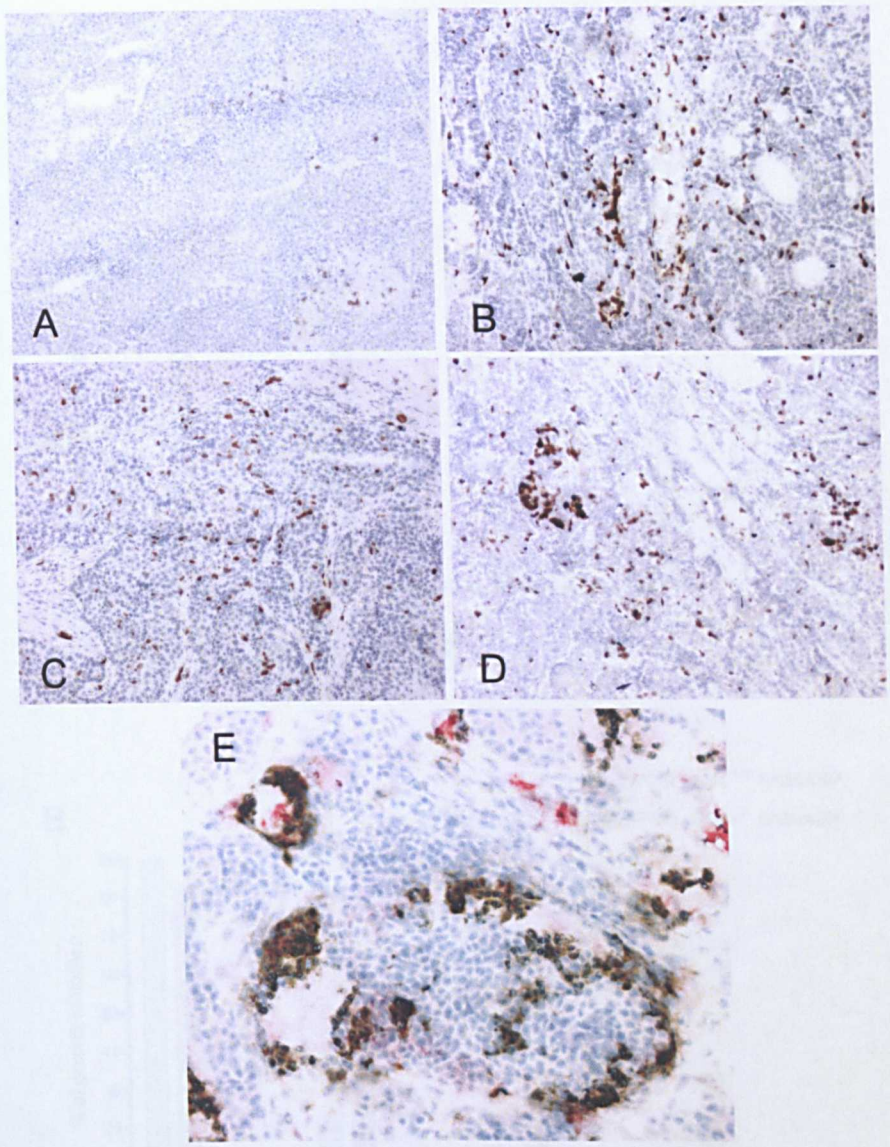

Fig.12 Myeloid cells recruitment in SN25A and SN25ASP tumors from *Sparc*$^{+/+}$ and *Sparc*$^{-/-}$ mice. Myeloid cells were stained with a mAb to GR-1. In *Sparc*$^{+/+}$ mice a major number of myeloid cells were recruited into SN25ASP tumors (**A**) in comparison to the parental ones (**B**). In *Sparc*$^{-/-}$ mice a large number of myeloid cells infiltrated both SN25A (**C**) and SN25ASP (**D**) tumors. (**E**). GR-1+ cells attack tumor cells into SN25A tumors from *Sparc*$^{-/-}$ mice such to create area of necrosis and vascular lacunae as showed by a staining of GR-1 cells (brown) with CD31 (red) that identifies vascular structures.

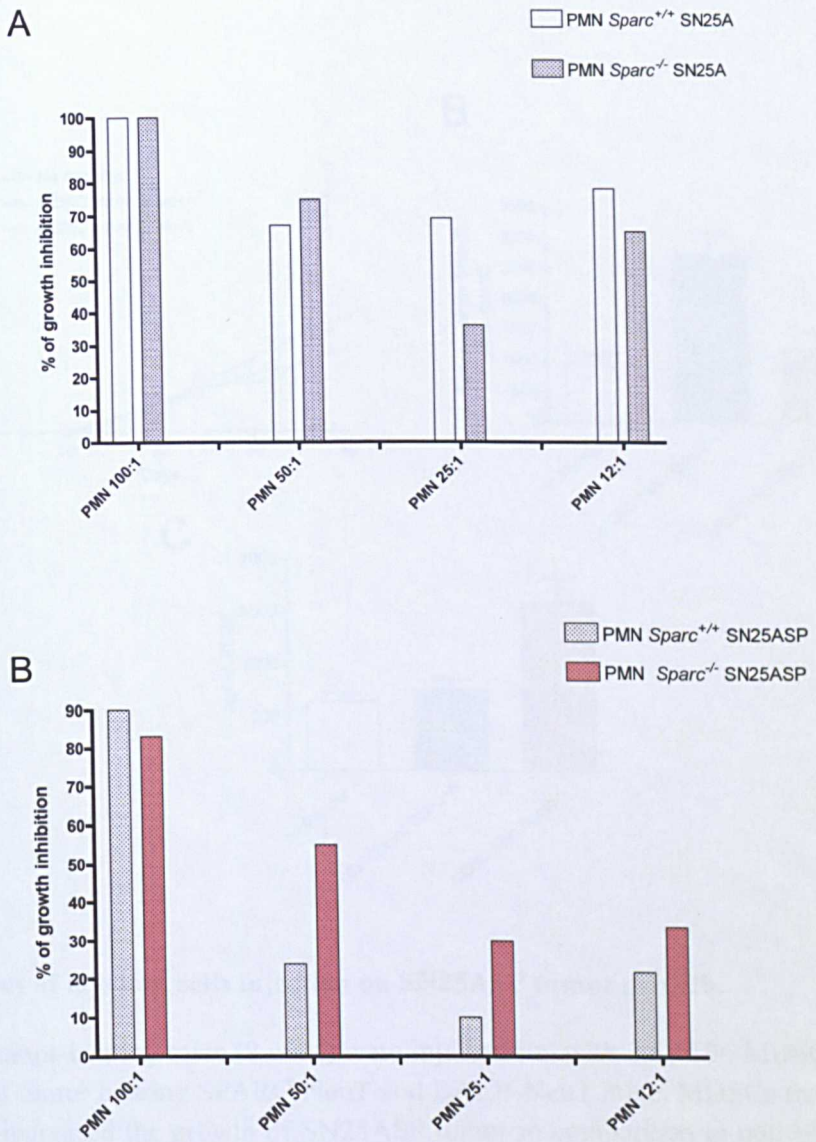

Fig. 13 In vitro proliferation assay of SN25A and SN25ASP cell lines co-cultured with *Sparc*$^{+/+}$ and *Sparc*$^{-/-}$ PMN. The capability of PMN from *Sparc*$^{+/+}$ mice to inhibit tumor proliferation is reduced in SN25ASP in comparison to the parental cell line (**A-B** white-grey bars). This effect is partially reverted in the presence of PMN from *Sparc*$^{-/-}$ mice (**B**).

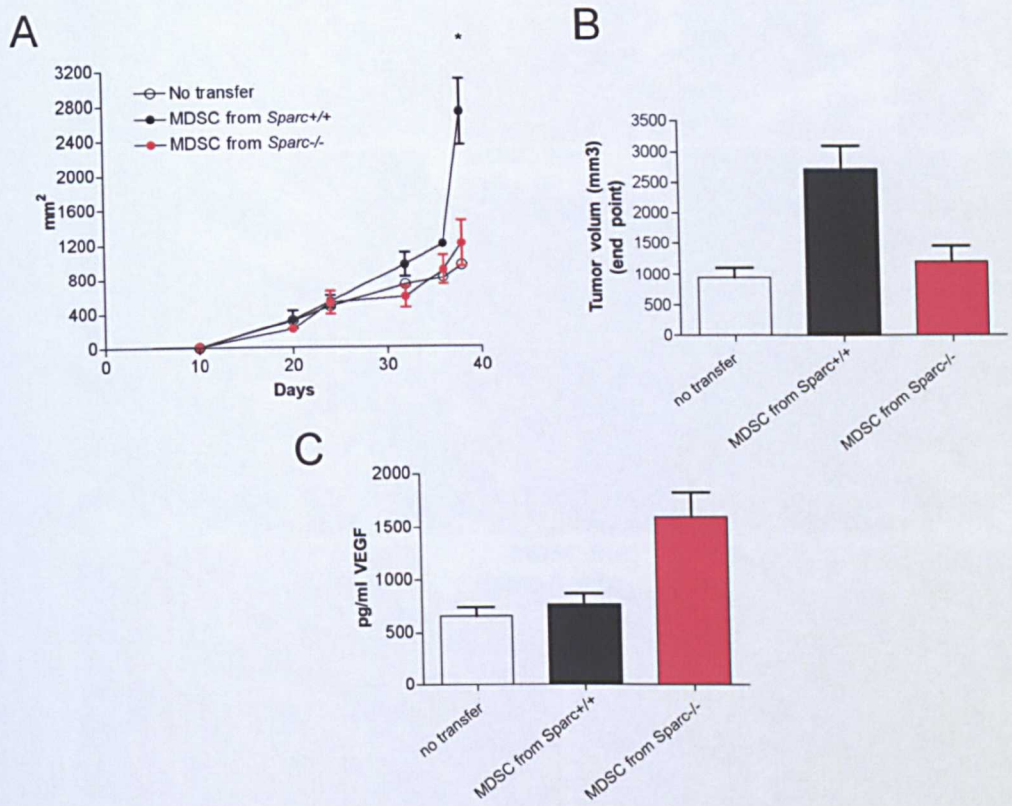

Fig. 14 Effect of myeloid cells injection on SN25ASP tumor growth.

SN25ASP tumor-bearing mice (8 mm^3) were injected i.v. with 2,5 *106 MDSC isolated from the spleen of tumor bearing SPARC-NeuT and BALB-NeuT mice. MDSCs from *Sparc*$^{+/+}$ but not *Sparc*$^{-/-}$ increased the growth of SN25ASP tumor in comparison to untreated mice (**A-B**) although MDSCs from *Sparc*$^{-/-}$ mice were most effecting in mobilizing VEGF in the serum (ELISA assay) (**C**), a factor that has been implicated in mammary tumors growth.

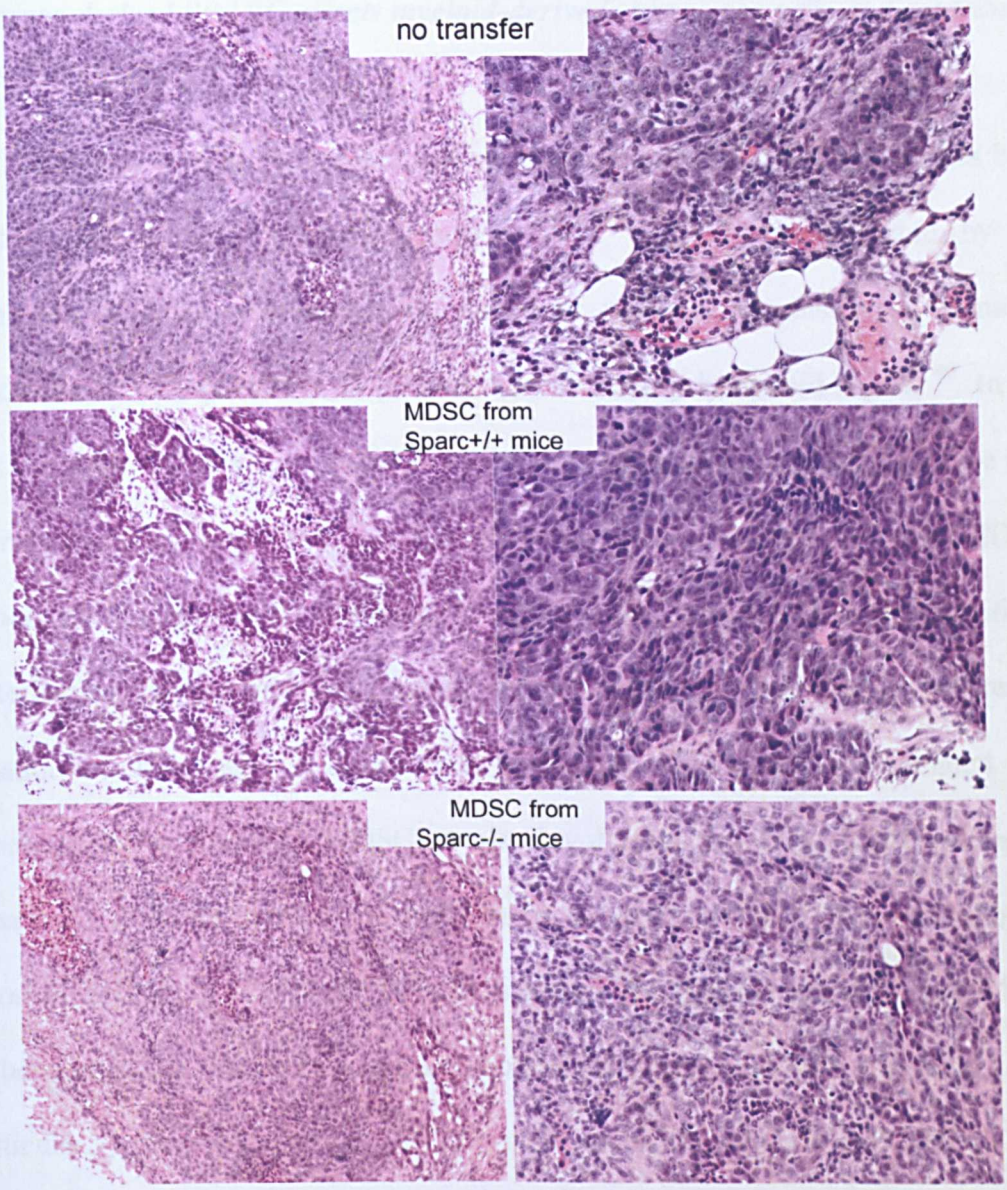

Fig.15 MDSCs from *Sparc*$^{+/+}$ mice induces EMT in vivo.

Sparc$^{-/-}$ mice were injected with SN25ASP cells and adoptively transferred with MDSCs isolated from tumor-bearing *Sparc*$^{-/-}$ and *Sparc*$^{+/+}$ donors. Forty-days later recipient mice were sacrificed and tumor histologically evaluated for EMT. We found that myeloid cells from *Sparc*$^{+/+}$, but not from *Sparc*$^{-/-}$ mice were able to promote EMT in SN25ASP tumors injected into *Sparc*$^{-/-}$ mice as H&E staining showed an increased tumor grade, the presence of spindle-shape cells, the loose of tumor septa and margins.

4.1.6 Tumor-derived SPARC affects myeloid-derived suppressor cells and contribute to tumor immunosuppression

The injection of transplantable murine breast carcinoma cells in mice has been associated with marked leukemic reaction [144, 145, 146, 147] characterized by the accumulation of neutrophils within the blood or with the expansion of immature myeloid cells including MDSC, in primary and secondary lymphoid organs [49]. In this context the spleen is now considered a crucial organ for tumor-induced tolerance as it is the main lymphoid organ that undergoes myeloid-derived suppressor cells (MDSC) expansion during tumor development in mice. This suggests that the functional characterization of myeloid cells could be performed in the spleen, where the purification of these cells is easier than in tumors. Beside being associated with immunosuppressive activities, MDSC are also involved in promoting EMT, prompting the idea that a different myeloid cells expansion or activation might be induced by the injection of SN25A or SN25ASP tumors in mice. The fine discrimination of MDSC could be exerted, by FACS, by using a mAb to Ly6C combined with a mAb to Ly6G. In particular, within the gate of CD11b+ cells, monocytic MDSCs (M-MDSC) are defined as Ly6G ^{low}/Ly6C^{high} whereas granulocytic MDSCs (G-MDSC) are Ly6G ^{high}/Ly6C^{low} [148]. Under this premises, I analyzed peripheral blood, spleen and BM of mice bearing SN25A versus SN25ASP tumors. I found that both cell lines determined an expansion of myeloid cells and of their precursors in the spleen and bone marrow (**Fig.16**). The only minor difference I observed among the two cell lines was in the peripheral blood, where I found a higher percentage of M-MDSC in SN25ASP tumor-bearing mice (**Fig. 17**). As these differences were too small to explain the different phenotypes of SN25A and SN25ASP tumors *in vivo,* we considered the possibility that tumor-derived SPARC might affect the modulation of the phenotype of myeloid cells,

rather than just promoting their expansion. The phenotype of myeloid cells could be evinced by gene expression or through a functional assay based on the capability of MDSC to suppress the proliferation of CD4 and CD8 T cells. In the first case the evaluation of myeloid cells phenotype through gene expression was based on some genes that mark MDSCs and overlap for expression those distinguishing N2 and N1-polarized neutrophils [149, 150]. Indeed MDSC and N2-neutrophils express Arginase-I, CCL2, CCL5, VEGF, MMP9 and STAT3 whereas N1-neutrophils express CCL3 but are low for CCL2, CCL5, Arginase and STAT3. I have purified M-MDSC and G-MDSC from the tumor and the spleen of SN25A and SN25ASP-tumor bearing mice by magnetic beads separation, and performed a quantitative PCR analysis to check the differential expression of the above listed chemokines. I found that M-MDSC isolated from the spleen of SN25ASP tumor-bearing mice express significantly higher levels of CCL2, CCL5, and STAT3 compared with M-MDSC isolated from the spleen of SN25A-bearers **(Fig. 18-A)**. Confirmatory results were obtained from MDSC isolated from the tumor, where I found that CCL2 gene was more highly expressed by M-MDSC isolated from SN25ASP rather than from SN25A tumors (20 vs 40 fold change expression) **(Fig. 18-B)**. Accordingly I have compared the ability of spleen-purified MDSC from SN25A and SN25ASP-tumor-bearing mice to suppress a-CD3 and a-CD28 induced T cells proliferation. I found that MDSCs spleen-purified from SN25ASP tumor bearing mice have a higher capacity to suppress T cells proliferation **(Fig. 19-A-B)**.

These data indicates that M-MDSC induced by SN25ASP are more suppressive than those induced by SN25A tumors. Thus, tumor-derived SPARC modulates the phenotype of tumor-induced MDSCs toward immunosuppression. In agreement, *in vivo* analysis of cytokine production showed an increased production of IL-10 the most potent immunosuppressive cytokine in the microenvironment of SN25ASP tumors compared with the wt counterpart (**Fig. 19-C**).

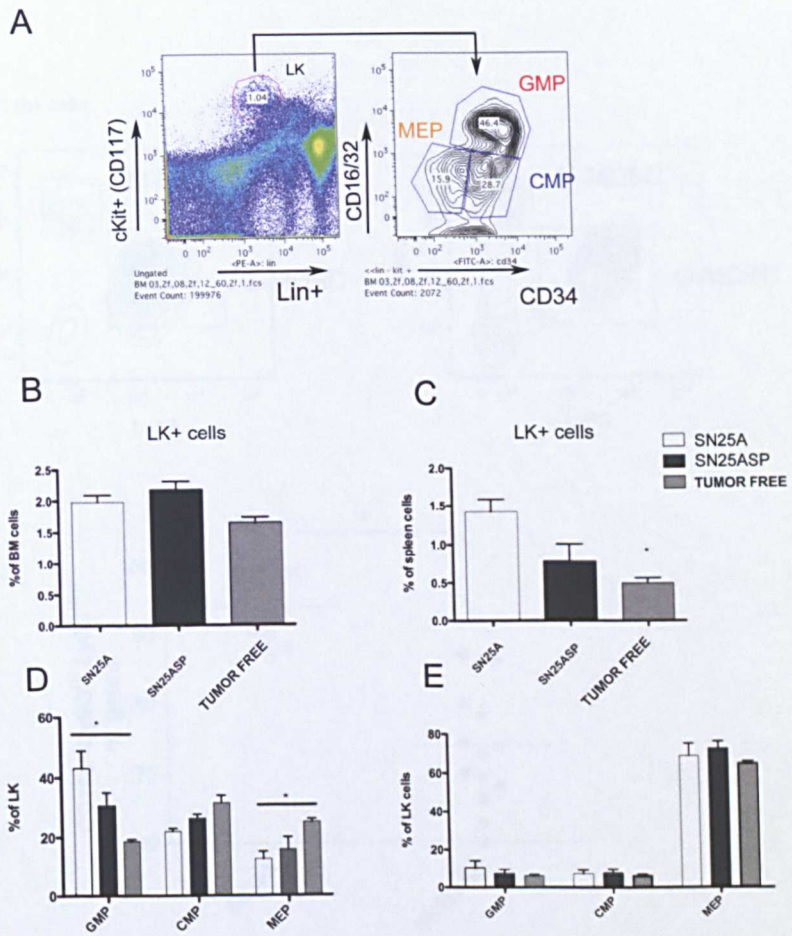

Fig.16 Analysis of myeloid cells precursors populations in BM and SPL of BALB/c injected with SN25A and SN25ASP cell lines.

FACS analysis for myeloid cells precursors was performed in BM and spleen, of BALB/c mice injected with SN25A and SN25ASP cell lines. Lin−cKit+ (LK), common myeloid progenitor (CMP), granulocyte-macrophage progenitor (GMP), megakaryocytic/erythroid progenitor (MEP), have been determined by staining BM or spleen cells with antibodies for lineage (Lin) positive cells including CD3, CD11b, CD45R, Ly-6G, CD4, CD8, Ter-119, for stem cell and progenitors including CD117, CD34, and CD16/CD32. (**A**) Representative plots showing the gating strategy that has been used: LK are gated first and, within the LK gate, the three GMP, CMP and MEP populations are identified according to the different expression of CD34 and CD16/32 (**B-C**). Percentage of LK cells in BM and spleen cell suspension showing an increased frequency of LK+ cells in the spleen of tumor bearing mice injected with SN25A and SN25ASP tumors in comparison to tumor-free mice. This difference was not found in the BM according to the spleen as major organ buffering myeloid cells expansion in mice. (**D-E**) Fraction of GMP, CMP, MEP precursors in BM and spleen showing that SN25ASP tumor-bearing mice have an increased frequency of MEP ($p<0.05$) whereas SN25A tumor bearing mice presented a slightly increased in GMP precursors ($p<0.05$ significance).

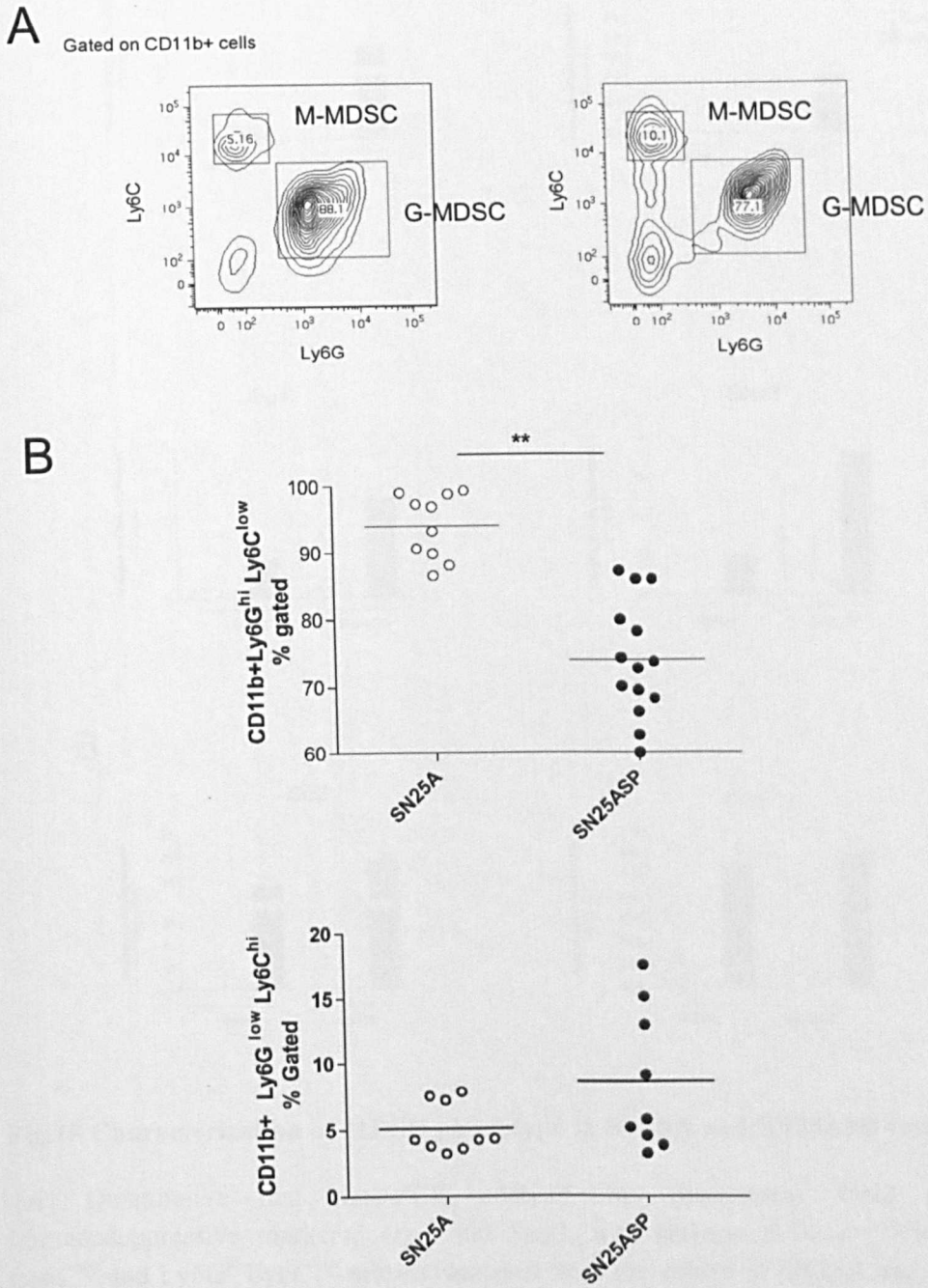

Fig.17 Analysis of MDSC subsets in PBMC of BALB/c injected with SN25A and SN25ASP cell lines.

(**A**) Representative plot showing the gating strategy used to identify the different myeloid cells subsets. Granulocytic-MDSC and Monocytic-MDSC are identified within the gate of CD11b+ cell based on the expression of Ly6G and Ly6C markers. Granulocytic-MDSC are $Ly6G^{hi}$ $Ly6C^{low}$ cells whereas Monocytic-MDSC are $Ly6G^{low}Ly6C^{hi}$ cells. (**B**) Frequency of granulocytic and monocytic MDSC in the PBMC of SN25A and SN25ASP tumor-bearing mice showing the increased frequency of monocytic MDSC in the spleen of SN25SP tumor-bearing mice ($p< 0.05$; *Student t test*).

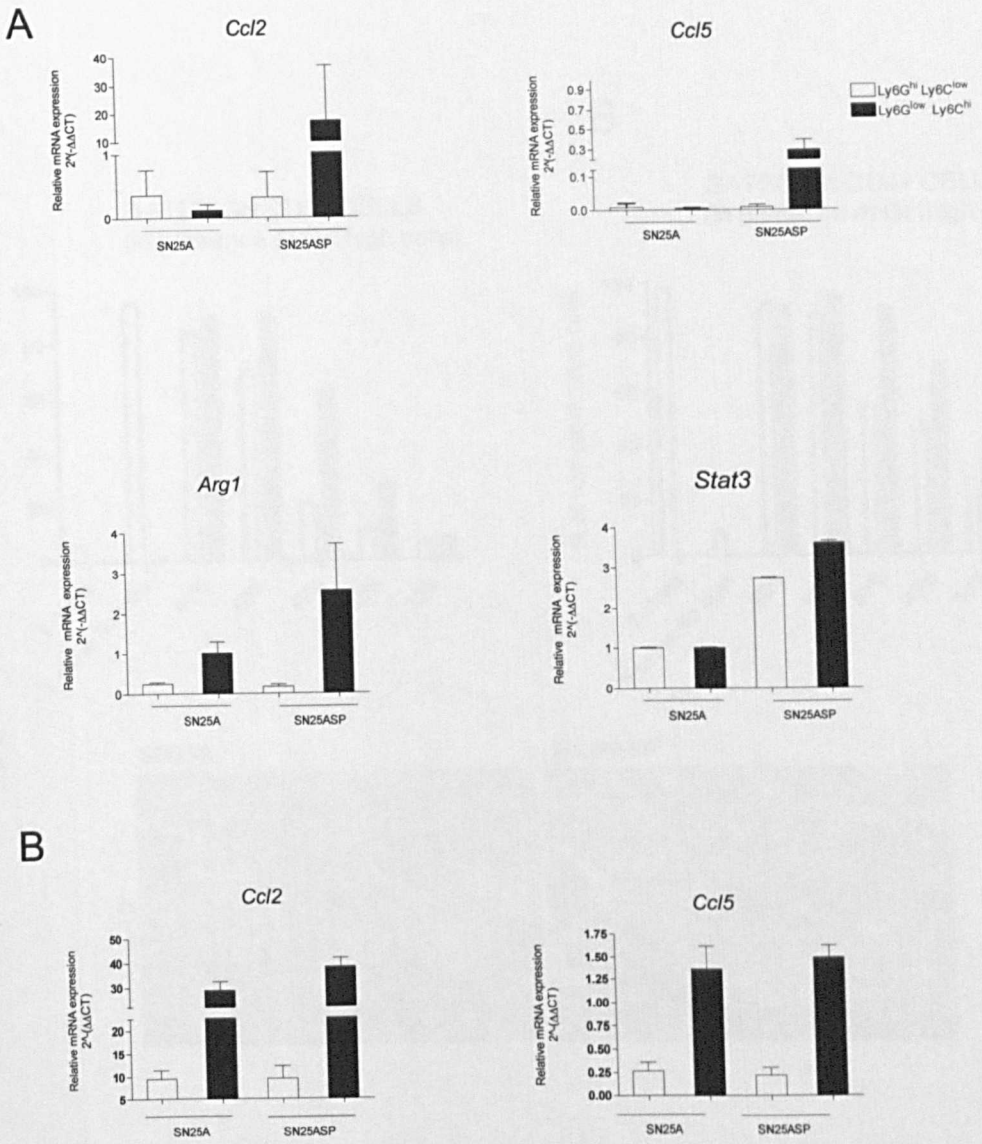

Fig.18 Characterization of MDSC phenotype in SN25A and SN25ASP tumors.

(**A**) Quantitative real time-PCR analysis for protumoral, *Ccl2* and *Ccl5,* or immunosuppressive markers, *Arg1* and *Stat3*, was performed on myeloid cells ($Ly6G^{hi}$ $Ly6C^{low}$ and $Ly6G^{hi}$ $Ly6C^{low}$ subsets) isolated from the spleen of SN25A and SN25SP tumor-bearing mice. The picture shows data from a pool of RNA extracted from n=10/group mice. Data are representative of 3 independent experiments. The fold change in expression of the target genes relative to the internal control gene (GAPDH) is shown. The mean fold change in expression of the target gene is calculated as $2^{-\Delta\Delta CT}$ where ΔΔCT= (*CT*,Target-*CT*,GAPDH)sample- (*C*T,Target-*C*,GAPDH)internal control. (**B**) The same analysis was performed on $Ly6G^{hi}$ $Ly6C^{low}$ and $Ly6G^{hi}$ $Ly6C^{low}$ myeloid cells subsets isolated from the tumor of SN25A and SN25SP tumor-bearing mice. Data are indicative of 2 independent experiments. Overall the analysis shows a significantly increased expression pro-tumoral and immunosuppressive markers in myeloid cells isolated from SN25ASP tumor-bearing mice.

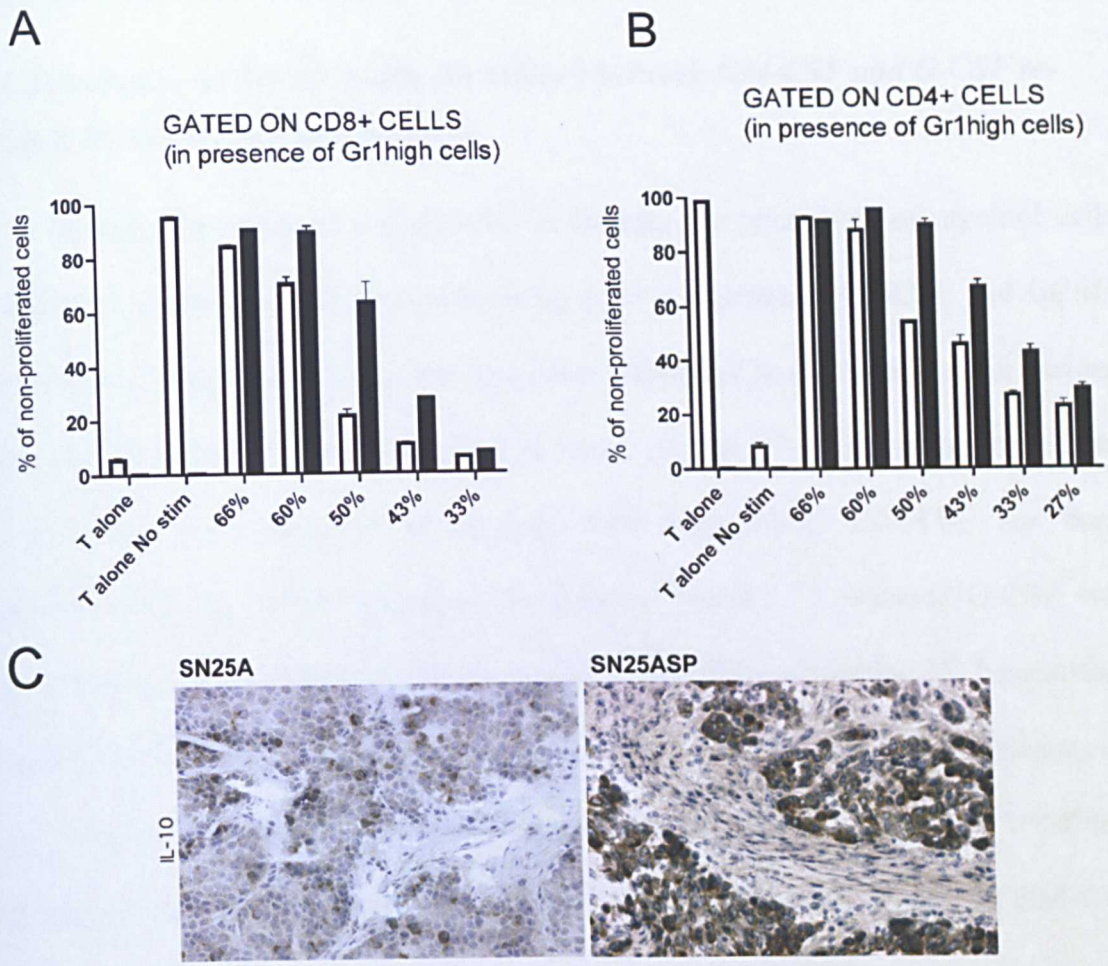

Fig. 19 Tumor-derived SPARC influences MDSC immune suppressive activity.

Myeloid derived suppressor cells were purified using CD11b-conjiugated microbeads and Myeloid-Derived Suppressor Cell Isolation Kit. 4 x 10^5 naïve BALB/c splenocytes have been labeled with CFSE and co-cultured with the different MDSC population at different ratio in presence of 2 mg/ml of soluble anti-CD3 and 1 mg/ml of anti-CD28 to activate lymphocytes. Each sample is seeded in triplicate. Proliferation of CD4 and CD8 T cells has been assessed 2 and 3 days later, by and evaluating CFSE dilution in the CD4+ and CD8+ gated populations. Results are shown as percentage of proliferated cell. (**A-B**). Immune suppressive activity of the two subsets of MDSC from the spleen of SN25A and SN25ASP tumor bearing mice on CD4 and CD8 T cell proliferation in vitro; samples in triplicates. Experiment performed 3 times with overlapping results. (**C**) Immunohistochemistry for IL-10 performed on SN25A or SN25ASP frozen sections showing that SN25ASP tumor cells strongly express IL-10.

4.2 SPARC REGULATION OF MDSC FUNCTIONS: POSSIBLE MECHANISMS

4.2.1 Tumor-derived SPARC shifts the balance between GM-CSF and G-CSF re-directing the tumor microenvironment

Having demonstrated that SPARC modulates the phenotype of myeloid cells we then investigated mechanisms underlying such a regulation. GMCSF and GCSF, are two main important hematopoietic cytokines expressed at different level in various tumor subtype, which act as modulators of tumor growth [151]. Most importantly these two cytokines were involved in myeloid cells polarization: GM-CSF has been implicated with the differentiation of pro-tumoral MDSC [152], whereas G-CSF was linked to the production of anti-tumoral myeloid cells (N1-neutrophils) [153]. I quantified GMCSF and GCSF production in the supernatants of SN25A and SN25ASP tumor cell lines. To this end tumor cells were seeded onto a 6-well plate at a density of $1*10^6$/ml; supernatants were collected after 48 h for ELISA. I found a higher amount of GM-CSF in the supernatants of SN25ASP tumor cell lines compared with the wt counterpart. By contrast, supernatants from the same cell lines showed a decreased amount of G-CSF (**Fig. 20-A-B**). These results indicated that SPARC transduction in SN25A cells shifted the synthesis of G-CSF towards GM-CSF. According to these *in vitro* data, the amount of G-CSF in the sera was higher in SN25A tumor-bearing mice, whereas GM-CSF was undetectable in sera from all groups (**Fig. 20-B**). Collectively these data suggest that the unbalanced production of GMCSF on GCSF within the tumor microenvironment might be responsible for the different re-direction of myeloid cells toward an immunosuppressive phenotype in SN25ASP tumor-bearing mice. These data were in line with the proliferation assay (*Section 4.1.5*; **Fig. 13**), in which we showed that SN25A and SN25SP tumor cells were differently sensitive to the cytostatic effect of

PMN. In particular, SN25A (high G-CSF) was more sensitive to the cytostatic effect of PMN; in fact, at lower doses of PMN (50:1, 25:1 and 12:1 ratio), the inhibition of tumor proliferation was nearly 70%, whereas the same dose of PMN resulted in a 10-20% inhibition in the SN25ASP cell line (producing higher GM-CSF) indicating that, as for our hypothesis, this cell line is capable to re-direct PMN toward a more immunosuppressive phenotype (**Fig. 13**).

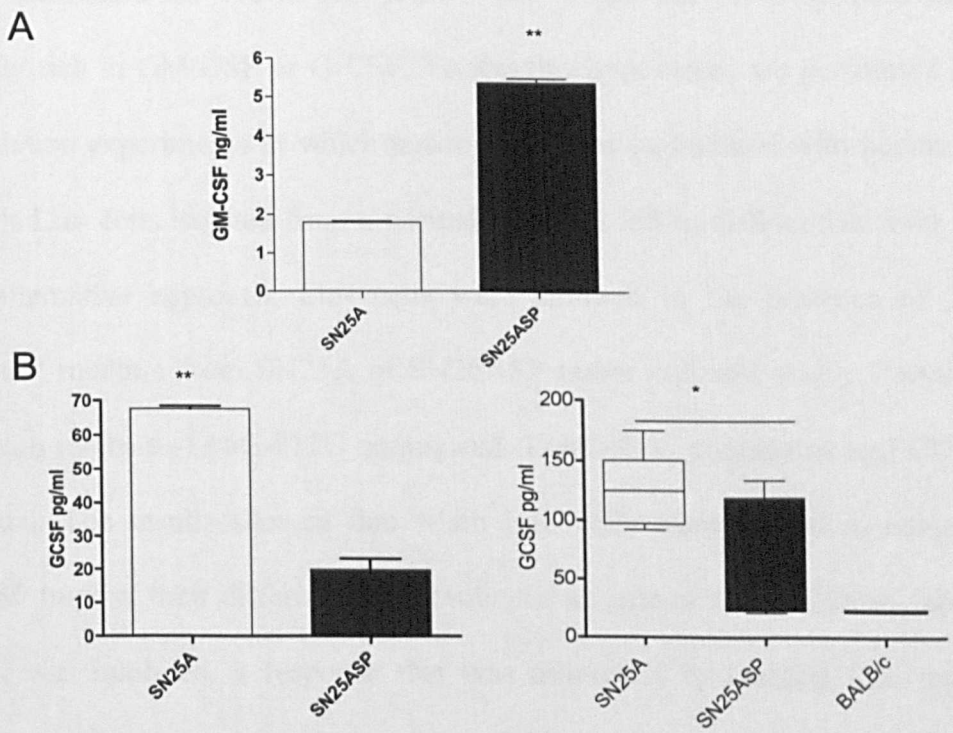

Fig. 20 SPARC shifts the balance between GMCSF and GCSF production.

(A) GMCSF production by SN25A versus SN25ASP cell line was measured through ELISA assay performed on supernatant collected 48 h after cell seeding; *$p < 0.05$, ***$p < 0.001$ (n=2). **(B)** GCSF level in supernatants of SN25A and SN25ASP cell lines and in PB (peripheral blood) of SN25A and SN25ASP BALB/c tumor bearing mice. Two independent experiments are shown.

4.2.2 SPARC blocks the differentiation and maturation of myeloid cells

The immunosuppressive phenotype of MDSC is linked with the maintenance of their "immature" state. The maintenance of this phenotype within the tumor is granted by various growth factors including TGF-β[154]. Our group has contributed to demonstrating that SPARC regulates TGF-β signaling in immune cells, particularly macrophages. We reasoned that the modulatory effect that we found on myeloid cells could be in part related to the ability of SPARC to modulate TGF-β signaling, a function dependent on cell-to-cell contact that might act on a microenvironment differently rich in GM-CSF or G-CSF. To test this hypothesis, we performed *in vitro* differentiation experiments in which tumor cells were co-cultured with hematopoietic stem cells Lin- cells isolated from a normal BM, and left to differentiate over 7 days. As an alternative approach, Lin- cells were cultured in the presence of 30% of conditioned medium from SN25A or SN25ASP tumor cell and at day 7 analyzed at FACS with mAbs to Ly6G-FITC conjugated, Ly6C-APC conjugated and CD11bPE-conjugated. The results showed that when Lin- cells were seeded in contact with SN25ASP tumors, their differentiation, evaluated as gain of CD11b, Ly6C, and Ly6G markers, was inhibited, a response that was mimicked by treating Lin- cells with recombinant TGF-β. By contrast, supernatants from SN25A and SN25ASP tumors were similarly capable of promoting Lin- cells differentiation in different subtypes of myeloid cells without notable differences (**Fig. 21**). The same result was obtained by seeding Lin- cells onto SN25A and SN25ASP tumors monolayer in the presence of a transwell that abrogated the contact between tumor cells and Lin- cells. The results indicated that SPARC modulates the phenotype of myeloid cells by both molding the cytokines microenvironment and by a cell-to-cell contact-mediated effect, probably TGF-ß -dependent.

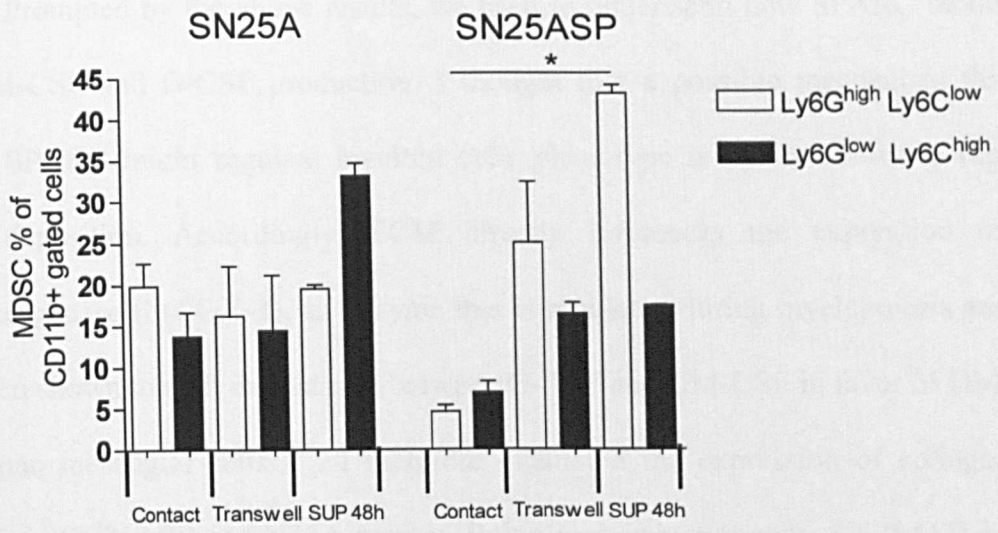

Fig.21 Effect of SPARC-tumor derived on hematopoietic stem cells (LK) differentiation.

Lin- cells were isolated from the BM by negative selection using a Lineage Cell Depletion Kit (Miltenyi). For co-culture experiments, 10^4 Lin-cells were seeded into a 24-well plate in contact or not with a monolayer of SN25A or SN25ASP cells. Alternatively Lin- cells were cultured in presence of 30% of conditioned medium from SN25A or SN25ASP tumor cell. Lin- cells differentiation was evaluated 7 days later at FACS with mAbs to Ly6G-FITC conjugated, Ly6C-APC conjugated and CD11bPE-conjugated. The results showed that when Lin- cells were seeded in contact with SN25ASP tumors their differentiation, the gain of CD11b, Ly6C, and Ly6G markers was inhibited, a condition that was mimicked by the treatment of Lin- cells with recombinant TGF-β. On the contrary supernatants from SN25A and SN25ASP tumors were similarly capable to promote Lin- cells differentiation in the different myeloid cells subtypes without any differences. Data are representative of two experiments.

4.2.3 Cox-2 involvement in SPARC-regulation of MDSC functions

Prompted by the above results, we tried to understand how SPARC modulates the GM-CSF and G-CSF production. I thought that a possible mechanism through which SPARC might regulate myeloid cells phenotype is by its ability to regulate ECM deposition. Accordingly, ECM directly influences the expression of the cyclooxygenase II (COX-2), an enzyme that is regulated during myelopoiesis and that has been shown to shift the balance between G-SCF and GM-CSF in favor of GM-CSF in human mesangial cells [100]. I therefore evaluated the expression of collagen and COX-2 in SN25ASP vs SN25A tumors. Being mesenchymal cells, SN25ASP cells *in vivo* express higher levels of collagens compared with SN25A cells (**Fig. 22**). Moreover, I found that SN25ASP tumor showed a higher COX-2 expression, especially in infiltrating immune cells (**Fig.23-A**). Quantitative qPCR analysis performed on MDSC isolated from SN25A and SN25ASP tumors showed that monocytic MDSC from SN25ASP but not SN25A tumors express COX-2 together with NOS2 and Arginase I (**Fig.23-B**). This enzyme plays a key role in tumor progression also by affecting immune cells for example by blocking M2 Macrophage Differentiation [155], we therefore hypothesized that it could also be involved in MDSC functions, such as promoting EMT.

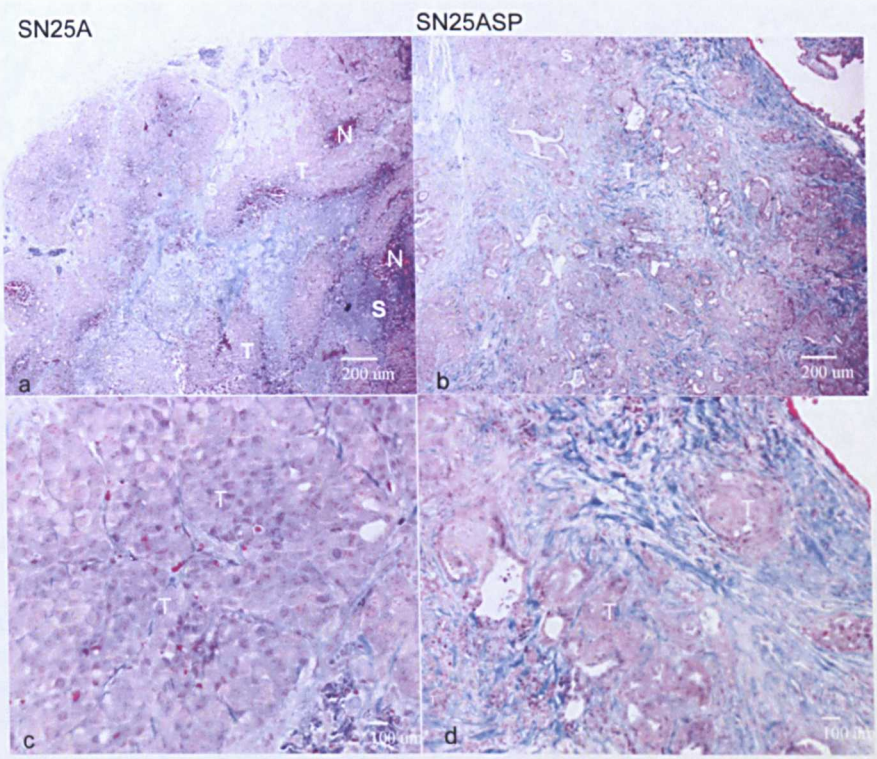

Fig.22 Masson's trichrome stain of SN25A and SN25ASP tumors.

SN25ASP shows an overall increased collagen deposition in comparison to the wt counterpart. **a-b**) (original magnification x100); **c-d**) (original magnification x200).

A

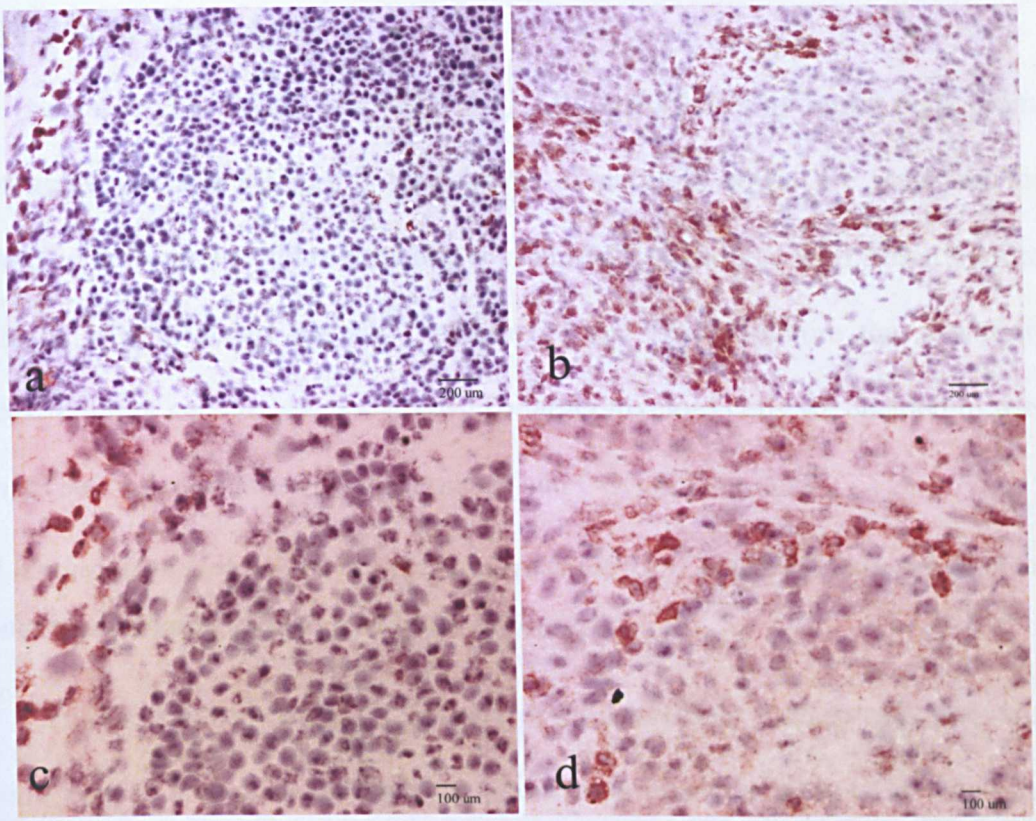

B

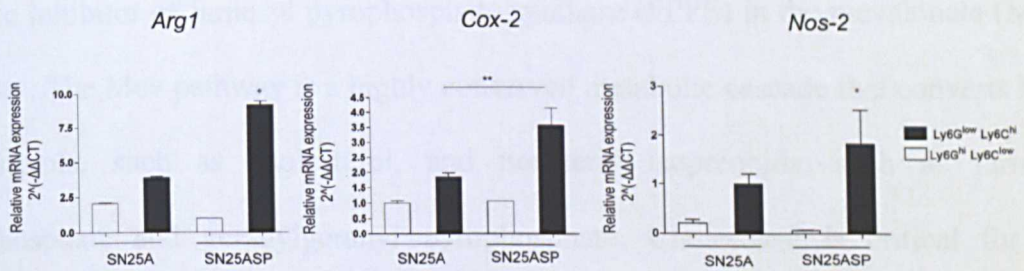

Fig.23 SPARC transduction regulates COX-2 expression in SN25A tumors.

(**A**) Immunohistochemistry analysis for Cox-2 expression was performed on SN25A and SN25ASP frozen sections. The poorly differentiated SN2ASP tumor expressed COX-2 both in tumor cells and within the myelo-monocytic infiltrate. (**b-d**). On the contrary SN25A tumors were negative for Cox-2 expression or slightly positivity in stromal cells (**a-c**). (**a-b**) (original magnification x100) ; (**c-d**) (original magnification x200) . (**B**) Quantitative qPCR analysis for *Cox-2*, *Nos-2*, *Arg1* genes was performed on Ly6GhighLy6Clow and $Ly6G^{low}$ $Ly6C^{high}$ myeloid cells subsets isolated from the tumor of SN25A and SN25SP tumor-bearing mice. Data are indicative of 2 independent experiments. The analysis shows a significative upregulation in *Cox-2* gene expression in $Ly6G^{low}$ $Ly6C^{high}$ cells isolated from SNA25SP tumors. *Cox-2* upregulation in these cells was associated with an increased expression of *Arg1* and *Nos-2* genes. The analysis included a pooled RNA extracted from n=10/group mice. (*** p= 0,0159; *≤0.05, *Student* t test.

4.3 MYELOID DERIVED SUPPRESSOR CELLS TARGETING AS STRATEGY TO IMPROVE CHEMOTHERAPY

So far we have demonstrated that SPARC production by tumor cells promotes tumor aggressiveness through a modulation of myeloid cells. We reasoned that if myeloid cells are ultimately responsible for the EMT phenotype their specific targeting should be able of revert the EMT phenotype and finally restore the sensitivity of SN25ASP tumor cells to chemotherapy. To target myeloid cells we decided to use two different strategies: amino-bisphosphonates and COX-2 inhibitors.

4.3.1 Aminobisphosphonates reduces aggressiveness of SN25ASP tumors in vivo without significantly affecting MDSCs expansion

Aminobisphosphonates (NBPs) are drugs commonly used to treat bone disease in solid cancer and multiple myeloma, and to prevent bone loss in osteoporosis. Zoledronic acid (Zometa), the most potent NBP currently available for clinical use, is a specific inhibitor of farnesyl pyrophosphate synthase (FPPS) in the mevalonate (Mev) pathway. The Mev pathway is a highly conserved metabolic cascade that converts Mev into sterols, such as cholesterol, and nonsterol isoprenoids, such as farnesyl pyrophosphate and geranylgeranyl pyrophosphate. Cholesterol is critical for the physicochemical properties of all eukaryotic cells, whereas isoprenoids are required for the isoprenylation and activation of small G-proteins, like Ras and Rho, that control cell proliferation, cytoskeleton remodeling, motility and angiogenesis. The metabolic consequences of Zometa-induced FPPS inhibition are two-fold: (1) a decreased content of intracellular isoprenoids leading to dysfunctional G-proteins and alterations of their downstream signaling pathways; and (2) an intracellular accumulation of isopentenyl pyrophosphate (IPP) leading to the formation of 1-adenosin-5′-yl ester 3-(3-methylbut-3-enyl) ester triphosphoric acid, a pro-apoptotic ATP analog generated by combination

of IPP with AMP by aminoacyl-tRNA-synthetase. In our laboratory, Melani et al. have demonstrated that, by reducing MDSCs expansion, Zometa treatment overcomes the tumor-induced immune suppression and improves the generation and maintenance of antitumor immune response induced by immunization against the p185/HER-2. The study, however, did not identify the pathway (i.e. Mev pathway) affected in MDSCs by the Zometa treatment[49]. Reproducing the experiment by Melani et al [49] SN25ASP tumor-bearing mice were daily treated with 0,1 mg/kg of Zoledronic acid (Zometa) (subcutaneously). Treated and untreated mice were checked once a week for MDSC expansion in the peripheral blood and, at the end of the experiment, tumors were harvested for histology and IHC **(Fig. 24-25)**. In contrast with Melani et al, I found that the treatment did not significantly affect tumor growth, as BALB/c mice injected with SN25ASP and treated with Zometa presented no significant changes in tumor volume reduction at the end point of the experiment **(Fig. 24)**. However, histological analysis of SN25ASP tumors from Zometa treated mice indicated a complete reversion of the EMT phenotype *in vivo* **(Fig. 25)**. IHC analysis for iNOS expression performed on frozen tumor sections showed downregulation of iNOS production in myeloid cells from Zometa-treated tumors that was associated to an unchanged number of Ly6G+ cells in tumors **(Fig. 26-A)**. Again, these results suggest the possibility that an altered phenotype of myeloid cell, in this case associated with the Zometa treatment, rather than impairing recruitment, might be responsible for EMT reversion. Interestingly, the PB (peripheral blood) of Zometa treated mice showed an imbalance in the frequency of CD11b+Ly6G^{high} Ly6C^{low} and CD11b+Ly6G^{low} Ly6C^{high} subset of myeloid cells in favor of the CD11b+Ly6Ghigh population **(Fig. 26-B)**. In agreement with the EMT reversion, SN25ASP tumor-bearing mice treated with Zometa, showed a reduction in the frequency of lung metastasis **(Fig. 27)**. Finally, SN25ASP tumor bearing mice

treated with Zometa showed an increased infiltration of granulocytes in the lung associated with a reduced number of infiltrating tumor cells.

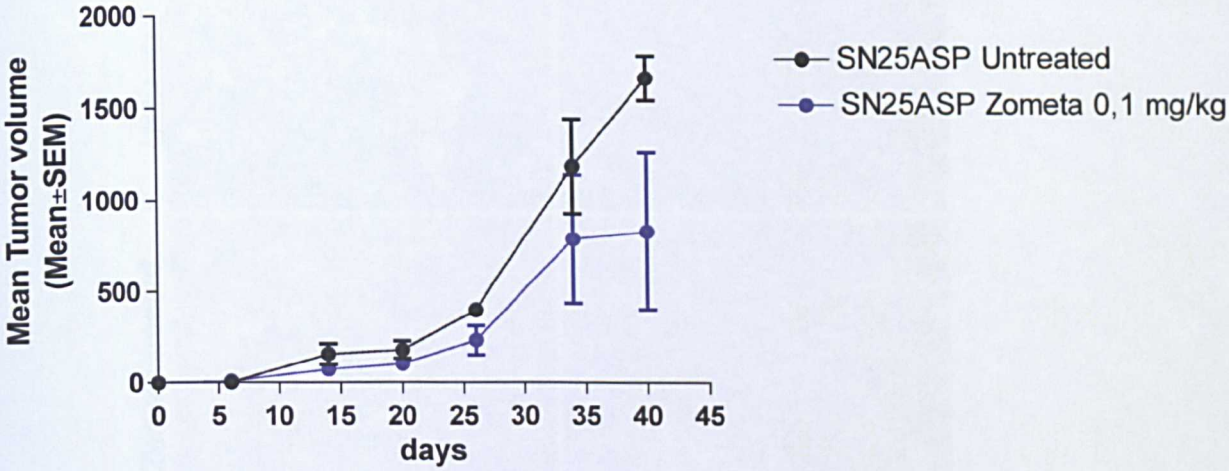

Fig. 24 Zoledronate don't affect significantly tumor growth of SN25ASP tumors.

BALB/c mice were subcutaneously injected with SN25ASP cells and treated with Zometa (0,1 μ g/mouse, s.c.). Treatment was started on day 15 and continued every day until sacrifice. Results are presented as mean tumor volume $\pm$ SEM. *P<0.05. Data are representative of three independent experiments.

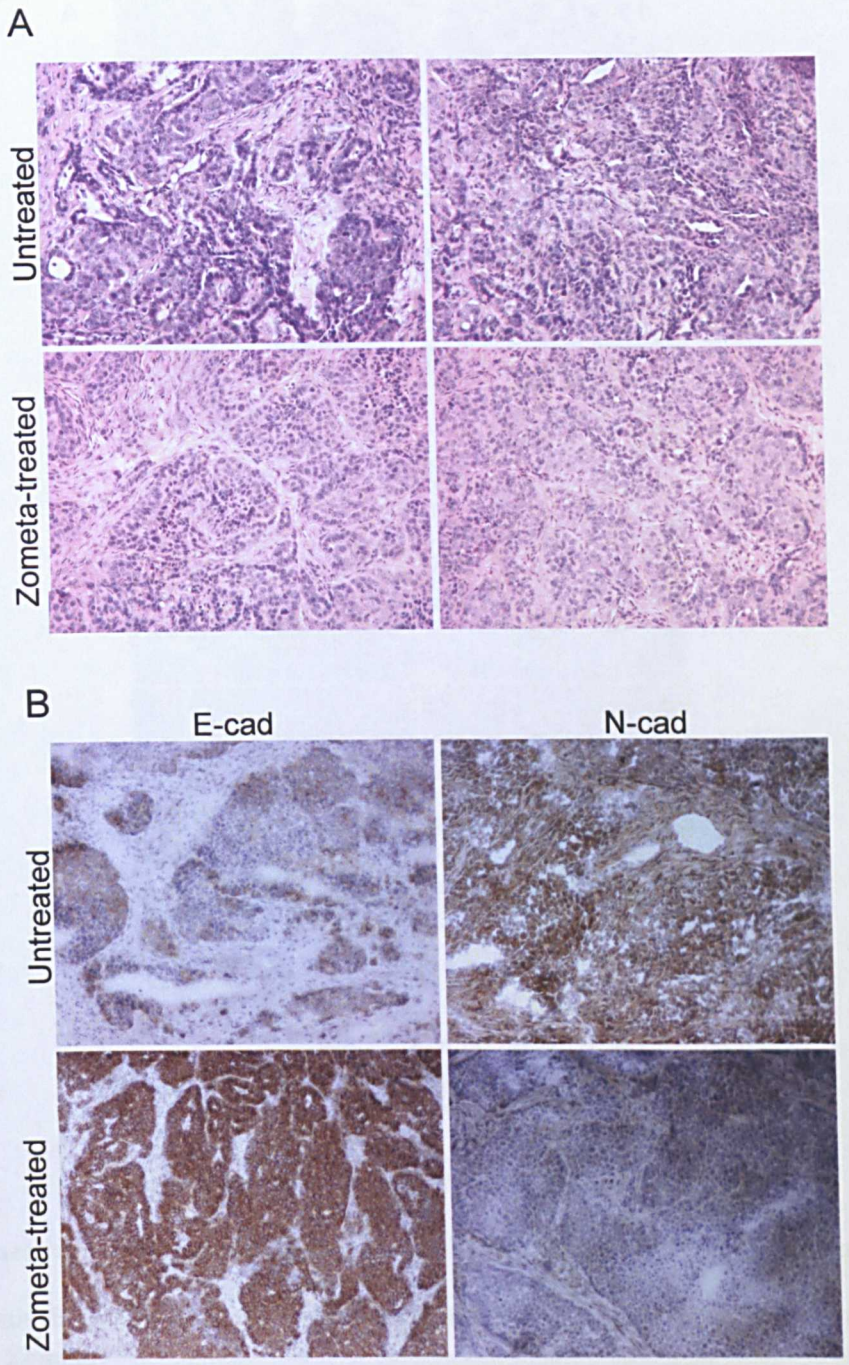

Fig. 25 Zometa reverts the mesenchymal phenotype of SN25ASP tumors.

(**A**) Histological (H&E) analysis of SN25ASP tumors treated with Zometa shows that the drug changed the tumor morphology from a mesenchymal to a more epithelial phenotype. Scale bars 100 um. (**B**) IHC analysis for E-cadherin and N-cadherin markers in SN25ASP tumors treated or not with Zometa shows E-cadherin strongly re-expressed in SN25ASP treated tumors. SN25ASP untreated tumors showed an increased N-cadherin expression; Zometa treatment reduces N-cadherin expression in SN25ASP tumor.

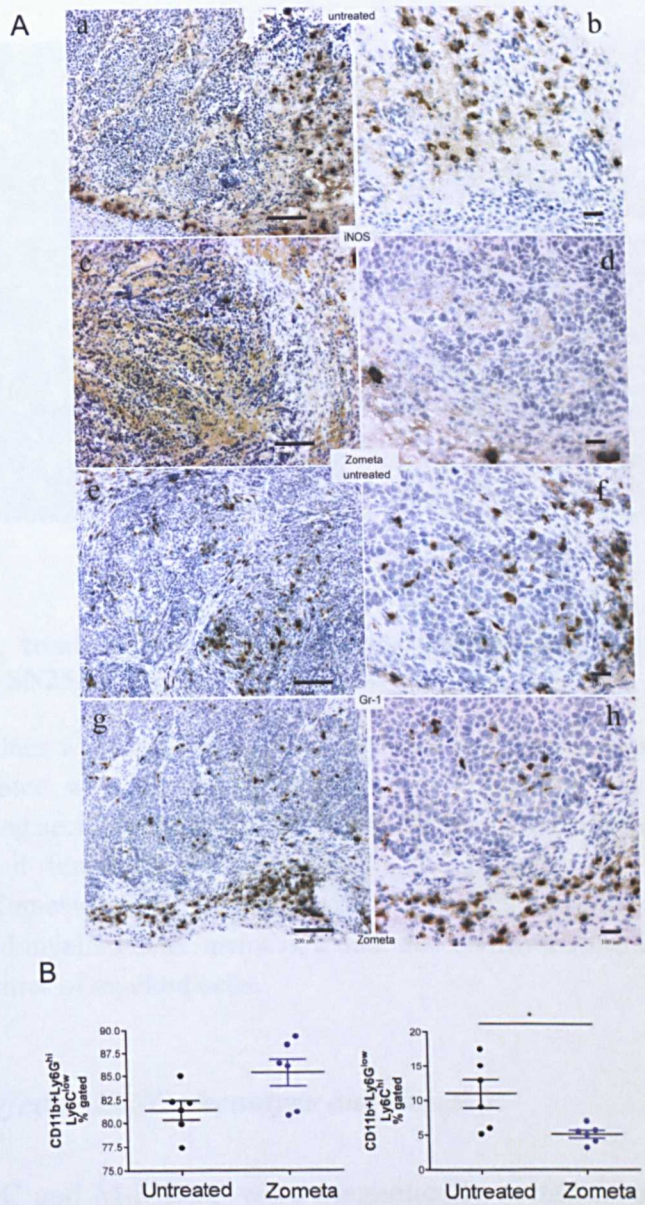

Fig.26 Zometa treatment affects the activity of MDSC but not their expansion.

(A) IHC analysis for Gr-1 and iNOS performed on frozen section of SN25ASP tumors treated or not with Zometa.

SN25ASP untreated and Zometa-treated tumorwere checked for myeloid cells infiltration and immunosuppressive activity. Tumors sections were stained with Gr- 1 mAb for myeloid cells and a polyclonal antibody against iNOS (Cayman) for ROS production (**a-b**); (**c-d**). Zometa-treated and untread tumors were equally infiltrated by Gr-1+ myeloid cells (**e-f**); (**c;d**) however Zometa-treated tumors showed a reduction in the number of infiltrating iNOS+ myeloid cells (**c-d**); (**a-b**). **(B)** FACS analysis for circulating myeloid cells performed on PB from SN25ASP tumor-bearing mice treated or not with 0.1 mg/kg of Zometa. ($p \leq 0.05$, *Student t* test).

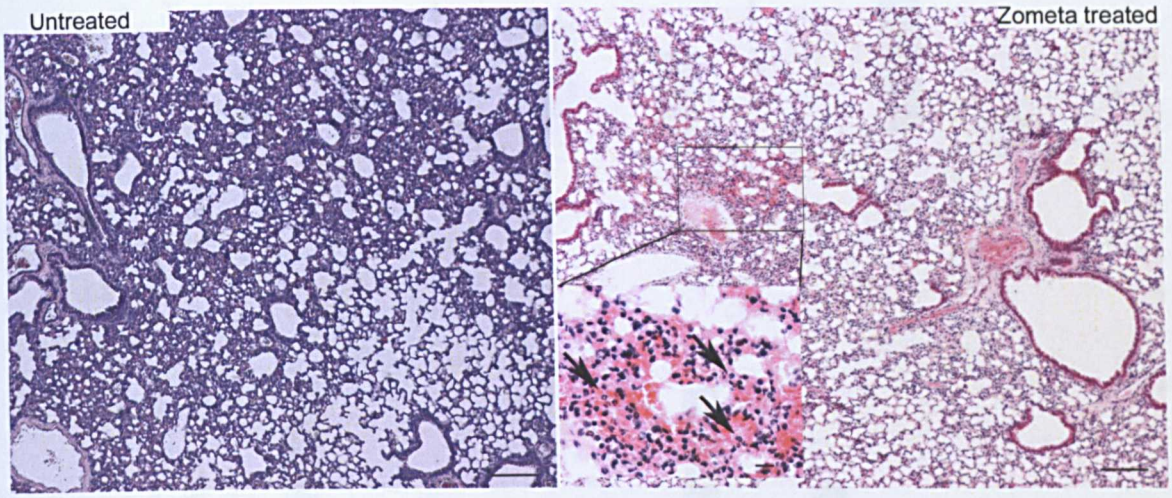

Fig.27 Zometa treatment reduces lung metastasis and increases the number of granulocytes in SN25ASP tumor bearing mice.

SN25ASP cell lines were injected in BALB/c mice and tumors treated or not with Zometa. 40-days later mice were sacrificed and lungs removed for histological analysis. H&E performed on lung sections showed that Zometa treatment overall reduced the lung cellularity that in untreated tumors was associated to the presence of infiltrating tumor cells. Interestingly, Zometa-treatment increased lung infiltration by anti-tumor granulocytes (hypersegmented myeloid cells, arrows), a data that confirmed the ability of Zometa to elicit anti-tumor activities of myeloid cells.

4.3.2 Zometa affects MDSC phenotype and function

G-MDSC and M-MDSC were magnetically sorted from the spleen of SN25A and SNA25ASP tumor-bearing mice treated or not with Zometa. Quantitative real-time PCR was performed to evaluate the expression of the MDSC pro-tumoral markers (*Section 4.1.6*) CCL2, CCL5, NOS2 and STAT3. Overall, I observed a significant downregulation of these markers particularly in the M-MDSC subset, where Zometa treatment strongly reduced CCL2, CCL5 and NOS2. In M-MDSC, moreover, I found a significant reduction in NOS2 and STAT3 (**Fig. 28**).

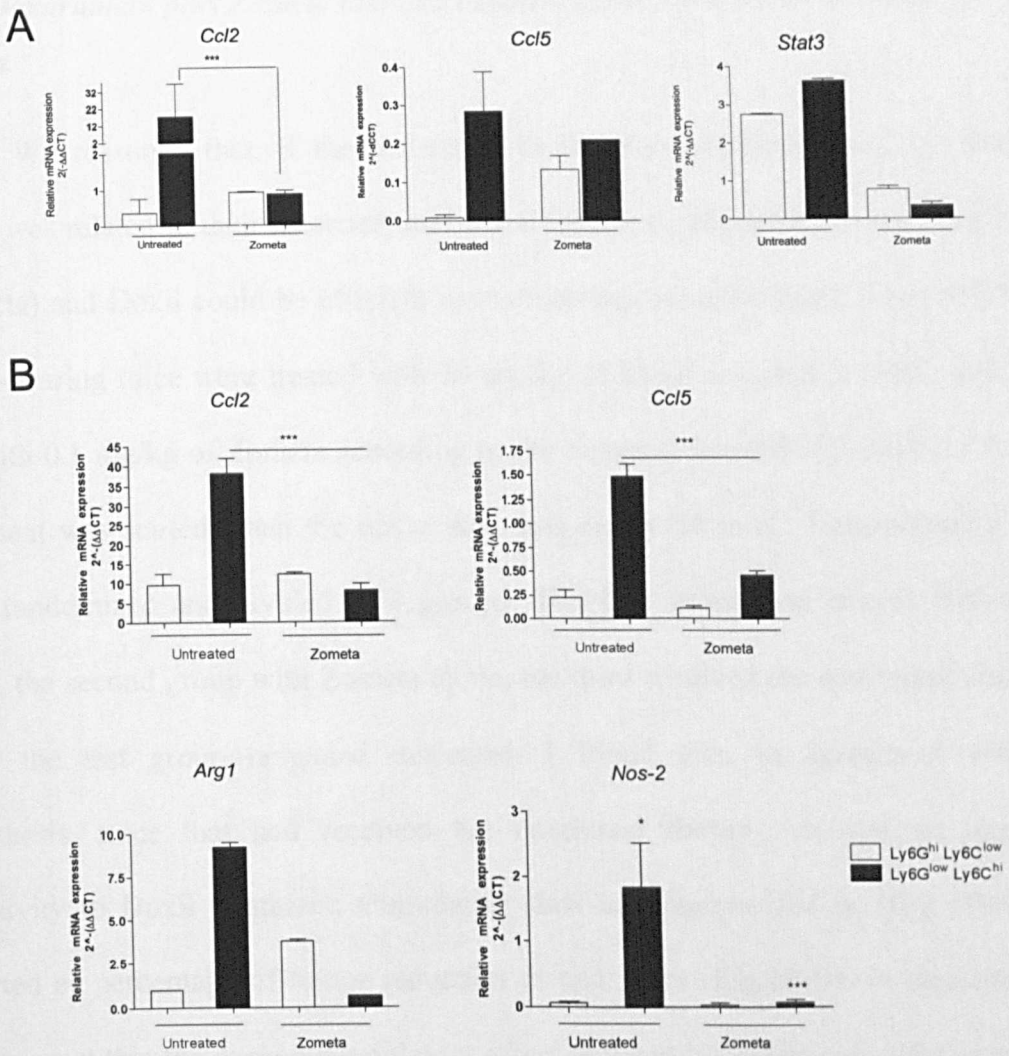

Fig.28 Zometa treatment reduces pro-tumoral and immunosuppressive markers in myeloid cells.

(A) Quantitative RT-PCR analysis for CCL2, CCL5, STAT-3 was performed on splenic $Ly6G^{low}Ly6C^{high}$ and $Ly6G^{high}Ly\text{-}6C^{low}$ myeloid cells subsets isolated from SN25ASP tumor bearing mice treated or not with Zometa. Data show that Zometa treatment significantly reduces the expression of CCL2, CCL5 and Stat3 on $Ly6G^{low}Ly6C^{high}$ myeloid cells (student t test*p ≤ 0.05). **(B)** Quantitative RT-PCR analysis for CCL2, CCL5 and ArgI was performed on $Ly6G^{low}$ $Ly6C^{high}$ and $Ly6C^{high}$ $Ly\text{-}6C^{low}$ myeloid cells sorted from tumor of SN25ASP tumor bearing mice treated or not with Zometa. Zometa promotes a significantly downregulation of protumoral markers CCL2 (-4 fold-change), CCL5 (-2 fold change). M-MDSC isolated from ZA-treated tumors significantly downregulated also immunesupressive markers Arg-I and NOS2 (-18 fold change). This data show that monocytic myeloid cells (M-MSDC) isolated from SN25ASP tumor bearing mice acquired an anti-tumor phenotype after Zometa treatment. Data are indicative of 2 independent experiments.(*** $p \leq 0.01$;** $p = 0.02$, *Student t test*).

4.3.3 Doxorubicin plus Zometa increases Doxil efficacy in SN25ASP-resistant tumors

We reasoned that, if the resistance to Doxil treatment showed by SN25SP tumor was related to their mesenchymal phenotype, a combination of Zoledronic acid (Zometa) and Doxil could be efficient in overcoming this phenotype. Thus SN25ASP tumor-bearing mice were treated with 10 mg/kg of Doxil i.v. once a week, and daily s.c. with 0.1 mg/kg of Zometa according to the reported schedule (*Section 2.2.1).* The treatment was started when the tumor size was nearly 20 mm^3. Tumor-bearing mice were randomized and divided in 4 groups. The first group was treated with Doxil alone, the second group with Zometa alone, the third received the combined treatment while the last group remained untreated. I found that, in agreement with my hypothesis, mice that had received the combined therapy showed an increased sensitivity to Doxil treatment. Cumulative data are summarized in **(Fig 29-A)** and reported as percentage of tumor reduction at end point **(Fig.29-B)**. In summary, the data suggest that the immunomodulatory effect induced by Zoledronic acid in myeloid cells could improve chemotherapy response. Finally, I have evaluated the possibility that Zometa-treatment, particularly in combination with Doxil, might also interfere with the immunosuppressive activity of myeloid cells, so I tested whether myeloid cells isolated from the spleen of Zometa+Doxil-treated SN25ASP tumor-bearing mice had a reduced ability to suppress the proliferation of a-CD3/aCD28 stimulated splenocytes. I found that MDSC isolated from Zometa+Doxil treated mice was significantly less efficient in inhibiting the proliferation of CD8 T cells **(Fig.30-A-B)**.

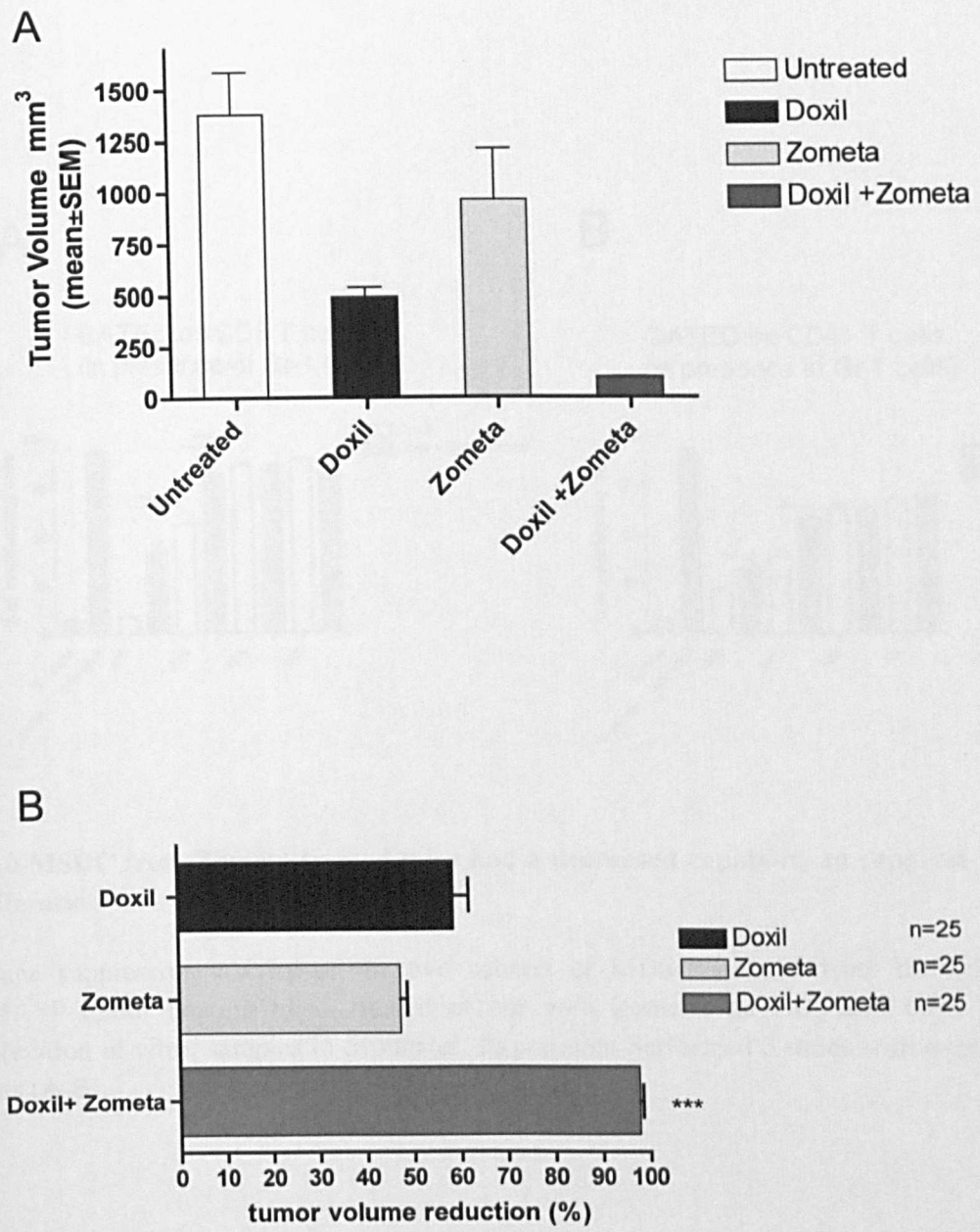

Fig.29 Zometa treatment enhances Doxil efficacy on SN25ASP tumors.

SN25ASP tumor-bearing mice were daily injected with 0.1 mg/kg of Zoledronic acid (Zometa) and treated once a week with 10 mg/kg of Doxil. **(A)** Bars refers to cumulative data show mean of tumor volume (mm3) relative to SN25ASP tumors injected in BALB/c mice and treated with Doxil , Zometa alone or combined drugs at the endpoint of the experiments. Data are reported as (mean±SEM) n=25. **(B).** Zometa alone reduced tumor volume (mm3) ($p \geq 0.05$) 50%; Doxil alone 60% ($p \geq 0.05$); Doxil + Zometa 100% tumor reduction (***p=0,0005). SN25ASP tumors treated with Zometa are more responsive to Doxil (Zometa vs Doxil+Zometa * $p \leq 0.05$). Tumor reduction was calculated at endpoint of the experiment. Statistical analysis were done using one-way ANOVA with Dun's multiple comparison Test.

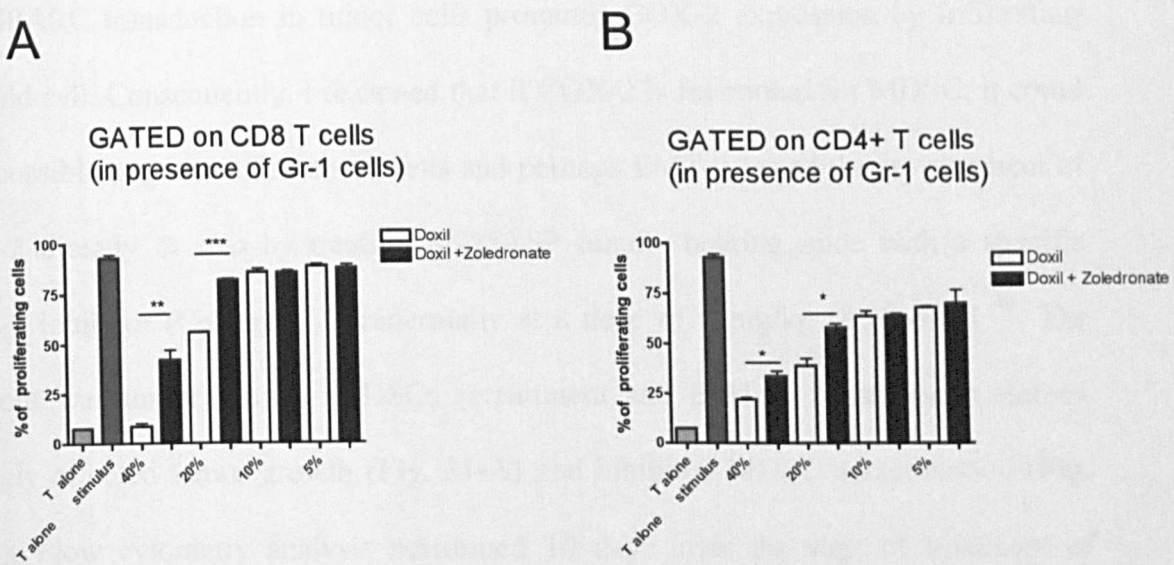

Fig.30 MSDC from Zometa-treated mice had a decreased capability to suppress T cells proliferation.

Immune suppressive activity of the two subsets of MDSC isolated from the spleen of SN25ASP tumor bearing mice, treated or not with Zometa, on CD4 and CD8 T cells proliferation in vitro; samples in triplicates. Experiment performed 3 times with overlapping results (**A-B**).

4.3.4 COX-2 inhibitors affects MDSC recruitment and ameliorate the sensitivity to Doxil treatment.

The use of COX-2 inhibitors in our models stemmed from my original finding that SPARC transduction in tumor cells promotes COX-2 expression by infiltrating myeloid cell. Consequently, I reasoned that if COX-2 is functional for MDSC, it could be a possible target to affect these cells and perhaps EMT. I tested the involvement of COX-2 directly *in vivo* by treating SN25ASP tumor- bearing mice with a specific COX-2 inhibitor (Celebrex), intradermally at a dose of 5 mg/kg as reported [59]. The read-out was tumor growth, MDSCs recruitment and EMT. I found that Celebrex strongly affected tumor growth (**Fig. 31-A**) and inhibited MDSC accumulation (**Fig. 31-B**). Flow cytometry analysis performed 10 days after the start of treatment of PBMC revealed that Celebrex significantly reduced the level of MDSC (**Fig. 31-B**). In keeping with my hypothesis, histological analysis of tumor showed that the COX-2 inhibitors were able to revert the mesenchymal phenotype of SN25ASP tumors (**Fig. 32-A**). Following a procedure similar to that used for NBTs, Celebrex was used in combination with Doxil. Again, I found that the combined therapy decidedly improved the response to Doxil treatment (**Fig. 32-B**). Taken together, these data suggest that the response to therapy of mesenchymal tumors might be enhanced by the association of conventional therapeutics with immunomodulatory drugs like aminobisphosphonates and COX-2 inhibitors.

A

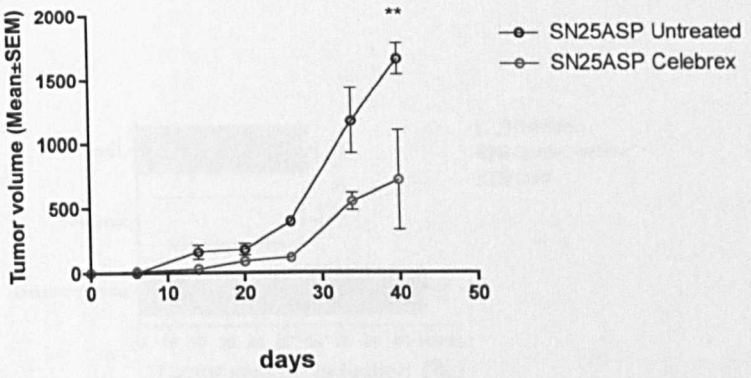

B

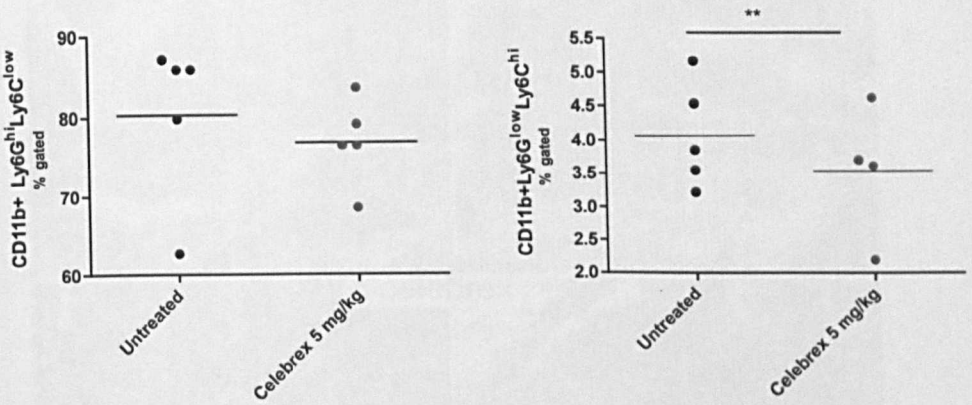

Fig.31 Celebrex treatment reduces tumor growth and PBMC MDSC in SN25ASP tumors.

(A) Tumor growth of SN25ASP untreated and SN25ASP Zometa treated tumors. Data are shown as tumor volume mean ±SEM n=5 volume at 40 day **(B)** Reduction in the frequency of $Ly6C^{hi}$ $Ly6G^{low}$ (M-MDSC) and $Ly6G^{hi}Ly6C^{low}$ (G-MDSC in the PB of SN25ASP tumor-bearuing mice treated with Celebrex (student t test; * $p< 0.05$).

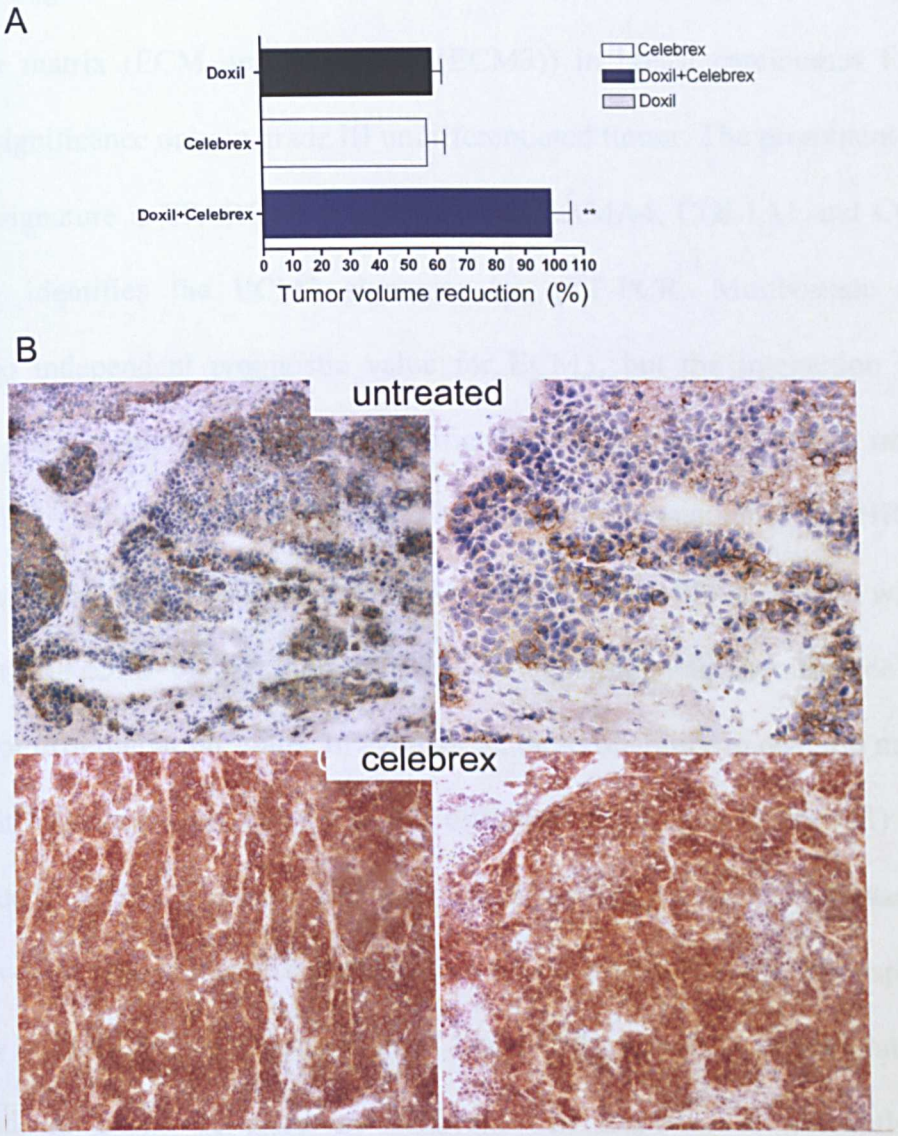

Fig.32 Celebrex modulates tumor differentiation and ameliorates Doxil resistance.

(**A**) Cumulative data show % of tumor volume reduction of SN25ASP tumors treated alone with Doxil, Celebrex (ns) or Doxil plus Celebrex treatment (**p=0,0041). Bars refer to mean values ±SEM. (**B**) E-Cadherin staining on SN25ASP tumors treated alone with 5 mg/kg of Celebrex. Ecadherin is strongly re-expressed by SN25ASP tumors after Celebrex treatment. (left panels original magnification x100) (right panels original magnification x200).

4.4 THE RELEVANCE TO HUMAN BREAST CANCER OF SN25A/SN25ASP TUMOR MODELS

Dr. Tagliabue at the Istituto Nazionale Tumori identified a peculiar extracellular matrix (ECM gene signature (ECM3)) in breast carcinomas featuring prognostic significance only in grade III undifferentiated tumor. The prominent gene of the ECM3 signature is SPARC that, together with LAMA4, COL1A1 and COL5A2, consistently identifies the ECM3 signature by qRT-PCR. Multivariate analysis indicated no independent prognostic value for ECM3, but the interaction between ECM3 and grade resulted strongly and significantly associated with hazard ratio (HR) of relapse (HR=5.35, p=0.001) in untreated breast carcinoma patients. The HR relative to ECM3 was markedly different in grade I-II (HR=0.6, p=0.08) compared with grade III tumors (HR=2.5, p=0.038), indicating that ECM3 prognostic significance depends on the tumor differentiation status. In agreement, the probability to develop metastases in a 10-year follow-up was 10% for ECM3 differentiated tumors (grade I-II) and 55% for the grade III ECM3. Moreover, the analysis of two data sets of neo-adjuvant treated patients revealed that, among the grade III tumors, pathological complete response was reached by 15% of ECM3 versus 85% of non-ECM3 tumors. Comparison between ECM3 and all others revealed no difference in response to chemotherapy in differentiated (grade I-II) tumors. The data on the biology of SPARC presented here might in part explain why the same signature is detected in well-differentiated and undifferentiated tumors but with a different outcome. These data in fact support the possibility that, in well-differentiated tumors, SPARC might drive stroma deposition, whereas in grade III tumors it might contribute to the EMT phenotype and chemoresistance. Accordingly, in grade III tumors the ECM3 signature defines the subgroup that undergoes EMT. If SPARC regulation of EMT occurs through MDSCs recruitment and COX-2 activation, correlative human data should be found comparing

ECM3 with ECM0 tumors. In collaboration with Dr. Tripodo from the University of Palermo, I have analyzed infiltration by immature myeloid cells (in human identified by the marker CD33) and their COX-2 production in ECM3 versus non-ECM3 tumors. We found that ECM3 grade III tumors, in keeping the (differential) SPARC expression of tumor and stroma, showed an increased infiltration by COX-2+ immune cells (**Fig. 33**). By contrast, non-ECM3 tumors showed COX-2 expression only by tumor cells. Finally, GEP (Gene Expression Profile analysis) showed that ECM3 tumors are enriched for genes related to myeloid cells, whereas non-ECM3 tumors had a signature associated with T-cells (**Fig. 34**).

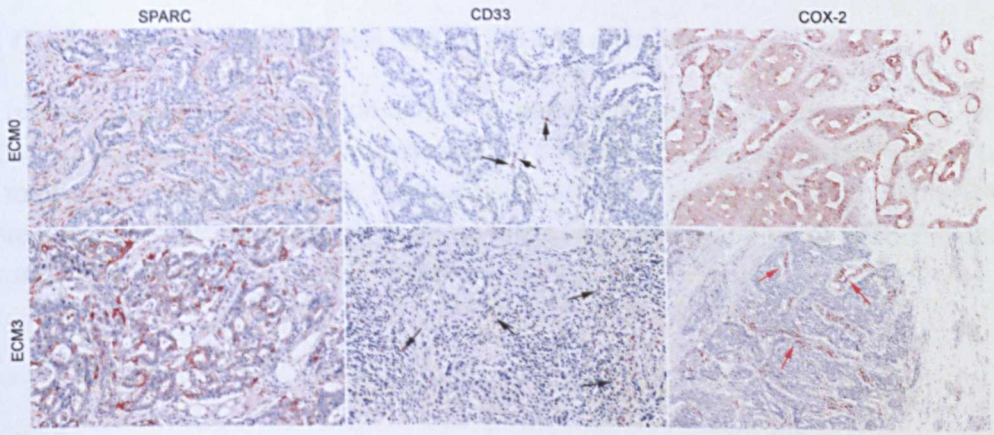

Fig.33 SPARC expression correlates with COX-2 activity of CD33+ infiltrating myeloid cells in ECM3 tumors.

ECM0 tumors SPARC is widely distributed in tumor **(a)** and is associated to a reduced number of CD33+ infiltrating myeloid cells **(b)** COX-2 is expressed by tumor cells. ECM3 tumors are characterized for a strongly SPARC expression **(d)** present an high number of infiltrating CD33+ myeloid cells **(e)** that specifically expressed Cox-2 **(f).**

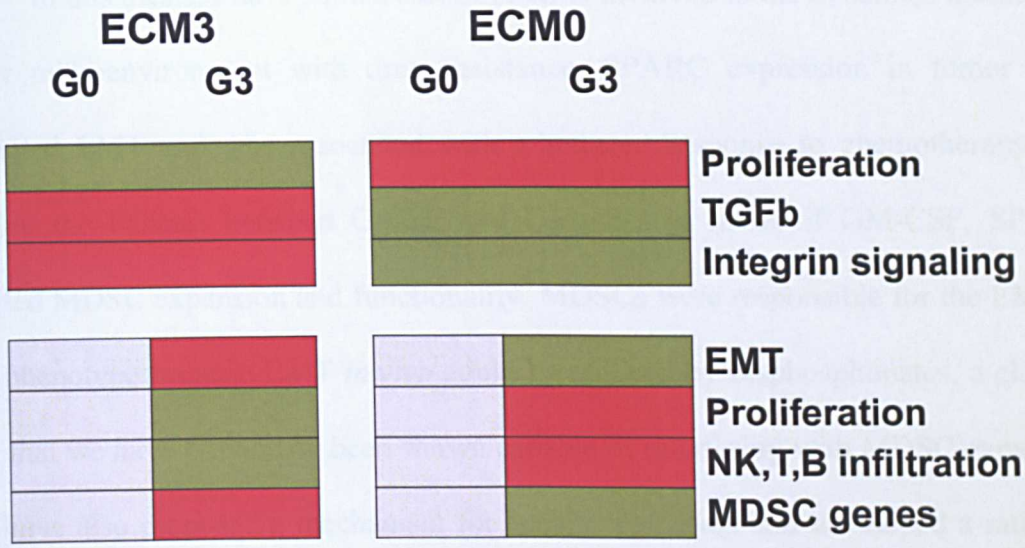

Fig. 34 Gene set enrichment analysis (GSEA) in two datasets.

ECM3 is represented by up-regulation of TGF β pathways, and membrane integrins, whereas non-ECM3 is characterized by overexpression of proliferation genes. Among grade III non-ECM3 tumors are enriched for genes representative of NK, T and B cells, and involved in cell cycle progression, while EMT, hypoxia genes and genes representative of MDSC cells were significantly up-modulated in ECM3 tumors.

5.DISCUSSION

In this thesis, I have shown that SPARC is involved in the dynamics linking the tumor microenvironment with drug resistance. SPARC expression in tumor cells promoted EMT and was associated with a reduced response to chemotherapy. By altering the balance between G-CSF and GM-CSF in favor of GM-CSF, SPARC affected MDSC expansion and functionality. MDSCs were responsible for the EMT *in vivo* phenotype because EMT *in vivo* could be reduced by bisphosphonates, a class of drug that we have previously been shown capable of interfering with MDSC expansion [49]. I have also proposed a mechanism for such a regulation and developed a rationale for the use of COX-2 inhibitors or amino-bisphosphonates in combination with conventional chemotherapy to treat a specific subset of breast cancer patients. Tagliabue and colleagues analyzed the expression of extracellular matrix (ECM) genes in breast carcinomas and identified four different profiles (ECM1, 2, 3 and 4) [156]. Among them they found that the peculiar signature "ECM3" had prognostic significance only in grade III tumors. The prominent gene of this signature was *SPARC,* together with LAMA4, COL1A1 and COL5A2. Multivariate analysis indicated that the interaction between ECM3 and grade was strongly and significantly associated with hazard ratio (HR) of relapse (HR=5.35, p=0.001) in untreated breast carcinoma patients. The HR relative to ECM3 was markedly lower in grade I-II (HR=0.6, p=0.08) compared with grade III tumors (HR=2.5, p=0.038), indicating that ECM3 prognostic value varies according to the tumor differentiation status. In addition, the comparison between grade III and grade I-II ECM3 showed that undifferentiated grade III tumors are also less responsive to therapy. This raises the query of how the same gene signature could predict a worse prognosis in grade III than in grade I-II tumors. Triulzi and colleagues showed that ECM3 is a robust cluster that

characterizes breast carcinomas with EMT features and increased metastatic potential only in undifferentiated grade III tumors, but the authors did not provide any biological mechanism to explain why the same ECM signature, enriched for SPARC, had prognostic significance only in grade III tumors but not in grade I tumors. Data from this PhD thesis might help explain at least in part this apparent inconsistency. Our initial finding in SPARC biology [157] was that in well-differentiated adenocarcinoma, where both tumor and stromal cells express SPARC (N2C, N3D and N1G cell lines), SPARC was required to correctly assemble collagen type IV fibers in the stroma. These tumors expressed SPARC at higher levels but were indolent tumors, unable to promote metastasis formation [138] and were responsive to chemotherapy (N2C cell line/Doxorubicin; Sangaletti S. unpublished). By contrast, in our SN25ASP model that mimics the human basal type (among which are ECM3G3), a higher SPARC expression than in the parental counterpart was associated with metastasis and resistance to therapy. Thus, although SPARC was expressed by adenocarcinomas and metastatic tumors its role was different and dependent on the tumor differentiation status. In well-differentiated tumors, SPARC controlled stroma deposition [138], whereas in grade III tumors, SPARC contributed to the EMT phenotype. In the SN25SP/N3DSPARC murine model, SPARC expression promoted a mesenchymal phenotype and tumor immunosuppression. This could be in line with the more general concept that mesenchymal cells might promote immunosuppression. Accordingly, cell therapy with mesenchymal stromal cells (MSC) has emerged as a promising tolerance-inducing strategy, as MSC are potent modifiers of immune cells within the adaptive as well as the innate arm of the immune system. Casiraghi F. et al. have hypothesized that MSC-cell therapy may be useful to promote kidney transplantation tolerance[158]; Ghannan et al. showed that mesenchymal stem cells are able to inhibit human th17 cell

differentiation and function, and induce a regulatory T cell phenotype [159] via IL-10. I found that SN25ASP tumor cells *in vivo* elicit the expression of the potent immune-suppressive cytokine IL-10 while, *in vitro,* they are capable of converting the phenotype of activated neutrophils into pro-tumor neutrophils. Our data seems to suggest that, unlike epithelial cells, mesenchymal tumor cells may possess the machinery, which is normally provided by accessory cells (i.e. mesenchymal stromal cells), to either promote tumor progression (collagens and ECM proteins among others) or immune-suppression (by re-directing myeloid cells functions) also suggesting that immune-modulatory drugs might be beneficial for the treatment of refractory ECM3G3 tumors. The analysis for the expression of CD33 (myeloid cells) and of COX-2 in human ECM0 vs ECM3 tumors highlighted the increased presence of COX-2+ infiltrating cells in ECM3 but not ECM0 tumors that were associated with the recruitment of CD33+ cells. Interestingly, the GEP (Gene Expression Profile analysis) analysis of ECM3 vs ECM0 tumors showed a different enrichment in genes related to immune cells infiltration: ECM3 tumors were enriched in genes related to myeloid cells (the csf-receptor) whereas ECM0 tumors were enriched in genes related to T cells. This data, together with data from murine models, suggested that a different ECM might results in a different immune-microenvironment. This would confirm that the ECM is not merely a scaffold but has a regulatory function. Accordingly, Sangaletti et al have recently demonstrated that that loss of SPARC in secondary lymphoid organs results in disruption of the ECM and defective collagen remodeling, promoting B cell activation and lymphomagenesis. In our breast tumor model, SPARC was shown to regulate MDSC function. We assumed that SPARC regulation occurs through the activation of COX-2 that shifts the balance between G-CSF and GM-CSF, together with a not well characterized, cell-to-cell mediated contact effect on myeloid

cells. I hypothesized that this effect could be related to the capability of SPARC to regulate TGFbeta signaling, similarly to what occurs in macrophages during fibrosis. In this model, SPARC-deficiency renders macrophages unable to modulate TGF-ß signaling and, as consequence, to dampen inflammation or reduce TNF production. Stressing our hypothesis about the involvement of TGF-ß signaling, we found that NBPs reverted the phenotype of MDSC also by down-modulating TGF-ß signaling in these cells, which in turn determined a reduced NF-kb activation. The use of NBPs as anti-cancer drug is not new: NBPs have entered clinical practice in the treatment of bone metastases from several neoplasms, including breast and prostate adenocarcinoma, as an anti-resorptive therapy. At the same time, evidence has accumulated of the direct anti-tumor effects of NBPs. NBPs were, for example, found to down-regulate hTERT gene expression in breast tumor cells [160] and to promote apoptosis. The possibility of a synergistic NBPs action with conventional drugs in the context of a subtype of tumors has been recently proposed as a new strategy that fits well with the approach of targeted therapies. Is is nonetheless necessary to consider that prior the reversion of the EMT-phenotype caused by NBPs-treatment, SN25ASP tumors showed an increased proliferation index (number of Ki-67+ cells). This suggests that the increased sensitivity to Doxil treatment was probably related to the increased incorporation of the DNA-intercalating agent by SN25ASP cells that, being less mesenchymal and more epithelial, proliferate more *in vivo*. A major question that remains open is why the injection of SN25ASP tumors in *Sparc*-null mice was sufficient to revert the EMT phenotype. *Sparc*-null mice were initially used to prove that SN25ASP mesenchymal phenotype was immune-mediated and particularly related to immunosuppression. Accordingly, our group has extensively reported an increased-M1 activation in the absence of SPARC[121]. It is likely that, in the total absence of

SPARC, the myeloproliferative stimulation is not promoted by the tumor production of GM-CSF, but is rather mediated by a BM or splenic stroma. These hematopoietic organs are, on one hand, capable of amplifying the myeloproliferative response by generating more myeloid cells [122] and, on the other hand, they may favor the generation of activated, anti-tumor myeloid cells in a process similar to that recently described in the context of lymphomagenesis[161]. In the context of lymphomagenesis in a *Sparc*-null background, the myeloproliferative spur provided by Fas mutation causes the generation of splenic neutrophils with high expression of genes related to class II and co-stimulation molecules, and the IFN signature indicating that these neutrophils were activated and primed toward immunogenic cells death. Taken together, these results suggest that both the over-expression of SPARC in tumor cells and its absence in host cells are capable of modulating the behavior of myeloid cells, so that the modulation of myeloid cells function could be the possible off-target in all diseases or tumors characterized by altered SPARC expression. Regarding tumors, this picture could be further complicated by the different roles of SPARC enrichment in tumors depending on their differentiation status. Data from this thesis suggest a new use of Bisphosphonates or Cox-2 inhibitors that, impairing MDSC expansion from the bone marrow, can be a component of drug combinations expected to be more effective in treating grade III breast-TM patients.

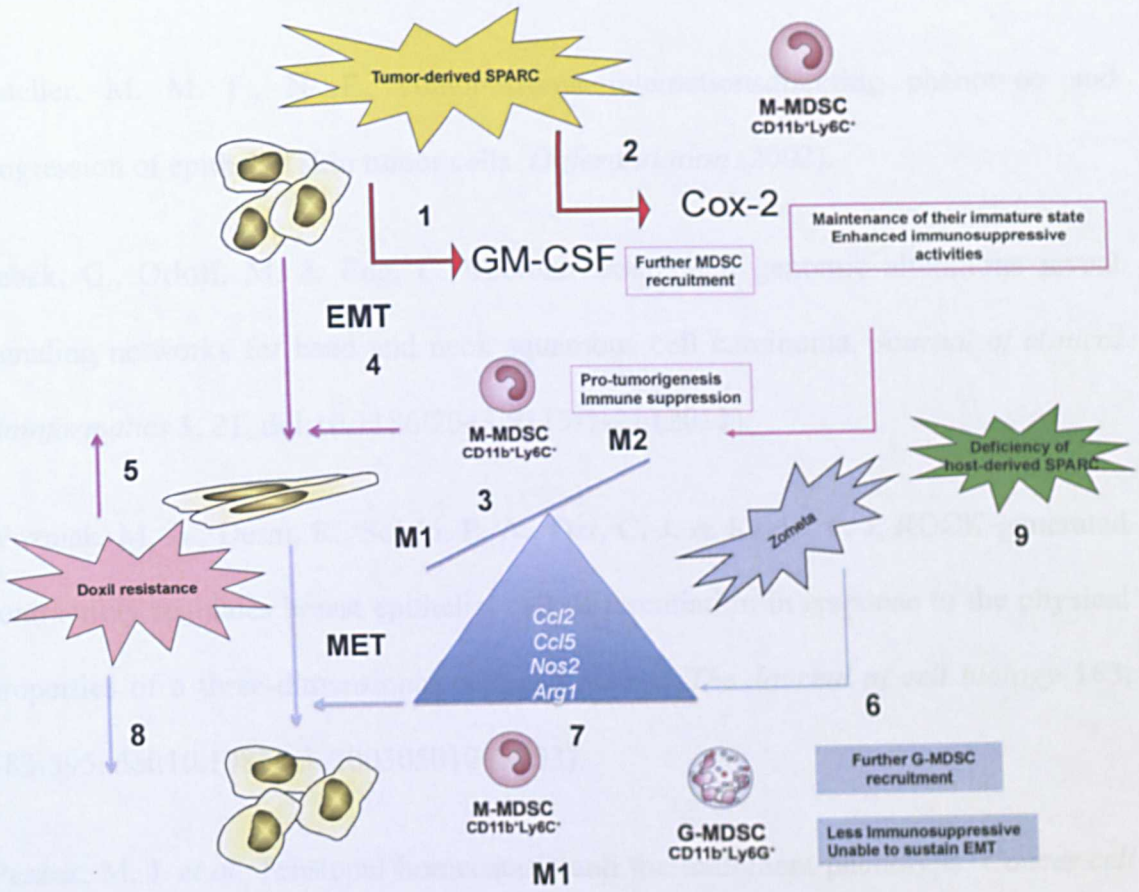

Fig.35 SUMMARY DIAGRAM

1. Tumor-derived SPARC in SN25ASP tumors alter the balance in the production of GMSCF and GCSF cytokines in favor of GMCSF, and promotes MDSC recruitment. **2.** SPARC-overexpressing tumors up-regulate selectively ***Cox-2*** gene in monocytic myeloid cells fraction (M-MDSC), characterized by higher surface marker expression of Ly6C. ***Cox-2*** activation, a consequence of SPARC expression in tumor cells, maintains M-MDSC cells in an immature state increasing their ability to suppress *ex vivo* CD8 T cells activity. **3.** In M-MDSC isolated from spleen and tumor of SN25ASP tumor-bearing mice, there is an up-regulation of ***Ccl2***, ***Ccl5*** pro-tumoral genes and of ***Arg1*** and ***Nos2*** immunosuppressive genes, which is characteristic of a Th2 response. **4.** Enhanced pro-tumor and immunosuppressive activity in M-MDSC in SPARC-overexpressing tumors activate EMT program *in vivo.* **5.** EMT features in SN25ASP tumors are associated with a reduced response to Doxil *in vivo.* **6.** Treatment of SN25ASP tumors with aminobisphosphonates increases recruitment of circulating G-MDSC cells that are less suppressive and unable to sustain EMT. **7.** In conjunction with an increased frequency of G-MDSC myeloid cells, M-MDSC isolated from SN25ASP tumors treated with Zometa also show a significant reduction of ***Ccl2***, ***Ccl5*** pro-tumor markers and immunosuppressive genes typical of Th1 response, reverting EMT to MET. **8.** The association of Zometa with Doxil treatment enhances sensitivity to Doxil. **9.** The EMT phenotype results from a cross-talk between tumor and myeloid cells, so that the injection of SN25ASP tumor cell lines in *Sparc*$^{-/-}$ mice reverts EMT and restores Doxil efficacy, mimicking Zometa treatment.

REFERENCES

1 Mueller, M. M. F., N. E. Tumor-stroma interactionsdirecting phenotype and progression of epithelial skin tumor cells. *Differantiation* (2002).

2 Bebek, G., Orloff, M. & Eng, C. Microenvironmental genomic alterations reveal signaling networks for head and neck squamous cell carcinoma. *Journal of clinical bioinformatics* **1**, 21, doi:10.1186/2043-9113-1-21 (2011).

3 Wozniak, M. A., Desai, R., Solski, P. A., Der, C. J. & Keely, P. J. ROCK-generated contractility regulates breast epithelial cell differentiation in response to the physical properties of a three-dimensional collagen matrix. *The Journal of cell biology* **163**, 583-595, doi:10.1083/jcb.200305010 (2003).

4 Paszek, M. J. *et al.* Tensional homeostasis and the malignant phenotype. *Cancer cell* **8**, 241-254, doi:10.1016/j.ccr.2005.08.010 (2005).

5 Levental, K. R. *et al.* Matrix crosslinking forces tumor progression by enhancing integrin signaling. *Cell* **139**, 891-906, doi:10.1016/j.cell.2009.10.027 (2009).

6 Coussens, L. M. & Werb, Z. Inflammation and cancer. *Nature* **420**, 860-867, doi:10.1038/nature01322 (2002).

7 Gordon, S. & Taylor, P. R. Monocyte and macrophage heterogeneity. *Nature reviews. Immunology* **5**, 953-964, doi:10.1038/nri1733 (2005).

8 Mantovani, A., Bottazzi, B., Colotta, F., Sozzani, S. & Ruco, L. The origin and function of tumor-associated macrophages. *Immunology today* **13**, 265-270, doi:10.1016/0167-5699(92)90008-U (1992).

9 Zhang, X. & Mosser, D. M. Macrophage activation by endogenous danger signals. *The Journal of pathology* **214**, 161-178, doi:10.1002/path.2284 (2008).

10 Hamilton, J. A. *et al.* The critical role of the colony-stimulating factor-1 receptor in the differentiation of myeloblastic leukemia cells. *Molecular cancer research : MCR* **6**, 458-467, doi:10.1158/1541-7786.MCR-07-0361 (2008).

11 Gouon-Evans, V., Rothenberg, M. E. & Pollard, J. W. Postnatal mammary gland development requires macrophages and eosinophils. *Development* **127**, 2269-2282 (2000).

12 Pollard, J. W. Trophic macrophages in development and disease. *Nature reviews. Immunology* **9**, 259-270, doi:10.1038/nri2528 (2009).

13 Guiducci, C. *et al.* Intralesional injection of adenovirus encoding CC chemokine ligand 16 inhibits mammary tumor growth and prevents metastatic-induced death after surgical removal of the treated primary tumor. *J Immunol* **172**, 4026-4036 (2004).

14 Hagemann, T. *et al.* "Re-educating" tumor-associated macrophages by targeting NF-kappaB. *The Journal of experimental medicine* **205**, 1261-1268, doi:10.1084/jem.20080108 (2008).

15 Gibbons MA, M. A., Ramachandran P, Dhaliwal K, Duffin R, Phythian-Adams AT, van Rooijen N, Haslett C, Howie SE, Simpson AJ, Hirani N, Gauldie J, Iredale JP, Sethi T, Forbes SJ. Ly6Chi monocytes direct alternatively activated profibrotic macrophage regulation of lung fibrosis *American journal of respiratory and critical care medicine* **184** (2011).

16 Duffield, J. S. *et al.* Selective depletion of macrophages reveals distinct, opposing roles during liver injury and repair. *The Journal of clinical investigation* **115**, 56-65, doi:10.1172/JCI22675 (2005).

17 Dvorak, H. F. Tumors: wounds that do not heal. Similarities between tumor stroma generation and wound healing. *The New England journal of medicine* **315**, 1650-1659, doi:10.1056/NEJM198612253152606 (1986).

18 Dineen, S. P. *et al.* Vascular endothelial growth factor receptor 2 mediates macrophage infiltration into orthotopic pancreatic tumors in mice. *Cancer research* **68**, 4340-4346, doi:10.1158/0008-5472.CAN-07-6705 (2008).

19 Lin, E. Y. *et al.* Vascular endothelial growth factor restores delayed tumor progression in tumors depleted of macrophages. *Molecular oncology* **1**, 288-302, doi:10.1016/j.molonc.2007.10.003 (2007).

20 Mauri, G. *et al.* Ultrasound-guided intra-tumor injection of combined immunotherapy cures mice from orthotopic prostate cancer. *Cancer immunology, immunotherapy : CII* **62**, 1811-1819, doi:10.1007/s00262-013-1486-7 (2013).

21 Lecis, D. *et al.* Smac mimetics induce inflammation and necrotic tumour cell death by modulating macrophage activity. *Cell death & disease* **4**, e920, doi:10.1038/cddis.2013.449 (2013).

22 Gershon, R. K. & Kondo, K. Dependence of concomitant tumor immunity on continued antigenic stimulation. *Journal of the National Cancer Institute* **46**, 1169-1175 (1971).

23 Gershon, R. K. & Kondo, K. Cell interactions in the induction of tolerance: the role of thymic lymphocytes. *Immunology* **18**, 723-737 (1970).

24 Fujimoto, S., Greene, M. & Sehon, A. H. Immunosuppressor T cells in tumor bearing host. *Immunological communications* **4**, 201-217 (1975).

25 Malek, T. R. & Castro, I. Interleukin-2 receptor signaling: at the interface between tolerance and immunity. *Immunity* **33**, 153-165, doi:10.1016/j.immuni.2010.08.004 (2010).

26 Malek, T. R., Yu, A., Vincek, V., Scibelli, P. & Kong, L. CD4 regulatory T cells prevent lethal autoimmunity in IL-2Rbeta-deficient mice. Implications for the nonredundant function of IL-2. *Immunity* **17**, 167-178 (2002).

27 Bayer, A. L., Yu, A., Adeegbe, D. & Malek, T. R. Essential role for interleukin-2 for CD4(+)CD25(+) T regulatory cell development during the neonatal period. *The Journal of experimental medicine* **201**, 769-777, doi:10.1084/jem.20041179 (2005).

28 Burchill, M. A., Yang, J., Vogtenhuber, C., Blazar, B. R. & Farrar, M. A. IL-2 receptor beta-dependent STAT5 activation is required for the development of Foxp3+ regulatory T cells. *J Immunol* **178**, 280-290 (2007).

29 Valzasina, B. *et al.* Triggering of OX40 (CD134) on CD4(+)CD25+ T cells blocks their inhibitory activity: a novel regulatory role for OX40 and its comparison with GITR. *Blood* **105**, 2845-2851, doi:10.1182/blood-2004-07-2959 (2005).

30 Brunkow, M. E. *et al.* Disruption of a new forkhead/winged-helix protein, scurfin, results in the fatal lymphoproliferative disorder of the scurfy mouse. *Nature genetics* **27**, 68-73, doi:10.1038/83784 (2001).

31 Wildin, R. S. *et al.* X-linked neonatal diabetes mellitus, enteropathy and endocrinopathy syndrome is the human equivalent of mouse scurfy. *Nature genetics* **27**, 18-20, doi:10.1038/83707 (2001).

32 Fontenot, J. D. *et al.* Regulatory T cell lineage specification by the forkhead transcription factor foxp3. *Immunity* **22**, 329-341, doi:10.1016/j.immuni.2005.01.016 (2005).

33 Fontenot, J. D., Gavin, M. A. & Rudensky, A. Y. Foxp3 programs the development and function of CD4+CD25+ regulatory T cells. *Nature immunology* **4**, 330-336, doi:10.1038/ni904 (2003).

34 Hori, S., Takahashi, T. & Sakaguchi, S. Control of autoimmunity by naturally arising regulatory CD4+ T cells. *Advances in immunology* **81**, 331-371 (2003).

35 Fontenot, J. D., Dooley, J. L., Farr, A. G. & Rudensky, A. Y. Developmental regulation of Foxp3 expression during ontogeny. *The Journal of experimental medicine* **202**, 901-906, doi:10.1084/jem.20050784 (2005).

36 Takeda, K. *et al.* Induction of tumor-specific T cell immunity by anti-DR5 antibody therapy. *The Journal of experimental medicine* **199**, 437-448, doi:10.1084/jem.20031457 (2004).

37 Feuerer, M., Hill, J. A., Mathis, D. & Benoist, C. Foxp3+ regulatory T cells: differentiation, specification, subphenotypes. *Nature immunology* **10**, 689-695, doi:10.1038/ni.1760 (2009).

38 Mailloux, A. W. & Young, M. R. Regulatory T-cell trafficking: from thymic development to tumor-induced immune suppression. *Critical reviews in immunology* **30**, 435-447 (2010).

39 Jordan, M. S. *et al.* Thymic selection of CD4+CD25+ regulatory T cells induced by an agonist self-peptide. *Nature immunology* **2**, 301-306, doi:10.1038/86302 (2001).

40 Sakaguchi, S., Yamaguchi, T., Nomura, T. & Ono, M. Regulatory T cells and immune tolerance. *Cell* **133**, 775-787, doi:10.1016/j.cell.2008.05.009 (2008).

41 Tran, D. Q., Ramsey, H. & Shevach, E. M. Induction of FOXP3 expression in naive human CD4+FOXP3 T cells by T-cell receptor stimulation is transforming growth factor-beta dependent but does not confer a regulatory phenotype. *Blood* **110**, 2983-2990, doi:10.1182/blood-2007-06-094656 (2007).

42 Burchill, M. A. *et al.* Linked T cell receptor and cytokine signaling govern the development of the regulatory T cell repertoire. *Immunity* **28**, 112-121, doi:10.1016/j.immuni.2007.11.022 (2008).

43 Lio, C. W. & Hsieh, C. S. A two-step process for thymic regulatory T cell development. *Immunity* **28**, 100-111, doi:10.1016/j.immuni.2007.11.021 (2008).

44 Salomon, B. *et al.* B7/CD28 costimulation is essential for the homeostasis of the CD4+CD25+ immunoregulatory T cells that control autoimmune diabetes. *Immunity* **12**, 431-440 (2000).

45 Medoff, B. D. *et al.* CD11b+ myeloid cells are the key mediators of Th2 cell homing into the airway in allergic inflammation. *Journal of immunology* **182**, 623-635 (2009).

46 Wing, K., Fehervari, Z. & Sakaguchi, S. Emerging possibilities in the development and function of regulatory T cells. *International immunology* **18**, 991-1000, doi:10.1093/intimm/dxl044 (2006).

47 Nakamura, K. *et al.* TGF-beta 1 plays an important role in the mechanism of CD4+CD25+ regulatory T cell activity in both humans and mice. *Journal of immunology* **172**, 834-842 (2004).

48 Gabrilovich, D. I. & Nagaraj, S. Myeloid-derived suppressor cells as regulators of the immune system. *Nature reviews. Immunology* **9**, 162-174, doi:10.1038/nri2506 (2009).

49 Melani, C., Sangaletti, S., Barazzetta, F. M., Werb, Z. & Colombo, M. P. Amino-biphosphonate-mediated MMP-9 inhibition breaks the tumor-bone marrow axis responsible for myeloid-derived suppressor cell expansion and macrophage infiltration in tumor stroma. *Cancer research* **67**, 11438-11446, doi:10.1158/0008-5472.CAN-07-1882 (2007).

50 Gabrilovich, D. Mechanisms and functional significance of tumour-induced dendritic-cell defects. *Nature reviews. Immunology* **4**, 941-952, doi:10.1038/nri1498 (2004).

51 Bronte, V. & Mocellin, S. Suppressive influences in the immune response to cancer. *J Immunother* **32**, 1-11, doi:10.1097/CJI.0b013e3181837276 (2009).

52 Movahedi, K. *et al.* Different tumor microenvironments contain functionally distinct subsets of macrophages derived from Ly6C(high) monocytes. *Cancer research* **70**, 5728-5739, doi:10.1158/0008-5472.CAN-09-4672 (2010).

53 Youn, J. I., Collazo, M., Shalova, I. N., Biswas, S. K. & Gabrilovich, D. I. Characterization of the nature of granulocytic myeloid-derived suppressor cells in tumor-bearing mice. *Journal of leukocyte biology* **91**, 167-181, doi:10.1189/jlb.0311177 (2012).

54 Youn, J. I. & Gabrilovich, D. I. The biology of myeloid-derived suppressor cells: the blessing and the curse of morphological and functional heterogeneity. *European journal of immunology* **40**, 2969-2975, doi:10.1002/eji.201040895 (2010).

55 Nefedova, Y. *et al.* Mechanism of all-trans retinoic acid effect on tumor-associated myeloid-derived suppressor cells. *Cancer research* **67**, 11021-11028, doi:10.1158/0008-5472.CAN-07-2593 (2007).

56 Eyles, J. *et al.* Tumor cells disseminate early, but immunosurveillance limits metastatic outgrowth, in a mouse model of melanoma. *The Journal of clinical investigation* **120**, 2030-2039, doi:10.1172/JCI42002 (2010).

57 Sushil Kumar, I. o. M. C. R., University of Zurich, Zurich, Switzerland. Zoledronate Nanoparticles Repolarize Neutrophils in Tumor Microenvironment to Impair Growth of Tumors Refractory to Anti Angiogenic Drugs. *AACR Congress , Tumor microenviroment cmplexity* (2011).

58 Obermajer, N., Muthuswamy, R., Lesnock, J., Edwards, R. P. & Kalinski, P. Positive feedback between PGE2 and COX2 redirects the differentiation of human dendritic cells toward stable myeloid-derived suppressor cells. *Blood* **118**, 5498-5505, doi:10.1182/blood-2011-07-365825 (2011).

59 Rodriguez, P. C. & Ochoa, A. C. Arginine regulation by myeloid derived suppressor cells and tolerance in cancer: mechanisms and therapeutic perspectives.

Immunological reviews **222**, 180-191, doi:10.1111/j.1600-065X.2008.00608.x (2008).

60 Kazlowska, K., Lin, H. T., Chang, S. H. & Tsai, G. J. In Vitro and In Vivo Anticancer Effects of Sterol Fraction from Red Algae Porphyra dentata. *Evidence-based complementary and alternative medicine : eCAM* **2013**, 493869, doi:10.1155/2013/493869 (2013).

61 Meads, M. B., Gatenby, R. A. & Dalton, W. S. Environment-mediated drug resistance: a major contributor to minimal residual disease. *Nat Rev Cancer* **9**, 665-674 (2009).

62 Georges Said, M. G., [...], and Hassan El Btaouri. Extracellular Matrix Proteins Modulate Antimigratory and Apoptotic Effects of Doxorubicin. *Chemotherapy Research and Practice* (2012).

63 Noborio-Hatano, K. *et al.* Bortezomib overcomes cell-adhesion-mediated drug resistance through downregulation of VLA-4 expression in multiple myeloma. *Oncogene* **28**, 231-242, doi:10.1038/onc.2008.385 (2009).

64 Sethi, T. *et al.* Extracellular matrix proteins protect small cell lung cancer cells against apoptosis: a mechanism for small cell lung cancer growth and drug resistance in vivo. *Nature medicine* **5**, 662-668, doi:10.1038/9511 (1999).

65 Folgiero, V. *et al.* Induction of ErbB-3 expression by alpha6beta4 integrin contributes to tamoxifen resistance in ERbeta1-negative breast carcinomas. *PloS one* **3**, e1592, doi:10.1371/journal.pone.0001592 (2008).

66 Vuoristo, M. *et al.* Increased gene expression levels of collagen receptor integrins are associated with decreased survival parameters in patients with advanced melanoma. *Melanoma research* **17**, 215-223, doi:10.1097/CMR.0b013e328270b935 (2007).

67 Borsellino, N. *et al.* Blocking signaling through the Gp130 receptor chain by interleukin-6 and oncostatin M inhibits PC-3 cell growth and sensitizes the tumor cells to etoposide and cisplatin-mediated cytotoxicity. *Cancer* **85**, 134-144 (1999).

68 Catlett, I. M. & Bishop, G. A. Cutting edge: a novel mechanism for rescue of B cells from CD95/Fas-mediated apoptosis. *J Immunol* **163**, 2378-2381 (1999).

69 Duan, Z. *et al.* Signal transducers and activators of transcription 3 pathway activation in drug-resistant ovarian cancer. *Clinical cancer research : an official journal of the American Association for Cancer Research* **12**, 5055-5063, doi:10.1158/1078-0432.CCR-06-0861 (2006).

70 Voorhees, P. M. & Orlowski, R. Z. Emerging data on the use of anthracyclines in combination with bortezomib in multiple myeloma. *Clinical lymphoma & myeloma* **7 Suppl 4**, S156-162 (2007).

71 Frassanito, M. A., Cusmai, A., Iodice, G. & Dammacco, F. Autocrine interleukin-6 production and highly malignant multiple myeloma: relation with resistance to drug-induced apoptosis. *Blood* **97**, 483-489 (2001).

72 Moshaver, B. *et al.* Chemotherapeutic treatment of bone marrow stromal cells strongly affects their protective effect on acute myeloid leukemia cell survival. *Leukemia & lymphoma* **49**, 134-148, doi:10.1080/10428190701593636 (2008).

73 Spiotto, M. T., Rowley, D. A. & Schreiber, H. Bystander elimination of antigen loss variants in established tumors. *Nature medicine* **10**, 294-298, doi:10.1038/nm999 (2004).

74 Bin Zhang 1 , N. A. B., Joseph K. Salama 2 , Hank Schmidt 2 , Michael T. Spiotto 1 , Andrea Schietinger 1 , Ping Yu 1 , Yang-Xin Fu 1 , Ralph R. Weichselbaum 2 , Donald A. Rowley 1 , David M. Kranz 3 , and Hans Schreiber 1. Induced sensitization of tumor stroma leads to eradication of established cancer by T cells *JEM* **204** (2007).

75 Triulzi, T. *et al.* Neoplastic and stromal cells contribute to an extracellular matrix gene expression profile defining a breast cancer subtype likely to progress. *PloS one* **8**, e56761, doi:10.1371/journal.pone.0056761 (2013).

76 Reiman, J. M., Knutson, K. L. & Radisky, D. C. Immune promotion of epithelial-mesenchymal transition and generation of breast cancer stem cells. *Cancer research* **70**, 3005-3008, doi:10.1158/0008-5472.CAN-09-4041 (2010).

77 Caiado, F. *et al.* Bone marrow-derived CD11b+Jagged2+ cells promote epithelial-to-mesenchymal transition and metastasization in colorectal cancer. *Cancer research* **73**, 4233-4246, doi:10.1158/0008-5472.CAN-13-0085 (2013).

78 Toh, B. *et al.* Mesenchymal transition and dissemination of cancer cells is driven by myeloid-derived suppressor cells infiltrating the primary tumor. *PLoS biology* **9**, e1001162, doi:10.1371/journal.pbio.1001162 (2011).

79 Kyriakides, T. R. & Bornstein, P. Matricellular proteins as modulators of wound healing and the foreign body response. *Thrombosis and haemostasis* **90**, 986-992, doi:10.1267/THRO03060986 (2003).

80 Said, N., Najwer, I. & Motamed, K. Secreted protein acidic and rich in cysteine (SPARC) inhibits integrin-mediated adhesion and growth factor-dependent survival signaling in ovarian cancer. *Am J Pathol* **170**, 1054-1063 (2007).

81 Sage, H., Johnson, C. & Bornstein, P. Characterization of a novel serum albumin-binding glycoprotein secreted by endothelial cells in culture. *The Journal of biological chemistry* **259**, 3993-4007 (1984).

82 Lane, T. F., Iruela-Arispe, M. L., Johnson, R. S. & Sage, E. H. SPARC is a source of copper-binding peptides that stimulate angiogenesis. *The Journal of cell biology* **125**, 929-943 (1994).

83 Yan, Q., Sage, E. H. & Hendrickson, A. E. SPARC is expressed by ganglion cells and astrocytes in bovine retina. *The journal of histochemistry and cytochemistry : official journal of the Histochemistry Society* **46**, 3-10 (1998).

84 Funk, S. E. & Sage, E. H. Differential effects of SPARC and cationic SPARC peptides on DNA synthesis by endothelial cells and fibroblasts. *Journal of cellular physiology* **154**, 53-63, doi:10.1002/jcp.1041540108 (1993).

85 Kupprion, C., Motamed, K. & Sage, E. H. SPARC (BM-40, osteonectin) inhibits the mitogenic effect of vascular endothelial growth factor on microvascular endothelial cells. *The Journal of biological chemistry* **273**, 29635-29640 (1998).

86 Motamed, K. & Sage, E. H. SPARC inhibits endothelial cell adhesion but not proliferation through a tyrosine phosphorylation-dependent pathway. *Journal of cellular biochemistry* **70**, 543-552 (1998).

87 Maillard, C., Malaval, L. & Delmas, P. D. Immunological screening of SPARC/Osteonectin in nonmineralized tissues. *Bone* **13**, 257-264 (1992).

88 Basu, A., Kligman, L. H., Samulewicz, S. J. & Howe, C. C. Impaired wound healing in mice deficient in a matricellular protein SPARC (osteonectin, BM-40). *BMC cell biology* **2**, 15 (2001).

89 Schwarzbauer, J. E., Musset-Bilal, F. & Ryan, C. S. Extracellular calcium-binding protein SPARC/osteonectin in Caenorhabditis elegans. *Methods in enzymology* **245**, 257-270 (1994).

90 Masson, S. *et al.* Remodelling of cardiac extracellular matrix during beta-adrenergic stimulation: upregulation of SPARC in the myocardium of adult rats. *Journal of molecular and cellular cardiology* **30**, 1505-1514, doi:10.1006/jmcc.1998.0714 (1998).

91 Stanton, L. W. *et al.* Altered patterns of gene expression in response to myocardial infarction. *Circulation research* **86**, 939-945 (2000).

92 Hasselaar, P., Loskutoff, D. J., Sawdey, M. & Sage, E. H. SPARC induces the expression of type 1 plasminogen activator inhibitor in cultured bovine aortic endothelial cells. *The Journal of biological chemistry* **266**, 13178-13184 (1991).

93 Weber, K. L., Bolander, M. E., Rock, M. G., Pritchard, D. & Sarkar, G. Evidence for the upregulation of osteogenic protein-1 mRNA expression in musculoskeletal neoplasms. *Journal of orthopaedic research : official publication of the Orthopaedic Research Society* **16**, 8-14, doi:10.1002/jor.1100160103 (1998).

94 Bolander, M. E., Young, M. F., Fisher, L. W., Yamada, Y. & Termine, J. D. Osteonectin cDNA sequence reveals potential binding regions for calcium and hydroxyapatite and shows homologies with both a basement membrane protein (SPARC) and a serine proteinase inhibitor (ovomucoid). *Proceedings of the National Academy of Sciences of the United States of America* **85**, 2919-2923 (1988).

95 Maurer, P. & Hohenester, E. Structural and functional aspects of calcium binding in extracellular matrix proteins. *Matrix biology : journal of the International Society for Matrix Biology* **15**, 569-580; discussion 581 (1997).

96 Kelm, R. J., Jr. & Mann, K. G. The collagen binding specificity of bone and platelet osteonectin is related to differences in glycosylation. *The Journal of biological chemistry* **266**, 9632-9639 (1991).

97 Xie, R. L. & Long, G. L. Role of N-linked glycosylation in human osteonectin. Effect of carbohydrate removal by N-glycanase and site-directed mutagenesis on structure and binding of type V collagen. *The Journal of biological chemistry* **270**, 23212-23217 (1995).

98 Iruela-Arispe, M. L., Vernon, R. B., Wu, H., Jaenisch, R. & Sage, E. H. Type I collagen-deficient Mov-13 mice do not retain SPARC in the extracellular matrix: implications for fibroblast function. *Developmental dynamics : an official publication of the American Association of Anatomists* **207**, 171-183, doi:10.1002/(SICI)1097-0177(199610)207:2<171::AID-AJA5>3.0.CO;2-E (1996).

99 Bradshaw, A. D., Graves, D. C., Motamed, K. & Sage, E. H. SPARC-null mice exhibit increased adiposity without significant differences in overall body weight.

Proceedings of the National Academy of Sciences of the United States of America **100**, 6045-6050, doi:10.1073/pnas.1030790100 (2003).

100 Alique, M., Calleros L., Luengo A., Griera M., Iniguez M.A., Punzon C., Fresno M., Rodruigues-Puyol M., Rodruiguez-Puyol D. & Chadee, K. Changes in extracellular matrix composition regulate cyclooxygenase-2 expression in human mesangial cells *Am J Physiol Cell Physiol* **300**, 963-969 (2011).

101 Sasaki, T. *et al.* Limited cleavage of extracellular matrix protein BM-40 by matrix metalloproteinases increases its affinity for collagens. *The Journal of biological chemistry* **272**, 9237-9243 (1997).

102 Sasaki, T., Hohenester, E., Gohring, W. & Timpl, R. Crystal structure and mapping by site-directed mutagenesis of the collagen-binding epitope of an activated form of BM-40/SPARC/osteonectin. *The EMBO journal* **17**, 1625-1634, doi:10.1093/emboj/17.6.1625 (1998).

103 Hakomori, S. Tumor malignancy defined by aberrant glycosyla- tion and sphingo(glyco)lipid metabolism. *Cancer Res.* **56**, 5309±5318. (1996).

104 Varki, A. Biological roles of oligosaccharides: all of the theories are correct. *Glycobiology* **3**, 97-130 (1993).

105 Yamamoto, H., Swoger, J., Greene, S., Saito, T., Hurh, J., Sweeley, C., Leestma, J., Mkrdichian, E., Cerullo, L., Nishikawa, A., and others. b1,6-N-acetylglucosamine-bearing N-glycans in human gliomas: implications for a role in regulating invasivity.. *Cancer research* **60** (2000).

106 Skelton, T. P., Zeng, C., Nocks, A. & Stamenkovic, I. Glycosylation provides both stimulatory and inhibitory effects on cell surface and soluble CD44 binding to hyaluronan. *The Journal of cell biology* **140**, 431-446 (1998).

107 Kaufmann, K., Bach, K. & Thiel, G. The extracellular signal-regulated protein kinases Erk1/Erk2 stimulate expression and biological activity of the transcriptional regulator Egr-1. *Biological chemistry* **382**, 1077-1081, doi:10.1515/BC.2001.135 (2001).

108 Yan, Q. & Sage, E. H. SPARC, a matricellular glycoprotein with important biological functions. *The journal of histochemistry and cytochemistry : official journal of the Histochemistry Society* **47**, 1495-1506 (1999).

109 Shankavaram, U. T., DeWitt, D. L., Funk, S. E., Sage, E. H. & Wahl, L. M. Regulation of human monocyte matrix metalloproteinases by SPARC. *Journal of cellular physiology* **173**, 327-334, doi:10.1002/(SICI)1097-4652(199712)173:3<327::AID-JCP4>3.0.CO;2-P (1997).

110 Gilles, C. *et al.* SPARC/osteonectin induces matrix metalloproteinase 2 activation in human breast cancer cell lines. *Cancer research* **58**, 5529-5536 (1998).

111 Raines, E. W. & Ross, R. Compartmentalization of PDGF on extracellular binding sites dependent on exon-6-encoded sequences. *The Journal of cell biology* **116**, 533-543 (1992).

112 Floege, J. *et al.* Glomerular cell proliferation and PDGF expression precede glomerulosclerosis in the remnant kidney model. *Kidney international* **41**, 297-309 (1992).

113 Kingsley, D. M. The TGF-beta superfamily: new members, new receptors, and new genetic tests of function in different organisms. *Genes & development* **8**, 133-146 (1994).

114 Francki, A. *et al.* SPARC regulates the expression of collagen type I and transforming growth factor-beta1 in mesangial cells. *The Journal of biological chemistry* **274**, 32145-32152 (1999).

115 Sage, H., Decker, J., Funk, S. & Chow, M. SPARC: a Ca2+-binding extracellular protein associated with endothelial cell injury and proliferation. *Journal of molecular and cellular cardiology* **21 Suppl 1**, 13-22 (1989).

116 Lane, T. F. & Sage, E. H. The biology of SPARC, a protein that modulates cell-matrix interactions. *FASEB journal : official publication of the Federation of American Societies for Experimental Biology* **8**, 163-173 (1994).

117 Sangaletti, S., Stoppacciaro, A., Guiducci, C., Torrisi, M. R. & Colombo, M. P. Leukocyte, rather than tumor-produced SPARC, determines stroma and collagen type IV deposition in mammary carcinoma. *The Journal of experimental medicine* **198**, 1475-1485, doi:10.1084/jem.20030202 (2003).

118 Sangaletti, S. *et al.* Accelerated dendritic-cell migration and T-cell priming in SPARC-deficient mice. *Journal of cell science* **118**, 3685-3694, doi:10.1242/jcs.02474 (2005).

119 Ledda, F., Bravo, A.I., Adris, S., Bover, L., Mordoh, J., Podhajcer, O.L. The expression of the secreted protein acidic and rich in cysteine

(SPARC) is associated with the neoplastic progression of human melanoma. *J. Invest. Dermatol.* (1997).

120 Alvarez, M. J. *et al.* Secreted protein acidic and rich in cysteine produced by human melanoma cells modulates polymorphonuclear leukocyte recruitment and antitumor cytotoxic capacity. *Cancer research* **65**, 5123-5132, doi:10.1158/0008-5472.CAN-04-1102 (2005).

121 Sangaletti, S. *et al.* SPARC oppositely regulates inflammation and fibrosis in bleomycin-induced lung damage. *Am J Pathol* **179**, 3000-3010, doi:10.1016/j.ajpath.2011.08.027 (2011).

122 Tripodo, C. *et al.* Stromal SPARC contributes to the detrimental fibrotic changes associated with myeloproliferation whereas its deficiency favors myeloid cell expansion. *Blood* **120**, 3541-3554, doi:10.1182/blood-2011-12-398537 (2012).

123 Kos, M., Kuebler, J. F., Luczak, K. & Engelke, W. Bisphosphonate-related osteonecrosis of the jaws: a review of 34 cases and evaluation of risk. *Journal of cranio-maxillo-facial surgery : official publication of the European Association for Cranio-Maxillo-Facial Surgery* **38**, 255-259, doi:10.1016/j.jcms.2009.06.005 (2010).

124 Demopoulos, K., Arvanitis, D. A., Vassilakis, D. A., Siafakas, N. M. & Spandidos, D. A. MYCL1, FHIT, SPARC, p16(INK4) and TP53 genes associated to lung cancer in idiopathic pulmonary fibrosis. *Journal of cellular and molecular medicine* **6**, 215-222 (2002).

125 Chin, D. *et al.* Novel markers for poor prognosis in head and neck cancer. *International journal of cancer. Journal international du cancer* **113**, 789-797, doi:10.1002/ijc.20608 (2005).

126 Wang, Y., Yu, Q., Cho, A.H., Rondeau, G.,Welsh, J., Adamson, E., Mercola, & D., M., M.,. Survey of differentially methylated promoters in prostate cancer cell lines. *Neoplasia* (2005).

127 Yamashita, K., Upadhay, S., Mimori, K., Inoue, H. & Mori, M. Clinical significance of secreted protein acidic and rich in cystein in esophageal carcinoma and its relation to carcinoma progression. *Cancer* **97**, 2412-2419, doi:10.1002/cncr.11368 (2003).

128 Mok, S. C., Chan, W.Y., Wong, K.K., Muto, M.G., Berkowitz, R.S.,. SPARC, an extracellular matrix protein with tumor-suppressing activity in human ovarian epithelial cells. *Oncogene* (1996).

129 Suzuki, M., Hao, C., Takahashi, T., Shigematsu, H., Shivapurkar, N., Sathyanarayana, & U.G. Aberrant methylation of SPARC in human lung cancers. *Br. J. Cancer* (2005).

130 Sato, N., Fukushima, N., Maehara, N., Matsubayashi, H., Koopmann, J., Su, & G.H. SPARC/osteonectin is a frequent target for aberrant methylation in pancreatic adenocarcinoma and a mediator of tumorstromal interactions. *Oncogene* (2003).

131 Puolakkainen, P. A., Brekken, R.A., Muneer, S., Sage, E.H. Enhanced growth of pancreatic tumors in SPARC-null mice is associated with decreased deposition of extracellular matrix and reduced tumor cell apoptosis. *Mol. Cancer Res.* (2004).

132 Lucchini, F. *et al.* Early and multifocal tumors in breast, salivary, harderian and epididymal tissues developed in MMTY-Neu transgenic mice. *Cancer Lett* **64**, 203-209 (1992).

133 Bradshaw, A. D. & Sage, E. H. SPARC, a matricellular protein that functions in cellular differentiation and tissue response to injury. *The Journal of clinical investigation* **107**, 1049-1054, doi:10.1172/JCI12939 (2001).

134 Morelli, D., Menard, S., Colnaghi, M. I. & Balsari, A. Oral administration of anti-doxorubicin monoclonal antibody prevents chemotherapy-induced gastrointestinal toxicity in mice. *Cancer research* **56**, 2082-2085 (1996).

135 Allen, G. J. R. C. a. T. M. Multiple Injections of Pegylated Liposomal Doxorubicin: Pharmacokinetics and Therapeutic Activity. *Pharmacology* **306** (2003).

136 Ottewell, P. D. *et al.* Sustained inhibition of tumor growth and prolonged survival following sequential administration of doxorubicin and zoledronic acid in a breast cancer model. *International journal of cancer. Journal international du cancer* **126**, 522-532, doi:10.1002/ijc.24756 (2010).

137 Schmittgen, T. D. *et al.* Real-time PCR quantification of precursor and mature microRNA. *Methods* **44**, 31-38, doi:10.1016/j.ymeth.2007.09.006 (2008).

138 Sangaletti, S., Stoppacciaro, A., Guiducci, C., Torrisi, M. R. & Colombo, M. P. Leukocyte, rather than tumor-produced SPARC, determines stroma and collagen type IV deposition in mammary carcinoma. *The Journal of experimental medicine* **198**, 1475-1485, doi:10.1084/jem.20030202 (2003).

139 Weaver, M. S., Workman, G. & Sage, E. H. The copper binding domain of SPARC mediates cell survival in vitro via interaction with integrin beta1 and activation of integrin-linked kinase. *The Journal of biological chemistry* **283**, 22826-22837 (2008).

140 Girotti, M. R. *et al.* SPARC promotes cathepsin B-mediated melanoma invasiveness through a collagen I/alpha2beta1 integrin axis. *The Journal of investigative dermatology* **131**, 2438-2447, doi:10.1038/jid.2011.239 (2011).

141 Santisteban, M. *et al.* Immune-induced epithelial to mesenchymal transition in vivo generates breast cancer stem cells. *Cancer research* **69**, 2887-2895, doi:10.1158/0008-5472.CAN-08-3343 (2009).

142 Ben-Baruch, A. The Tumor-Promoting Flow of Cells Into, Within and Out of the Tumor Site: Regulation by the Inflammatory Axis of TNFalpha and Chemokines. *Cancer microenvironment : official journal of the International Cancer Microenvironment Society* **5**, 151-164, doi:10.1007/s12307-011-0094-3 (2012).

143 Colombo, M. P. *et al.* Granulocyte colony-stimulating factor (G-CSF) gene transduction in murine adenocarcinoma drives neutrophil-mediated tumor inhibition in vivo. Neutrophils discriminate between G-CSF-producing and G-CSF-nonproducing tumor cells. *J Immunol* **149**, 113-119 (1992).

144 Demers, M. *et al.* Cancers predispose neutrophils to release extracellular DNA traps that contribute to cancer-associated thrombosis. *Proceedings of the National Academy of Sciences of the United States of America* **109**, 13076-13081, doi:10.1073/pnas.1200419109 (2012).

145 DuPre, S. A., Redelman, D. & Hunter, K. W., Jr. The mouse mammary carcinoma 4T1: characterization of the cellular landscape of primary tumours and metastatic tumour foci. *International journal of experimental pathology* **88**, 351-360, doi:10.1111/j.1365-2613.2007.00539.x (2007).

146 Kodama, T., Goto, T. & Kobayashi, H. [Proceedings: Immunological study of regression of metastatic neoplasm in lymph nodes]. *[Hokkaido igaku zasshi] The Hokkaido journal of medical science* **49**, 153-154 (1974).

147 Boggs, D. R. Transfusion of neutrophils as prevention or treatment of infection in patients with neutropenia. *The New England journal of medicine* **290**, 1055-1062, doi:10.1056/NEJM197405092901906 (1974).

148 Rose, S., Misharin, A. & Perlman, H. A novel Ly6C/Ly6G-based strategy to analyze the mouse splenic myeloid compartment. *Cytometry. Part A : the journal of the International Society for Analytical Cytology* **81**, 343-350, doi:10.1002/cyto.a.22012 (2012).

149 Piccard, H., Muschel, R. J. & Opdenakker, G. On the dual roles and polarized phenotypes of neutrophils in tumor development and progression. *Critical reviews in oncology/hematology* **82**, 296-309, doi:10.1016/j.critrevonc.2011.06.004 (2012).

150 Wen-Chin Yang, G. M. Polarization and reprogramming of myeloid-derived suppressor cells. *Journal of Molecular Cell Biology* (2013).

151 Dolcetti, L. *et al.* Hierarchy of immunosuppressive strength among myeloid-derived suppressor cell subsets is determined by GM-CSF. *European journal of immunology* **40**, 22-35, doi:10.1002/eji.200939903 (2010).

152 Morales, J. K., Kmieciak, M., Knutson, K. L., Bear, H. D. & Manjili, M. H. GM-CSF is one of the main breast tumor-derived soluble factors involved in the differentiation of CD11b-Gr1- bone marrow progenitor cells into myeloid-derived suppressor cells. *Breast cancer research and treatment* **123**, 39-49, doi:10.1007/s10549-009-0622-8 (2010).

153 Granot, Z. *et al.* Tumor entrained neutrophils inhibit seeding in the premetastatic lung. *Cancer cell* **20**, 300-314, doi:10.1016/j.ccr.2011.08.012 (2011).

154 Melissa G. Lechner, Daniel J. Liebertz and Alan L. Epstein. Characterization of cytokine-induced myeloid-derived suppressor cells from normal human peripheral blood mononuclear cells. *J Immunol* **185**, 2273-84, doi: 10.4049/jimmunol.1000901. (2010).

155 Na YR, Y. Y., Son DI, Seok SH. Cyclooxygenase-2 inhibition blocks M2 macrophage differentiation and suppresses metastasis in murine breast cancer model. *PloS one* (2013).

156 Bergamaschi, A. *et al.* Extracellular matrix signature identifies breast cancer subgroups with different clinical outcome. *The Journal of pathology* **214**, 357-367, doi:10.1002/path.2278 (2008).

157 Sangaletti S, C. M. *Cancer Lett* **267**, 245-253.

158 Casiraghi, F., Remuzzi, G., Abbate, M. & Perico, N. Multipotent mesenchymal stromal cell therapy and risk of malignancies. *Stem cell reviews* **9**, 65-79, doi:10.1007/s12015-011-9345-4 (2013).

159 Ghannam, S., Pene, J., Torcy-Moquet, G., Jorgensen, C. & Yssel, H. Mesenchymal stem cells inhibit human Th17 cell differentiation and function and induce a T regulatory cell phenotype. *J Immunol* **185**, 302-312, doi:10.4049/jimmunol.0902007 (2010).

160 Dalle Carbonare L, V. M., Bertoldo F, Fracalossi A, Balducci E, Azzarello G, Vinante O, Lo Cascio V. Amino-bisphosphonates decrease hTERT gene expression in breast cancer in vitro. *Aging Clin Exp Res.* (2007).

161 Sangaletti, S. *et al.* Defective Stromal Remodeling and Neutrophil Extracellular Traps in Lymphoid Tissues Favor the Transition from Autoimmunity to Lymphoma. *Cancer discovery*, doi:10.1158/2159-8290.CD-13-0276 (2013).